[American Journal of Science, Vol. 310, September, 2010, P. 523–574, DOI 10.2475/07.2010.01]

American Journal of Science

SEPTEMBER 2010

LITHOSTRATIGRAPHIC AND GEOCHRONOLOGICAL CONSTRAINTS ON THE EVOLUTION OF THE CENTRAL ASIAN OROGENIC BELT IN SW MONGOLIA: EARLY PALEOZOIC RIFTING FOLLOWED BY LATE PALEOZOIC ACCRETION

ALFRED KRÖNER*,†, JÉRÉMIE LEHMANN**,***, KAREL SCHULMANN**, ANTOINE DEMOUX*, ONDREJ LEXA***,****, DONDOV TOMURHUU§, PAVLA ŠTÍPSKÁ**, DUNYI LIU§§, and MICHAEL T. D. WINGATE‡

ABSTRACT. New SHRIMP U-Pb and evaporation Pb-Pb zircon ages, together with a revision of the lithostratigraphy of "suspect" terranes in SW Mongolia, suggest that the collage of continental and oceanic units in this region resulted from recurrent magmatic reworking and deformation of Silurian–early Devonian proximal and distal passive margin sequences of the Paleo-Asian Ocean. The zircon ages from early Ordovician volcaniclastic rocks and syntectonic felsic dikes reveal an heterogeneous stretching of the Precambrian Dzabkhan microcontinent (Lake Zone basement) during the Ordovician, followed by the development of a carbonate platform on a proximal margin (Gobi-Altai Zone), serpentinite breccias and Silurian chert sequences on a distal margin and possibly also the formation of oceanic crust. The assumed early Neoproterozoic South Gobi continental zone may either represent an allochthonous block detached from Dzabkhan or, less likely, the conjugate margin of a Paleo-Asian continental rift. Early Devonian volcanism subsequently affected both types of margins with back-arc spreading centers and arcs located in the core of the future Trans-Altai Zone. During the late Devonian to early Carboniferous a Japan-type magmatic arc developed on the previously stretched continental crust of the Gobi-Altai Zone. This event was associated with shortening of the entire domain, exhumation of the deep arc core and formation of intramontane basins with Devonian and Carboniferous detrital zircons of the adjacent Lake Zone continent. Clastic, flysch-type sedimentation occurred on the former distal margin and in oceanic areas. During this early Carboniferous contraction event the continental and oceanic units were imbricated and accreted to the continent in the north. Subsequently, late Carboniferous volcanic arc sequences and a Japan-type magmatic arc developed on the Trans-Altai oceanic crust and the southern South Gobi Zone, respectively. Finally, a Permian thermal event was localized in the Gobi-Altai–Lake Zone contact domain and was responsible for formation of Permian grabens, bimodal volcanism and substantial melting of the accreted crust.

Key words: Accretionary tectonics, Central Asian Orogenic Belt, Mongolia, Paleozoic, tectono-stratigraphy, zircon geochronology.

* Institut für Geowissenschaften, Universität Mainz, Becherweg 21, D-55099 Mainz, Germany, and Beijing SHRIMP Center, Chinese Academy of Geological Sciences, Beijing 100037, China
** Institut de Physique du Globe de Strasbourg, IPGS—UMR 7516, CNRS et Université de Strasbourg, 3 rue Michel-Ange, F-67084 Strasbourg, France
*** Czech Geological Survey, Klárov 3, 118 21 Praha 1, Czech Republic
**** IPSG, Univerzita Karlova, Albertov 6, Praha 2, Czech Republic
§ Institute of Geology and Mineral Resources, Mongolian Academy of Sciences, P. O. Box 118, Ulaanbaatar 210351, Mongolia
§§ Beijing SHRIMP Center, Chinese Academy of Geological Sciences, 26 Baiwanzhuang Road, 100037 Beijing, China
‡ Geological Survey of Western Australia, 100 Plain Street, East Perth, WA 6004, Australia
† Corresponding author: kroener@uni-mainz.de

INTRODUCTION

The Central Asian Orogenic Belt (CAOB), also known as Altaids, occurs in a broad area between the Siberian, North China and Tarim cratons (fig. 1, inset) and documents some of the most voluminous continental growth on Earth during the early Phanerozoic (Şengör and others, 1993; Mossakovsky and others, 1994; Windley and others, 2007). Formation of the belt is thought to be dominated by the accretion of magmatic arcs, back-arc terranes, accretionary complexes and continental blocks, from the latest Mesoproterozoic to the late Permian (Şengör and others, 1993; Şengör and Natal'in, 1996; Khain and others, 2003; Kröner and others, 2007; Windley and others, 2007).

The term Altaids was first used by Suess (1901) who recognized that Asia had grown peripherally during the Paleozoic, mainly to the west and south of the Angara/Siberia nucleus (see Şengör and Natal'in, 2007, for a review of central Asian terminology). Several models of accretion have been debated for the last 20 years. Şengör and others (1993) and Şengör and Natal'in (1996) proposed that the orogen formed by successive accretion and oroclinal bending of a long-lived single-subduction system (the ~7000 km long Kipchak-Tuva-Mongol arc), whereas other authors (Hsü, 1988; Coleman, 1989; Mossakovsky and others, 1994) suggested that the CAOB originated through the operation of several subduction systems with different polarities and by collision of various microcontinents. Windley and others (2007) speculated that some of the metamorphic and tectonic features observed in parts of the CAOB may have resulted from ridge subduction in a circum-Pacific environment, an idea already proposed by Kovalenko and others (1995). These different models have distinctive predictions with regard to: (1) the age of magmatic and metamorphic complexes in the belt, (2) the general style of accretion of juvenile crust and, (3) the paleogeographic position of the major lithotectonic units within the belt.

The SW Mongolian geological structure plays an important role in understanding the evolution of the CAOB because it covers two major regions that were affected by early Paleozoic (Caledonian in the old literature) and late Paleozoic (Hercynian in the old literature) tectonic events. In the last 60 years our study area has been subjected to extensive mapping including detailed lithostratigraphy and paleontological research, thus allowing the definition of lithostratigraphic formations and lithotectonic units (Sinitsyn, 1956; Amantov and others, 1970; Marinov and others, 1973; Markova, 1975; Ruzhentsev and Pospelov, 1992). In agreement with early models for the tectonic evolution of the CAOB (Amantov and others, 1968; Zonenshain, 1972, 1973; Ruzhentsev and others, 1991), the basement structure of Mongolia is divided into two super-units that differ from each other in structural style and ages of geological formations: 1) the Neoproterozoic northern super-unit (the Mongolian continent of Zonenshain, 1973) was predominantly affected by early Paleozoic orogenesis, whereas the early Paleozoic southern super-unit was predominantly affected by late Paleozoic deformation (fig. 1). The two super-units are separated by the Main Mongolian deep fault, later slightly modified and renamed as Main Mongolian Lineament (Tomurtogoo, 1997). These super-units were subdivided into zones and blocks, separated by faults and marked by distinct lithological assemblages, which were spatially correlated within individual tectonic zones in terms of facial variations of rocks with similar ages (Ruzhentsev and Pospelov, 1992; Ruzhentsev, 2001). Thus, four major tectonostratigraphic zones have been defined from north to south by Zaitsev and others (1970), Zonenshain (1973), Markova (1975), Ruzhentsev (2001): the northernmost Lake Zone, the Gobi-Altai Zone, the Trans-Altai Zone (sometimes South Mongolian Zone; for example, Zonenshain, 1973) and the southernmost South Gobi Zone. These zones correspond, in the same order, to the southern margin of the northern Mongolian continent of Zonenshain (1973), early Paleozoic passive margin sequences, an early

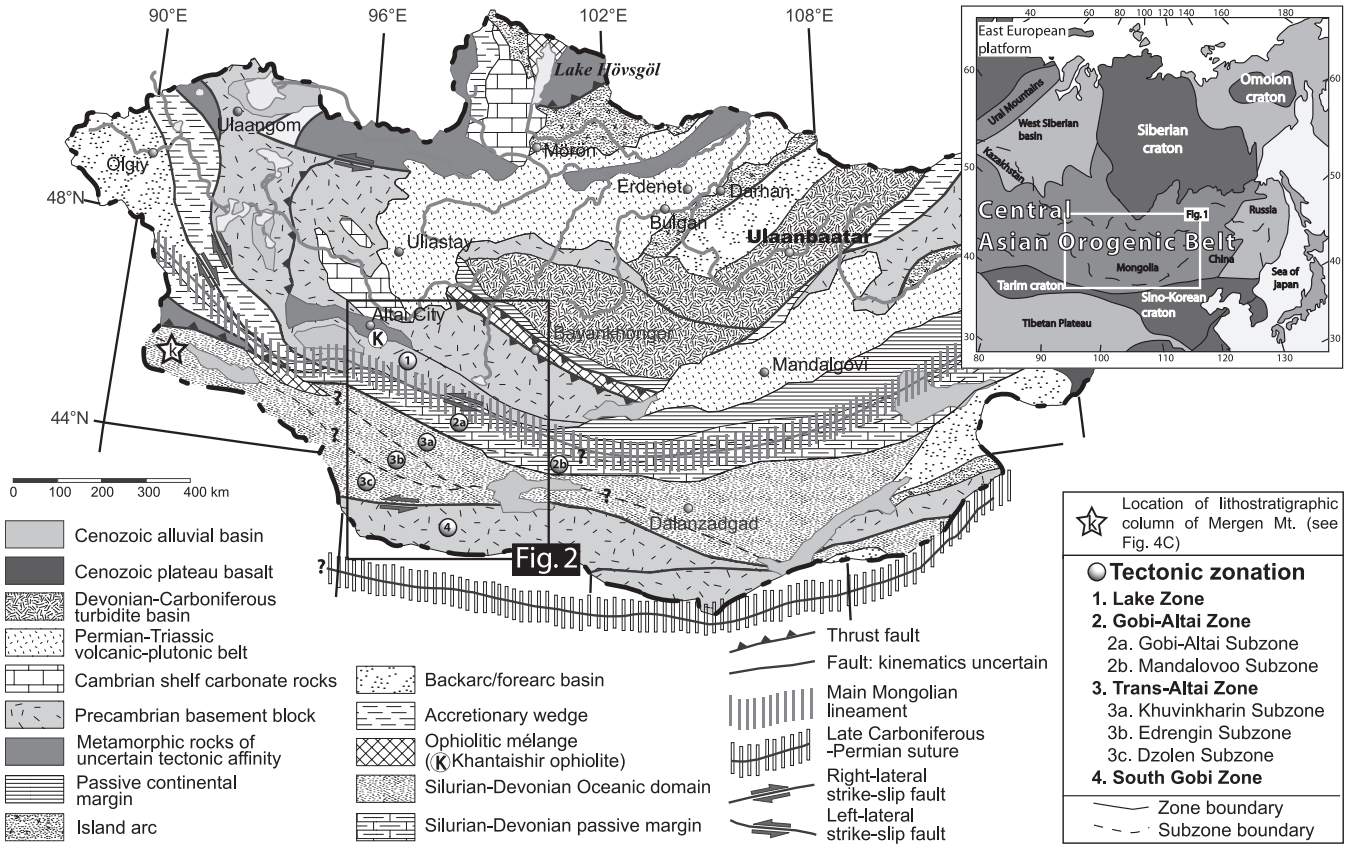

Fig. 1. Simplified geological map of Mongolia showing lithotectonic associations and location of fig. 2. Modified from Badarch and others (2002). Inset shows location of Central Asian Orogenic Belt and adjacent tectonic elements. Circled numbers in framed map section of fig. 2 refer to lithotectonic zones separated by dashed lines or faults (modified according to Markova, 1975 and Ruzhentsev, 2001).

Paleozoic oceanic domain and a southern continent, respectively. These tectonic zones were further subdivided into sub-zones that were later renamed as tectonostratigraphic terranes without major modifications of boundaries or lithological contents (Badarch and others, 2002) but with some revision of their geodynamic significance (fig. 1). This simple model was considerably modified by Şengör and others (1993) and Şengör and Natal'in (1996) who proposed an imbrication of Precambrian and early Paleozoic sequences forming a major Tuva-Mongol magmatic arc by strike slip motion and oroclinal bending.

Badarch and others (2002) subdivided the accretionary collage of Mongolia into 44 terranes, and defined a terrane, following the earlier literature, as "a fault-bounded assemblage or fragment whose geology differs from that of adjacent terranes." However, many of their proposed terrane boundaries are ill-defined, and lithostratigraphic analysis by earlier authors shows that there are frequently more similarities than differences between specific "terranes" so that their "exotic" origin is questionable. We therefore prefer to use the more neutral term "tectonic zone" to define distinct tectonostratigraphic domains, following Zaitsev and others (1970) and Markova (1975) and use "terrane" in inverted commas when referring to the nomenclature of Badarch and others (2002).

In this paper we summarize lithostratigraphic and paleontological information of critical (volcano)-sedimentary sequences, mainly published in the Russian literature, and evaluate these data on the basis of new single zircon ages for magmatic and sedimentary rocks and structural and petrological observations. Our study area covers a north-south transect that begins in the Lake Zone north of Chandman village in the north and extends to the Gobi-Altai, Trans-Altai and South Gobi Zones in the south (figs. 2 and 3). The principal tectonic units in our transect are formed by NW-SE trending Gobi-Altai ridges and their branches, piedmonts and the sub-meridionally trending Gobi-Tienshan Ridge juxtaposed with intermontane Meso- to Cenozoic depressions (fig. 2). The transect is 300 km long and about 70 km wide along which detailed structural and petrological analysis, combined with zircon dating of critical felsic magmatic and sedimentary rocks, were performed. This leads us to propose a modified tectonic model for crustal accretion in SW Mongolia (for details on the structural evolution and new tectonic model see Lehmann and others, 2010).

Lithostratigraphy and metamorphism of the Lake Zone (fig. 4a)

Rocks of the Lake Zone are exposed in the Erdene, Zamtyn and Bayantsagaan mountain ranges located north of the Main Mongolian Lineament (figs. 2 and 3). According to previous geological mapping and based on rock assemblages and metamorphic overprints, at least four contrasting lithotectonic groups have been distinguished (Markova, 1975).

The Khantaishir Ridge northwest of our study area represents a type section of the Lake Zone (fig. 4A). It is represented by the following sequence of lithotectonic units from bottom to top: the structurally lowest unit is represented by a compositionally heterogeneous gneiss-amphibolite-granite basement (Havchig Complex of Mitrofanov and others, 1981) of Proterozoic age, exposed north and NW of Altay City and considered to be part of the Dzabkhan microcontinent (Kozakov and others, 2007b). Kröner and others (2001) reported a SHRIMP zircon age of 1127 ± 1 Ma with a 1715 Ma zircon xenocryst for a porphyritic granite-gneiss just E of Altay City, whereas Yarmolyuk and others (2008a) found an age of 755 ± 3 Ma for an alkali granite, and Zhao and others (2006) reported a SHRIMP zircon age of 840 ± 9 Ma for leucosome within migmatitc gneisses from this complex. Some of the Neoproterozoic rocks contain zircon cores as old as Neoarchean (Y. Zhao, personal communication, 2008). Similarly, a felsic volcanic rock from the upper section of the late Riphean Zavkhan formation yielded a SHRIMP zircon age of 777 ± 6 Ma (Zhao and others, 2006), and

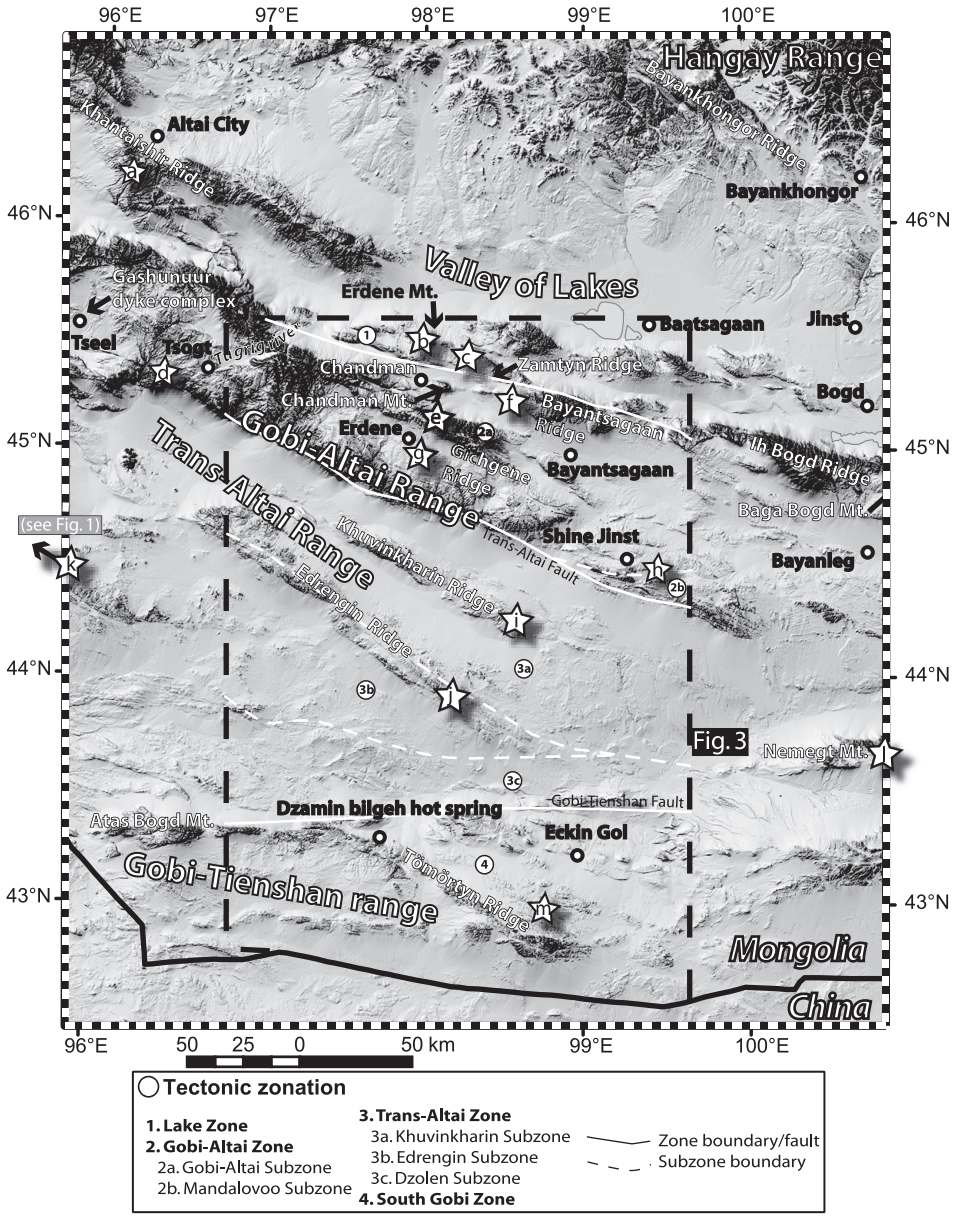

Fig. 2. Gray-scaled digital elevation model (SRTM 2) showing the geography and morphology of southern Mongolia mentioned in the text and location of fig. 3. Stars represent approximate location of lithostratigraphic columns of fig. 4.

this is in good agreement with ages of 774 ± 4 Ma and 803 ± 8 Ma reported by Levashova and others (2010) for the same formation. This basement is overlain by a tectonically dismembered ophiolite association (Khantaishir formation) composed of peridotite, gabbro, a sheeted dike complex, basaltic pillow lava boninite and chert (Zonenshain and Kuzmin, 1978; Matsumoto and Tomurtogoo, 2003). Zircons from a plagiogranite were dated at 568 ± 4 Ma (Gibsher and others, 2001). According to

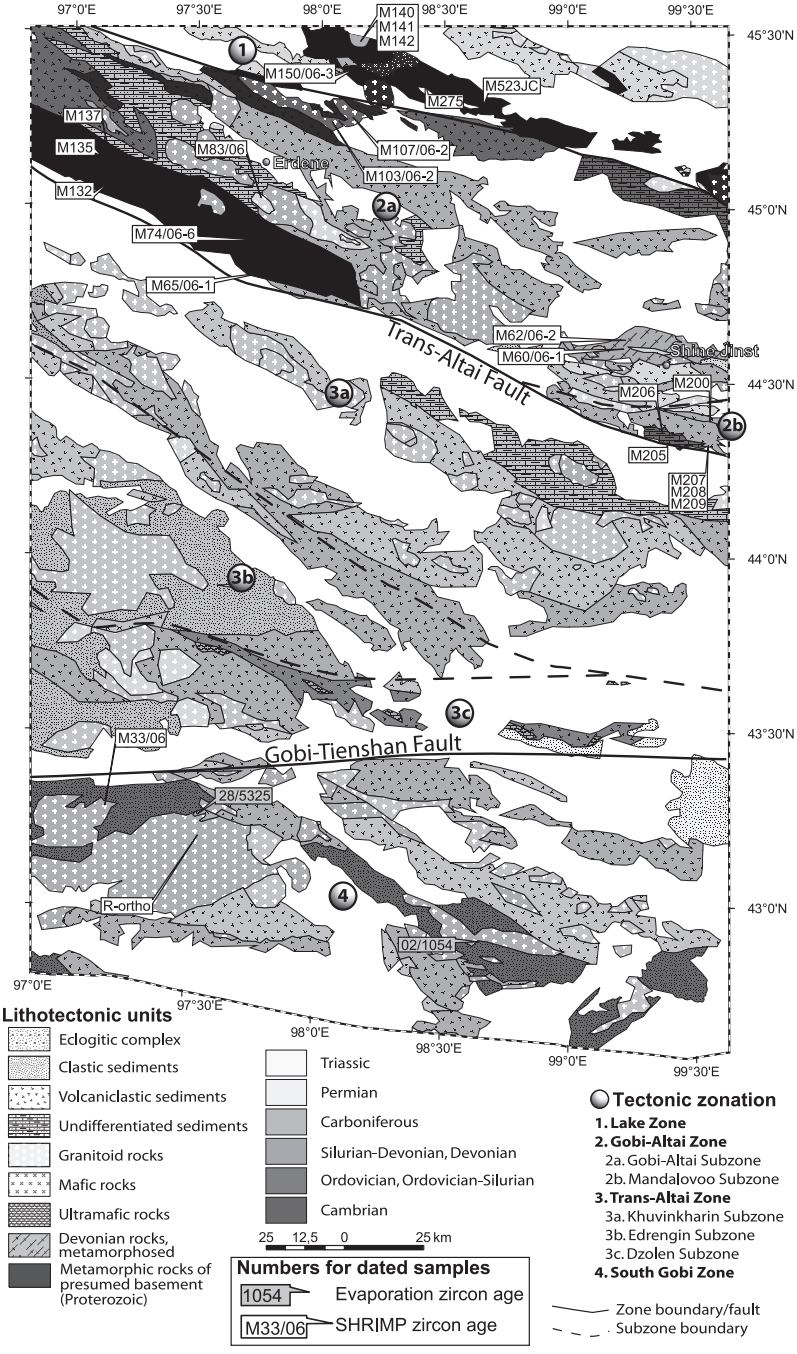

Fig. 3. Lithotectonic map of traverse in SW Mongolia showing pre-Jurassic units (compiled from Rauzer and others, 1987 and Tomurtogoo, 1998). MML: Main Mongolian Lineament. Circled numbers refer to lithotectonic zones separated by dotted lines (modified according to Markova, 1975 and Ruzhentsev, 2001). Numbers and locations of samples collected for zircon dating are also shown.

lithology and geochemical data, this assemblage was interpreted as a supra-subduction island arc complex (Markova, 1975; Zonenshain and Kuzmin, 1978; Kepezhinskas, 1986; Khain and others, 2003). The overlying paleontologically dated late Vendian–early Cambrian (Archaeocyatha, Markova, 1975) Tsakhir Uul formation is represented predominantly by chlorite schist and marble (fig. 4A). The hanging wall Naran formation was first assumed to be early Cambrian in age (Rauzer and others, 1987) but without paleontological evidence. Ruzhentsev and Burashnikov (1996) divided it in two different sequences. The lower sequence Arynbulag formation of Cambrian age (Photoconodonts, anabaritids, chiolites and molluscs, Ruzhentsev and Burashnikov, 1996) is composed of coarse epiclastic rocks in the northern part, whereas tuffitic-carbonate sediments occur in the south. The second sequence is the Naran formation of Cambrian age, represented by a flyschoid siliciclastic sequence. The uppermost position in the column, according to Rauzer and others (1987) and Markova (1975), is occupied by the middle Cambrian Ulaanshand formation that is essentially composed of mafic volcanic and corresponding pyroclastic rocks.

However, rocks that are considered to be an analogue of this assemblage in our study area differ from the type section in their higher grade of metamorphism. Basement rocks in our section are exposed north of the Main Mongolian Lineament (figs. 3 and 4A) as an E-W elongated belt that is flanked in the north by a Cretaceous basin. The structurally lowest and eastern part is represented by coarse-grained augen-gneiss at the base, banded amphibolites, amphibolitic gneisses and marbles with a minor proportion of metapelite of the Zamtyn Nuuru complex. The amphibolite-facies metamorphic assemblages are mostly characterized by hornblende, garnet and plagioclase in amphibolites and garnet and biotite in associated metapelites. These medium-grade metamorphic rocks occur in a wide area extending from the studied section to the west as far as the eastern end of the Khantaishir Ridge (fig. 2). Therefore, medium-grade metamorphism is one of the main features in the Neoproterozoic basement of the Lake Zone. The unit is intruded by leucogranite bodies of which zircons were dated at 518 Ma (Hrdličková and others, 2008). Diorites, granodiorites and leucocratic granites are widespread and were suggested to be Permian in age (Rauzer and others, 1987).

The lateral equivalent of the Khantaishir unit in our traverse is represented by rocks of the southeastern Erdene Mountain piedmont where serpentinized peridotites, a tonalite-trondhjemite suite, and abundant tholeiitic to calc-alkaline (Hanžl and Aichler, 2007) mafic to intermediate volcanic rocks are observed.

The third important sequence is represented by the Tsakhir Uul formation (fig. 4A), composed of fossiliferous volcano-sedimentary, sedimentary, and tuffaceous siliceous schists and marbles which were dated paleontologically in both the Khantaishir and Zamtyn Ridges by early Cambrian Archaeocyatha (Markova, 1975; Hanžl and Aichler, 2007). In our study area, these rocks also differ from the type section in the Khantaishir Ridge in their higher degree of metamorphism. The Tsakhir Uul formation essentially consists of marble, enclosing up to hundred m thick layers (tectonic lenses?) of eclogite and metapelite in the north. The central part of the unit is composed of a NE-SW trending belt of metagabbro, whereas the southern part is dominated by marble and metapelite. The eclogites contain a peak metamorphic assemblage of omphacite, garnet, barroisite, zoisite and phengite. The occurrence of garnet and chloritoid in the metapelites indicates that the metasediments also reached HP conditions. However, there are some metabasites which show only amphibolite-facies mineral assemblages, indicating that the unit did not reach eclogites-facies conditions as a whole. The metamorphic assemblages related to amphibolite-facies retrogression in the eclogites are associated with late shear zones and a late metamorphic fabric in the metapelites.

The uppermost assemblage of the Lake Zone is represented by clastic sequences distinguished as the Naran formation of presumed early and middle Cambrian age (Rauzer and others, 1987; Ruzhentsev and Burashnikov, 1996; Hanžl and Aichler, 2007). In the NW part of the transect, the Naran formation is represented by low-grade volcanic-derived shales dominated by muscovite and chlorite, silicate-rich sediments, metarhyolites, metaconglomerates and minor metabasalts which attest to lower greenschist-facies metamorphism (Markova, 1975; Rauzer and others, 1987; Hanžl and Aichler, 2007). Turbidites consisting of alternating sandstone and siltstone are similar to those described at the southern slope of the Khantaishir Ridge in the Naran zone. However in the studied section, these sediments do not contain fossils, and a Cambrian age was assumed on the basis of their stratigraphic position and lateral correlation with rocks of the Khantaishir Ridge. A small outlier of supposedly Devonian sandstone and conglomerate (fig. 4A) suggests a fluviatile depositional environment (Rauzer and others, 1987). On the southwestern foothill of the Zamtyn Range, a volcaniclastic formation of bimodal volcanic rocks and volcaniclastic sediments was dated as Permian (Hanžl and Aichler, 2007). The geochemistry of these rocks indicates a within-plate setting, and granites as well as rhyolites show an evolution from volcanic arc to within-plate settings (Hanžl and Aichler, 2007).

LITHOSTRATIGRAPHY OF THE GOBI-ALTAI ZONE (FIG. 4B)

Northern Slope of the Gichgene Ridge (Fig. 2)

The oldest lithostratigraphic unit of this zone is best developed in the Tsogt area along the valley of the Tugrig River (figs. 2 and 4B). Here, the lowermost part of the succession is composed of quartz-chlorite-schist, siliceous thinly laminated rocks, strongly altered metabasalt, epidote-actinolite-schist and massive diabase porphyry (fig. 4B). The intermediate part of the succession is composed of variably schistose clastic rocks and altered black to dark gray siltstones and schists. The lower and intermediate parts of this metamorphic succession constitute the so-called Tugrig formation of presumed early to middle Cambrian age. The uppermost part of this sequence is attributed by some authors to the late Cambrian–early Ordovician (Rauzer and others, 1987) Uhaanuruu formation which consists of felsic volcanic rocks as well as volcano-sedimentary, tuffaceous and clastic rocks with layers of limestone at the top. The uncertain stratigraphic position is due to a lack of reliable ages, both paleontological and isotopic. Even a Silurian age was proposed for the Tugrig formation which resulted from correlation with similar strata exposed east of our study area near Bayanleg (fig. 4B) where early Silurian tabulate corals, bryozoans and crinoids were found (Markova, 1975).

Rocks of the Tugrig formation are overlain by a sequence of sandstones, siltstones and graded conglomerates that is correlated with the paleontologically dated Ordovician Bayantsagaan formation farther east (brachiopods, trilobites and crinoids, Hanžl and Aichler, 2007). These sediments underwent very low grade metamorphism so that they often have the appearance of chlorite-sericite slates. The original contact with the Tugrig formation is obliterated by active faults but appears to be unconformable due to differences in deformation intensity and the degree of metamorphism. Early Devonian sediments unconformably overlie the medium-grade rocks of the Tugrig formation or volcaniclastic sediments of the Bayantsagaan formation. The Devonian rocks of the Takhit, Duchindavaa and Togoot formations essentially consist of mica-rich sandstones and siltstones which are intercalated with basal porphyries, tuffs and basaltic pillow lavas as well as large bodies of rugosa corals and crinoidea-bearing reef limestones, indicating early and middle Devonian depositional ages (Markova, 1975).

In our study area, the rocks exposed along the northern slope of the Gichgene Ridge, south of Chandman, are interpreted as a lateral continuation of the Tugrig

A.

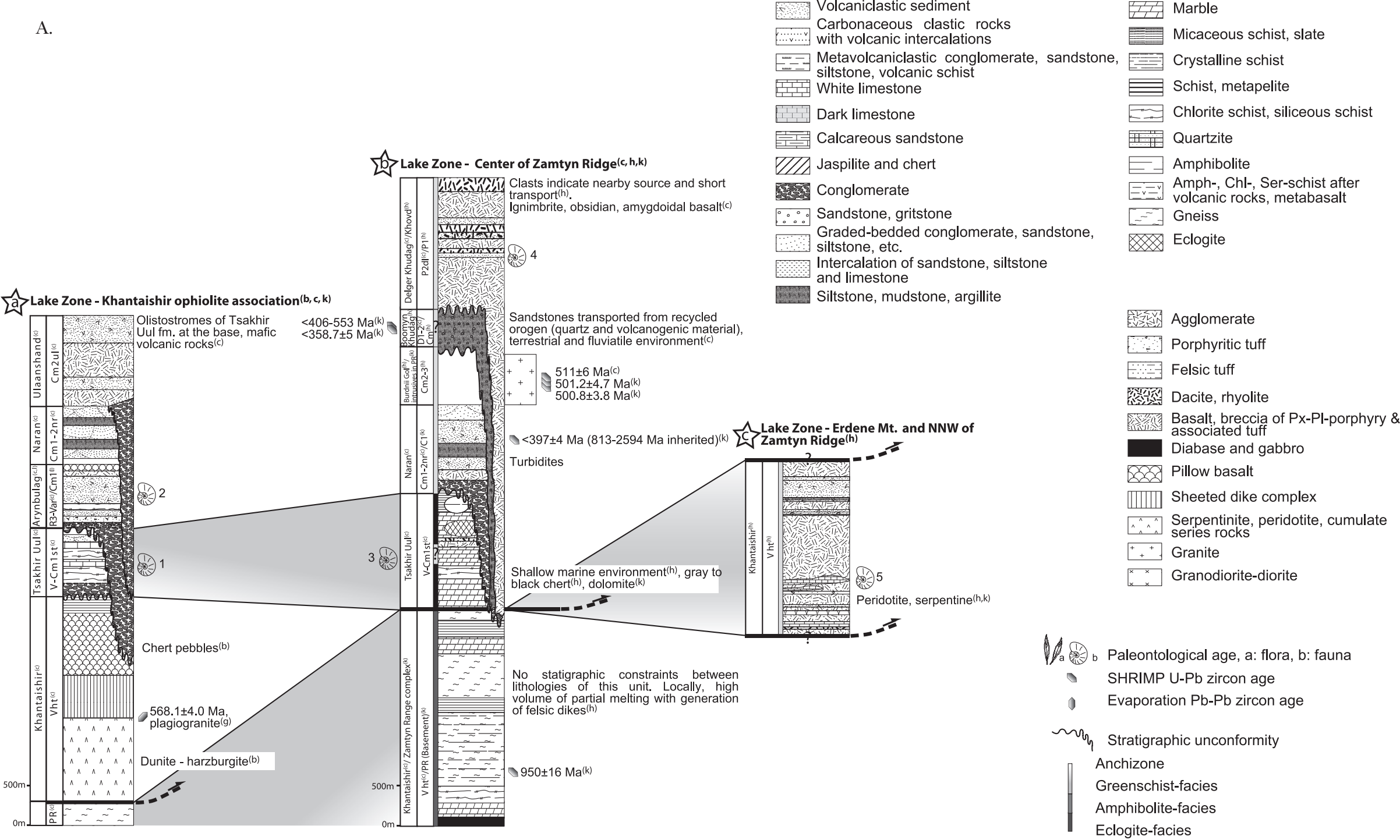

Fig. 4A. Stratigraphic columns for Lake Zone.

B.

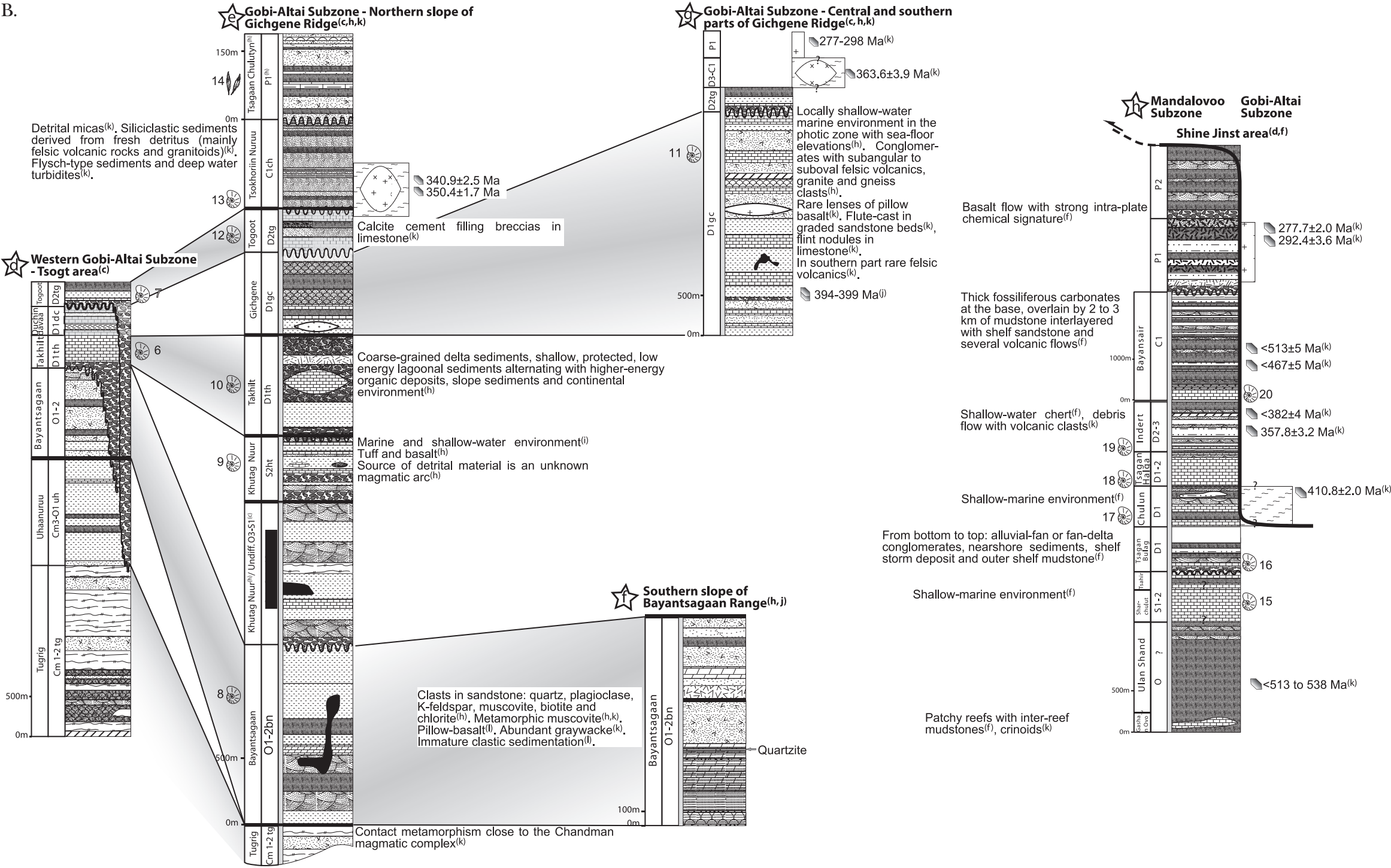

Fig. 4B. Stratigraphic columns for Gobi-Altai Zone.

C.

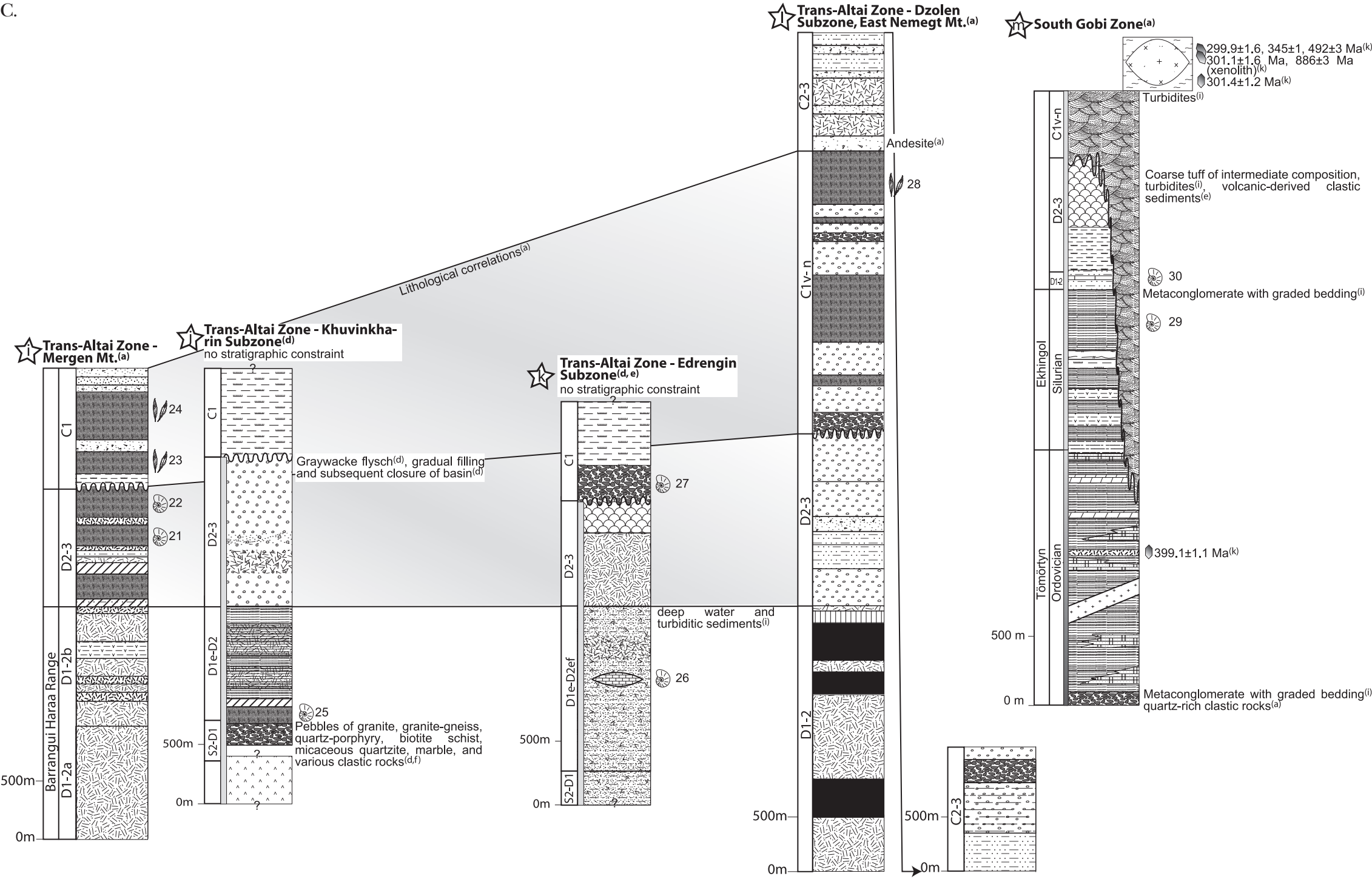

Fig. 4C. Stratigraphic columns for Trans-Altai and South Gobi Zones.

formation (figs. 2 and 3). These metamorphic rocks are mainly paragneisses, amphibolites and quartz-rich metapelites which contain a garnet-sillimanite-biotite peak metamorphic assemblage in the northern central parts of the section. To the south, the metapelites contain an andalusite-muscovite-biotite mineral assemblage in a wide belt bordering a domal structure of granitoid gneisses. Amphibolite lenses are interpreted as metamorphosed volcanic rocks (Hanžl and Aichler, 2007).

The andalusite-biotite schists are unconformably overlain by a thick sedimentary-volcanic sequence of the early-middle Ordovician Bayantsagaan formation containing calc-alkaline dacitic to rhyolitic volcanic rocks and tholeiitic basalt (Hanžl and Aichler, 2007) and well dated as Arenig to Llanvirn by brachiopods, trilobites and gastropods (Markova, 1975). This succession is followed by a thick sequence of fossil-free tuffaceous sediments, siltstones and rare limestones of probable late Ordovician or Silurian age. The structurally overlying Khutag Nuur formation is paleontologically dated as Ludlow to Wenlock (Markova, 1975; Hanžl and Aichler, 2007) and, in turn, is overlain by thick early Devonian coral-rich limestones (Markova, 1975). A large tectonic slice of the Tsokhoriin Nuruu formation containing siliclastic sediments is dated as early Carboniferous. Markova (1975) interpreted this sequence to have been deposited in intramontane basins. The structurally deepest rocks exposed in the vicinity of Chandman village in the Gobi-Altai Zone are represented by granites with dioritic enclaves,

Fig. 4. Stratigraphic columns for the study area. (A) Lake Zone, (B) Gobi-Altai Zone, (C) Trans-Altai and South Gobi Zones. Stars enclosing letters on top of each column refer to location indicated in fig. 2. Modified from a)—Markova (1975), b)—Zonenshain and Kuzmin (1978), c)—Rauzer and others (1987), d)—Ruzhentsev and Pospelov (1992), e)—Ruzhentsev (2001), f)—Lamb and Badarch (1997), g)—Gibsher and others (2001), h)—Hanžl and Aichler (2007), i)—Hanžl and Krejči (2008), j)—Demoux and others (2009a), k)—this study, l)—Ruzhentsev and Burashnikov (1996).

Sources of paleontological data: (1)—Oncolites, algae and archaeocyatha (Markova, 1975). (2)—Photoconodonts, anabaritids, chiolites and molluscs (Ruzhentsev and Burashnikov, 1996). (3)—Archaeocyatha, stromatolites, microbialites (Hanžl and Aichler, 2007). (4)—*Rufloria* sp. (Hanžl and Aichler, 2007). (5)—Oncoliths: *Ambigolamellatus horrida, Osagia nimia* (Hanžl and Aichler, 2007). (6)—Tabulata: *Favosites kovechovi, Squameofavosites* sp.; Bryozoa: *Fistulipora* sp. (Marvoka, 1975). (7)—Tabulata: *Favosites multiformis, Riphaeolites ramosus* sp., etc (Marvoka, 1975). (8)—Brachipods: *Orthidiella* sp., *Productorthis* sp., *Orthambonites* sp. and *Strophomenida* div. sp.; Trilobites: *Asaphidae* indet.; Crinoids: *Iocrinus* sp. and *Ramseyocrinus* sp. (Hanžl and Aichler, 2007). (9)—*Lykophyllina* indet.; Tabulata: *Favosites lichernarioides., Favosites* sp.; Amphiporida indet.; Stromatoporoida indet.; Crinoids: *Cyclomischus* sp., *Baryschir* sp. (Hanžl and Aichler, 2007). (10)—Crinoids: *Asperocrinus* sp., *Trybliocrinus* sp., *Mediocrinus* sp., *Salairocrinus* sp., *Pentamerostella* sp., *Mydodactylus* sp., *Pandocrinus* sp.; Corals and stromatoporoids: *Sutherlandinia* sp., *Rugosa* indet., *Parastriatopora* sp., *Cladochonus* sp., *Syringoporida* indet., and *Laccophyllum;* Gastropods: *Orthonychia* sp., *Cyrtocyclonema* sp.; Brachiopods: *Cymostrophia* sp.; Trilobites: *Gerastos* sp., *Crotalocephalina* aff. *Cordai;* Nautiloids: *Kopaninoceras* sp.; Dacryoconarid tentaculites: *Guerichina* sp. (Hanžl and Aichler, 2007). (11)—Crinoids: *Trybliocrinus* sp., *Mediocrinus* sp., *Salairocrinus* sp., *Cyclocaudex* sp.; Brachiopods: *Atrypa* sp., *Leptaenopyxis* sp., *Sieberella* sp., *Athyridae* indet., *Rhynchonellidae* indet.; Corals: *Cladopora* sp., *Favosites* div sp. and *Thamnopora, Lecomptia* sp. (Hanžl and Aichler, 2007). (12)—Crinoids: *Pentacauliscus* sp., *Cyclocaudex* sp. and *Melocrinites* sp.; Dracryoconarid tentaculites: *Viriatelina sp.* and *Styliolina* sp. (Hanžl and Aichler, 2007). (13)—Brachiopods, crinoids and lepidophytes (Rauzer and others, 1987). Crinoids: *Cyclocaudiculus* sp.; Ichnofossils: *Dictyodora liebeana.* (Hanžl and Aichler, 2007). (14)—Cordaites: *Rufloria* cf. *derzavinii* and *Rufloria* sp (Hanžl and Aichler, 2007). (15)—Tabulate and rugose corals, brachiopods (Menner and others, 1981; Sharkova, 1986; Rozman and Minzhin, 1988; Minzhin and others, 1993). (16)—Limestone corals of Ordovician to earliest Devonian (Alekseyeva, 1981; 1993). (17)—Tabulate corals, rugose corals, stromatoporoid and algae (Sharkova, 1986). (18)—Crinoids and Bryozoans (Alekseyeva, 1981; 1993). (19)—Brachiopods, conodonts, tabulate corals and radiolarians (Koneva, 1990; Lazarev and Suur'suren, 1992; Nyamsuren and Badarch, 1994). (20)—Unspecified brachiopods (Afanas'yeva, 1992; Lazarev and Suur'suren, 1992). (21)—Brachiopods: *Isorthis sibirica, Lamellispirifer mucronatus,* Atrypa *vandae;* Crinoids: *Dactilocrinus* cf. *spiniferus* (Marvoka, 1975). (22)—*Spinatrypa* exgr. *Bachatiensis* (Marvoka, 1975). (23)—*Archaeocalamites* sp. (Marvoka, 1975). (24)—*Angarodendron* vel., *Caenodendron* sp., *Knorria* sp., *Arcaheocalamites* sp., *Sphenopteris* sp., *Adiantities* sp., *Angaropteridium* sp., *Cardioneura* sp., *Cordaites* sp., *Carpolitus* sp. (Marvoka, 1975). (25)—Conodonts: *Pandorinellina steinhornensis, Polygnathus inversus,* "*Hindeodella*" sp. (Rhuzentsev, 2001). (26)—Brachiopods: *Brachyspirifer* sp., *Multispirifer* sp., (Ruzhentsev, 2001). (27)—Bryozoans, rugose corals, crinoids and brachiopods (Suyetenko and others, 1988). (28)—Not specified—(Marvoka, 1975). (29)—*Tentaculites sp.* Indet. (Marvoka, 1975). (30)—Tabulata: *Favosites archaensis;* Brachiopods: *Aulacella* sp., *Gladiostrophia* sp., *Leptagonia* sp., *Delthyris* sp. (Ruzhentsev, 2001).

diorites, and xenoliths of migmatitic amphibolitic gneisses and migmatites (fig. 3). Zircons from one of the granites were dated at 345 ± 2 Ma (Hrdličková and others, 2008). Locally, the granites and granodiorites were converted to orthogneiss and cut by granite veins and dikes that are locally folded and foliated. These observations indicate that magmatic activity and gneissification were synchronous processes. The orthogneisses and plutonic rocks have calc-alkaline compositions with trace element patterns of volcanic arc and within-plate granites (Hanžl and Aichler, 2007; Economos and others, 2008). This magmatic complex shows an intrusive contact with sillimanite- and andalusite-bearing schists of the Tugrig formation.

Southern Slope of the Gichgene Ridge (Fig. 2)

The second area of interest constitutes the core of the Tseel metamorphic "terrane" of Badarch and others (2002), south of Erdene village (fig. 3). The southernmost part of the Gichgene Ridge is formed by a pink granophyric granite-gneiss that is locally converted to greenschist-facies mylonite. Farther north, metamorphosed rocks are represented by amphibole-rich gneisses, felsic gneisses, as well as paragneisses with garnet and pyroxenite boudins, embedded in garnet-andalusite-bearing metapelites. To the north of these high-grade rocks occur low-grade metasediments rich in felsic volcanic rocks of presumed Neoproterozoic (Vendian) age (Rauzer and others, 1987; Tomurtogoo, 1998). Farther north occurs the above described early to middle Devonian sedimentary basin made up of siltstones, shales and numerous paleontologically dated reef limestones (fig. 4B) that, according to Rauzer and others (1987), are intruded by Devonian and Permian granites. Early Devonian metabasalts and felsic metavolcanic rocks show chemical and isotopic compositions at the transition between back-arc and arc settings (Demoux and others, 2009a).

Located in the Gobi-Altai Zone, some 10 km north of Shine Jinst village (fig. 2), a metamorphic basement unit of ~600 km^2 is considered to be of early Devonian age (Rauzer and others, 1987). The dominant lithology is represented by garnet-bearing migmatitic gneisses, amphibolitic gneisses, migmatitic gabbros, paragneisses and tonalites. Locally pink subvolcanic granites occur in association with other high-grade rocks. The southern boundary of this unit exposes mafic and granitoid intrusive rocks of Permian age as well as intraformational felsic volcanic rocks and volcaniclastic sediments of paleontologically determined Permian age (flora in Badarch, 1982), interpreted as an intracontinental basin (Lamb and Badarch, 1997). A thrust contact between the high-grade unit and these late Paleozoic sequences was locally observed.

The adjacent sedimentary sequence of the Mandalovoo Subzone (redefined as terrane by Badarch and others, 2002) was described in detail by Lamb and Badarch (1997), and we only provide a brief description based on their lithostratigraphic column and presented in figure 4B. The section begins with paleontologically undetermined but assumed Ordovician slates of the Ulan Shand formation. The overlying Silurian formations contain fossiliferous carbonate lenses (Menner and others, 1981; Sharkova, 1986; Rozman and Minzhin, 1988; Minzhin and others, 1993). The overlying early Devonian Tsagan Bulag formation contains basal conglomerates with clasts of limestone corals of Ordovician to earliest Devonian age (Alekseyeva, 1981, 1993), and these rocks evolve into sandstones and gritstones in the middle part of the section. The hanging wall fossiliferous shallow-marine Chulun formation was paleontologically dated (Sharkova, 1986) and is followed by early to middle Devonian crinoidea- and bryozoan-bearing reef limestones of the Tsagan Halga formation (Alekseyeva, 1981, 1993). Finally, middle to late Devonian volcaniclastic sandstones, siltstones and argillites of the Indert formation contain volcanic flows and tuffs of basaltic to rhyolitic composition. Detailed sedimentological analysis of Lamb and Badarch (1997) shows that the Shine Jinst Devonian and Carboniferous section records a marginal marine setting with periodic input from proximal volcanic centers. In addition, major and

trace element data for Devonian basalts suggest that these rocks correspond to volcanic arc basalts and were produced within a mature island arc or an arc forming on the outermost edge of a continent (Lamb and Badarch, 2001).

A fragment of granodiorite of unknown age separates the Permian basin from the Devonian carbonates, interpreted as the southern boundary of the Gobi-Altai "terrane" (Badarch and others, 2002). In this way, the thick Ordovician to Carboniferous sequence is considered to correspond to the western termination of the Mandalovoo Subzone (Badarch and others, 2002; see fig. 4B).

lithostratigraphy of the trans-altai zone (fig. 4c)

The northern part of the Trans-Altai Gobi Desert, located south of the Trans-Altai fault and north of the Gobi-Tienshan fault zone, was divided into a variety of zones and terranes by different authors: from north to south, this area is known as the Edrengin and Trans-Altai zones (Ruzhentsev and Pospelov, 1992), Edren, Baaran, Zoolen and Baytag terranes (Badarch and others, 2002) or Trans-Altai, Ajbogd and Gobian terranes (Tomurtogoo, 1997). We use the nomenclature and most of the lithostratigraphic sections of Ruzhentsev and Pospelov (1992) and some lithostratigraphic sections of Markova (1975) for comparison. We modify the zonation of Ruzhentsev (2001) and distinguish from north to south the Khuvinkharin, Edrengin and Dzolen Subzones or ridges. This large area (fig. 3) consists of the following lithostratigraphic sequences.

The oldest rocks are confined to the Trans-Altai fault and serve as a boundary between the Gobi-Altai and Trans-Altai Zones. The section mainly consists of clastic rocks made up of coarse-grained sediments in the lower part and sandstone, shale, tuffite and siliceous sinter and chert in the upper part (fig. 4C). The age of this sequence is early Devonian (Ruzhentsev and others, 1985; Suyetenko and others, 1988; Ruzhentsev and Pospelov, 1992). Devonian rocks are widely distributed in this area and were studied in the Khuvinkharin and Edrengin Ridges (fig. 2) where two different sections were distinguished (Ruzhentsev and Pospelov, 1992; Ruzhentsev, 2001). The northern section is exposed in the region of the Khuvinkharin Ridge where the Devonian consists of conglomerates with boulders of granite, quartz-porphyry, micaceous quartzite, gritstone and marble, which pass upwards into strata composed of intercalations of clay-rich siliceous shale, serpentinite, jasper and sheets of basalt flows (fig. 4C). A serpentinite mélange was locally recorded and is considered to represent the lowest part of the section (Ruzhentsev, 2001). The entire sequence ends with homogeneous middle to late Devonian graywacke flysch, up to 2000 m thick. Intermediate mafic volcanic rocks belong to a weakly differentiated low-Ti series which is ascribed to a back-arc basin environment (Ruzhentsev and Pospelov, 1992; Yarmolyuk and others, 2008c). The Devonian section of this zone is generally strongly deformed.

The southern section occurs along the Edrengin Ridge (fig. 4C) and is dominated by volcano-sedimentary sequences. These rocks consist of tuff, tuffite, and tuff-sandstone which contain lenses of limestone with Emsian brachiopods in the lower part (Ruzhentsev and others, 1985) as well as massive dacite, andesite and basaltic pillow lava with rare tuff in the upper part. The chemical composition of the sub-alkaline volcanic rocks is interpreted as reflecting an island-arc series (Ruzhentsev and Pospelov, 1992; Lamb and Badarch, 2001; Yarmolyuk and others, 2008c).

The Devonian rocks display important lateral variations so that in the west (Baruun Huurai area, Mergen Mountain, fig. 4C), the early Devonian is represented by a 3000 m thick sequence of mafic to intermediate volcanic rocks of marine environment, locally with fossils of Givetian and Frasnian age (Markova, 1975). The upper part grades into more felsic volcanic rocks associated with tuffaceous graywacke (Markova, 1975). Calc-alkaline granites of early Carboniferous age (Hanžl and others, 2008; Yarmolyuk and others, 2008b) are exposed in the SE part of this ridge. A similar

section is described to the east in the area of the Nemegt Mountain (fig. 4C) where the early Devonian is represented by a 2000 m thick volcanic sequence of basaltic tuff, porphyry and a gabbro sheet, progressively passing into a 1400 m thick middle Devonian rhyodacite sequence (Markova, 1975). Helo and others (2006) demonstrated that the geochemistry of Devonian volcanic rocks from the Nemegt Mountain exhibit both calc-alkaline, LREE-enriched island arc and tholeiitic LREE-depleted back-arc basin signatures of predominantly juvenile composition.

Ruzhentsev and others (1991) provided detailed lithological sections through the Trans-Altai Gobi Desert and suggested that the oldest rocks of this domain are found along the southern slope of the Dzolen Ridge (just east of fig. 2). Here a range of strongly serpentinized peridotite fragments occur, locally accompanied by gabbro, pillow lava and corresponding basaltic tuff. Radiolarian bedded jasper of Silurian–early Devonian age, sponges and quartz-hematite rocks are common (Zonenshain and others, 1975; Ruzhentsev and others, 1985). These fragments of oceanic lithosphere (fig. 4C) are interpreted to correspond to the eastern termination of the Dzolen "terrane" (Badarch and others, 2002), whereas Ruzhentsev and others (1991) interpreted them as the oldest rocks in the Silurian-Devonian oceanic Trans-Altai Zone. These authors also described several sections from the Gurvansaykhan Range, starting with jasper beds 200 to 300 m thick and followed by a thick volcanic sequence of tholeiitic basalt, epiclastic and tuffaceous material and basalt-andesite volcanic rocks. This sequence is overlain by middle Devonian clastic sediments. Helo and others (2006) have shown that the Devonian volcanics from the Gurvansaykhan and Dzolen Ranges exhibit intermediate, calc-alkaline compositions marked by LREE enrichment and high initial ϵ_{Nd}–values that are consistent with a juvenile intra-oceanic arc. Some rocks reveal features similar to adakites and high-Mg andesites that possibly evolved in a forearc environment. These authors also reported SHRIMP zircon ages of 421 ± 3.0 Ma and 417 ± 2.2 Ma, confirming an early Devonian age of volcanic activity.

The Devonian sequence is overlain unconformably by early Carboniferous volcanic and tuffaceous strata with a thick basal conglomerate where the calcareous cement contains brachiopods, trilobites and gastropods of Tournaisian age (Suyetenko and others, 1988). At other localities, the Devonian is covered by a thick clastic sequence (sandstones, conglomerates, shales and some tuffs) of early Carboniferous (Viseen-Namurian) age as shown by several flora findings (Markova, 1975). The Carboniferous strata consist of basalt, andesitic basalt, and andesite as well as corresponding tuff, tuff-sandstone, tuff-siltstone, and tuff-conglomerate. These rocks show lateral lithological variations which are expressed by a decrease in volcanic material and an increase in volcano-sedimentary rocks eastwards.

The thickness of the Lower Carboniferous is highly variable and ranges from 1000 m in the west to 2400 m in the east. However, the Upper Carboniferous is rather homogeneous both in facies and thickness, dominated by felsic and intermediate products of subareal volcanism of andesitic composition. The lower part of a 1000 to 1200 m thick sequence is composed of andesitic lava flows and agglomeratic tuff, whereas the upper part, also ~1000 m thick, is represented by a volcano-sedimentary sequence dominated by volcanic-derived sandstone, tuffite and tuff (Markova, 1975).

Lithostratigraphy of the South Gobi Zone (fig. 4C)

The South Gobi Zone (Ruzhentsev, 2001) or Atasbogd "terrane" (Badarch and others, 2002) occupies the southernmost part of the study transect and is separated from the northern part of the Trans-Altai Gobi by the E-W striking Gobi-Tienshan fault (fig. 3). The area exposes variably metamorphosed rocks ranging in age from presumed Ordovician to Carboniferous. These rocks occur in ridges that are juxtaposed against young intermontane basins filled with Mesozoic and Cenozoic sediments.

The oldest rocks are represented by a presumed Ordovician sequence (Tömörtyn formation of Sinitsyn, 1956; Markova, 1975) composed of siliceous clastic rocks, quartzite, sandstone, gritstone and conglomerate with coarse-grained sediments mainly occurring in the lower part (fig. 4C). These are conformably overlain by metamorphosed rocks consisting of amphibolite, amphibolite schist and hornfels, interlayered with gray-green chlorite or sericite-chlorite schists. The schists were assigned to the Silurian by Sinitsyn (1956) and Markova (1975). Although these authors suggested that the Ordovician and Silurian rocks constitute a conformable sequence showing both temporal and spatial relationships, the presumed Ordovician and Silurian ages were not well documented, and only some tentaculites found in the upper, clastic part of the succession indicate a Silurian age (Markova, 1975). The younger age limit of the above succession is defined by well dated hanging-wall Devonian strata.

The early Devonian is mainly represented by volcanic, volcano-sedimentary and sedimentary rocks with lenses and beds of limestone and quartzite (fig. 4C). Coarse-grained sediments represented by graywacke with graded bedding and conglomerates occur in the upper part of the sequence. The limestones contain fossils of early Devonian age (Šourek and others, 2003) and volcanic rocks are mostly represented by basaltic pillow lavas. The middle Devonian consists of black-gray, graded-bedded, slaty metamudstone, metasandstone and calc-silicate rocks.

All these early Paleozoic rocks are unconformably overlain by ~1000 m thick early Carboniferous sediments containing a brownish-gray conglomerate in the lower part ascribed to the Visean (fig. 4C). The Carboniferous rocks constitute the most widely developed lithologies in this area. Unclassified Carboniferous strata are represented by tuffaceous sandstone with graded bedding and thin layers of mudstone and conglomerate, and volcanic rocks of basalt, andesite, dacite and rhyolite compositions. These strata are ascribed to the Lower and Middle (or Middle-Upper) Carboniferous (fig. 4C). The Upper Carboniferous sequences are represented by tholeiitic basalt flows and hyaloclastites, followed by clastic sediments containing biogenic limestones and sandstones.

The structurally lowest unit is represented by the E-W trending Gobi-Tienshan magmatic complex, covering an area of about 3000 km^2 and described by Badarch and others (2002) as part of their Atasbogd "terrane." A late Carboniferous emplacement age of 302 ± 3 Ma was recently determined for a granodiorite of this batholith (Yarmolyuk and others, 2008b). The host rocks in the Tömörtyn zone, NE of the Gobi-Tienshan magmatic complex, consist of metapelites, metavolcanic rocks, marbles, paragneisses and amphibolite gneisses of presumed Ordovician to early Silurian age which are bounded, in the north, by the up to 500 m wide active Gobi-Tienshan fault. Peak metamorphic conditions are inferred from the presence of migmatitic melts showing hornblende- and plagioclase-rich leucosomes in gneisses which constitute the structurally lowest part of the magmatic complex. Towards the SE the gneisses pass into the main batholith which is composed of gabbro, granodiorite and granite. The predominant magmatic rock is a coarse-grained granodiorite composed of plagioclase, biotite, hornblende ± clinopyroxene ± titanite and containing numerous dioritic xenoliths. The granodiorite commonly alternates with sheets of biotite-bearing quartzitic hornfels. A progressive transition exists from the main granodiorite in the core of the pluton to schlieren-bearing, porphyric quartz-rich pink granite on the southeastern margin. Locally, rare leucocratic veins and foliated orthogneiss xenoliths were observed. To the SE, a granophyric pink granite intruded into shallow crustal levels as shown by spotted Devonian slates and Carboniferous volcaniclastic sediments. The entire structure of the Gobi-Tienshan plutonic complex with high-grade metamorphic rocks at the bottom, a mafic lower part of the magma chamber, a granodioritic core and a subsurface granophyric granite intruding weakly metamorphosed Devonian

sediments at the top indicates an increasing structural depth towards the NW in this huge magmatic complex.

LITHOSTRATIGRAPHIC CORRELATIONS AND PALEOGEOGRAPHIC IMPLICATIONS

An attempt is made here to demonstrate lithostratigraphic correlations within our study area and to present a preliminary paleogeographic model in which our samples are positioned. The Ordovician and Silurian deposits of the Gobi-Altai Zone were traditionally interpreted to have developed along the southern edge of the Mongolian continent (for example, Zaitsev and others, 1970; Zonenshain, 1973). According to early Russian studies the Ordovician sequences in the South Gobi Zone reflect a similar evolution, that is, a continental margin clastic sedimentation. This model was slightly modified by Lamb and Badarch (1997, 2001) who proposed evolution of the Ordovician sediments along the southern edge of an E-W trending sliver of continental crust or the remnant of an older island arc complex represented by the Ulaan Shand formation of the Lake Zone and the lower part of the Tugrig formation in the Gobi-Altai Zone. The Ordovician-Silurian sediments are undoubtedly ocean margin deposits, mainly proximal with a small component of bimodal effusives. The structuraly deepest formations are early Devonian deep marine deposits in the Trans-Altai Zone represented by radiolarian-bearing cherts unconformably overlying a serpentinite–gabbro mélange (Eengin, 1978; Ruzhentsev and Pospelov, 1992; Ruzhentsev, 2001). These sequences were interpreted as deep oceanic sediments by several authors (for example, Suyetenko, 1973; Zonenshain and others, 1975) and represent the axis of the South Mongolian oceanic basin (Zonenshain, 1973). Ordovican and Silurian deposits of the South Gobi Zone were regarded by earlier Russian authors (for example, Zaitsev and others, 1970; Zonenshain, 1973) as typical pericontinental sediments, similar to those described from the Gobi-Altai Zone.

Devonian and early Carboniferous deposits show significantly higher variability across the N-S and E-W sections (Ruzhentsev and Pospelov, 1992; Lamb and Badarch, 1997, 2001; Ruzhentsev, 2001). Traditionally, the Gobi-Altai Zone sequences are interpreted as typical passive margin deposits (for example, Zaitsev and others, 1970). However, modern studies of the Mandalovoo Subzone (Shine Jinst section) suggest nearshore to neritic conditions and deposition in a volcanic-arc setting due to proximal volcanic deposits known from the Chuluun and Indert formations (Lamb and Badarch, 1997). Devonian sequences (fossiliferous reef limestones) on the northern slope of the Gichgene Ridge indicate shallow marine conditions whereas pillow lavas and felsic volcanic rocks in the lower part of the section suggest opening of an intra-arc or backarc basin in this area (Demoux and others, 2009a). The lower Devonian oceanic rocks of the Trans-Altai Zone are locally covered by early Devonian intra-oceanic arc and back-arc volcanic rocks (Zonenshain and others, 1975; Lamb and Badarch, 2001; Helo and others, 2006). The middle to late Devonian volcanosedimentary deposits show north-south zoning which was interpreted in terms of a back-arc located to the north, an arc in the center and a forearc basin in the south (Lamb and Badarch, 1997). Middle-late Carboniferous deposits are generally seen as reflecting widespread volcanic arc activity affecting the Trans-Altai Zone in SW Mongolia (Markova, 1975). Devonian and Carboniferous deposits of the South Gobi Zone reflect shallow marine conditions and led some authors to propose the existence of a South Mongolian continental ribbon (for example Zonenshain, 1967; Zaitsev and others, 1970).

SUMMARY OF STRUCTURAL EVOLUTION

Deformational features and metamorphic fabrics were used by Lehmann and others (2010) to better constrain unconformities and the timing of several tectonic events. The earliest structures occur in the Lake Zone and are related to the

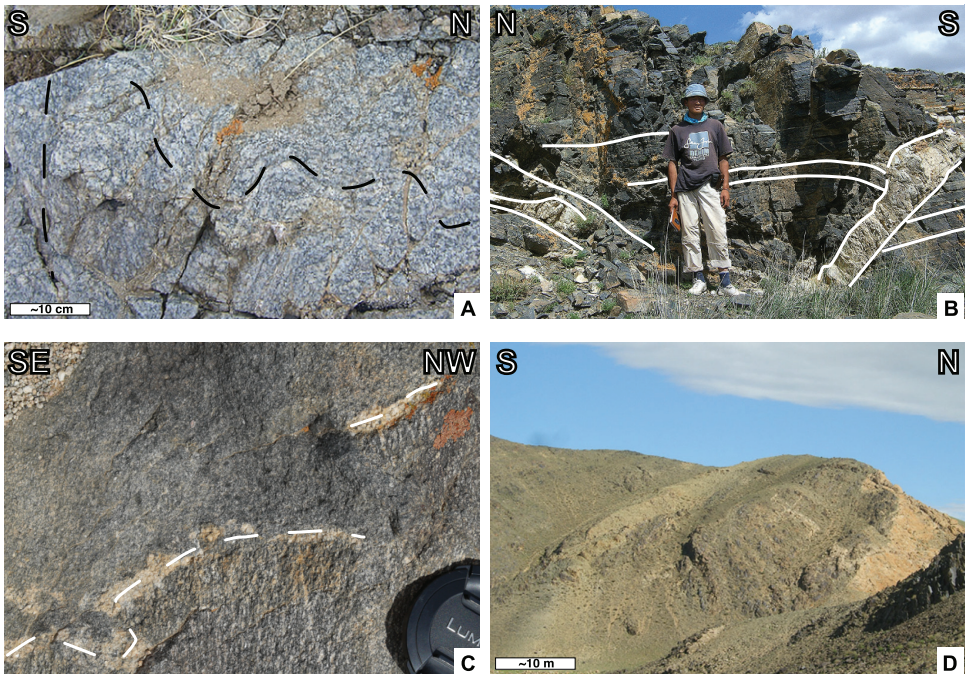

Fig. 5. Field photographs of selected dated rocks. (A) Folding of metamorphic foliation in orthogneiss of Zamtyn Range basement (sample M523JC); (B) horizontal metamorphic fabric in banded amphibolite of Zamtyn Range basement cut by granitic dikes (sample M150/06-3); (C) intrusive contact (dashed white line) between microgranite and granite-gneiss (sample M107/06-2) on Chandman Mountain; (D) Permian leucogranite (sample M83/06) near Erdene village.

emplacement of the Tsakhir Uul and Khantaishir ophiolite nappes over the Meso- to early Neoproterozoic basement of the Dzabkhan microcontinent. These structures are represented by a phengite-bearing foliation in eclogites and high pressure fabrics in associated metapelites and were dated by the ^{40}Ar-^{39}Ar method at 540 Ma (Lehmann and others, 2010). These cooling ages thus bracket ophiolite thrusting over the continental basement. The Lake Zone basement reveals a polyphase structural evolution with an early steep metamorphic fabric that was reworked by a second amphibolite-facies foliation (fig. 5A) that is crosscut by granite dikes which were dated in this study using the U-Pb method (fig. 5B; sample M150/06-3).

The Gobi-Altai Zone reveals a complex and polyphase structural evolution. The structurally oldest, possibly Cambrian, Tugrig formation shows a dominant flat greenschist-facies fabric which was superposed over poorly preserved earlier structures. The age of this fabric could not be determined by isotopic methods but is older than the unconformably overlying early Ordovician Bayantsagaan formation. These rocks are unconformably overlain by Devonian sediments (Markova, 1975; Lehmann and others, 2010). The entire sequence was affected by deformation associated with the exhumation of metamorphic and magmatic domes on both the northern and southern Gichgene Ridges in the late Devonian to early Carboniferous. This E-W oriented compression generated crustal-scale, N-S trending steep folds with gneissic and granitic cores marked by a strong magmatic fabric that passes into solid state deformation, thus suggesting syntectonic emplacement of magmatic complexes during deformation (fig. 5C). The development of early Carboniferous intramontane basins is most likely related to this event. Both Lake and Gobi-Altai Zones are affected by a strong and

steeply dipping lower greenschist-facies cleavage and folding of late Permian to Triassic age (Lamb and others, 2008; Lehmann and others, 2010). Early Permian granites which were mostly emplaced through passive mechanisms (fig. 5D) were either entirely reworked by this cleavage or represent rigid bodies around which the cleavage fronts are deflected.

The earliest deformation in the Trans-Altai Zone is preserved in strongly sheared serpentinites, ophicalcites, gabbros and early Devonian cherts, but this deformation is not developed in Devonian rocks (Ruzhentsev and Pospelov, 1992 and our own observations). However, the ultramafic rocks are imbricated with early to middle Devonian rocks and thrust over them at several localities in the form of thin thrust sheets and nappes (for example, Zonenshain and others, 1975). Detailed structural analysis of Lehmann and others (2010) has shown that thrusting was associated with gentle N-S trending folds that also affected early Carboniferous strata. However, the Permian volcanic rocks are not affected by this deformation so that the shortening event can be placed in the middle-late Carboniferous. The Trans-Altai Zone was also affected by intense late Permian to late Triassic folding and steep E-W trending cleavage development.

The South Gobi Zone reveals three principal deformation events. The first affected Ordovician and Silurian rocks of the Tömörtyn group and is represented by an originally sub-horizontal greenschist-facies fabric. The early Devonian rocks also reveal a metamorphic fabric, but its age and relationship to that affecting the Tömörtyn group remain uncertain. The second major deformation is related to WNW-ESE compression which produced a steep metamorphic foliation in high-grade orthogneiss, migmatite and granodiorite of the Gobi-Tienshan arc pluton. This fabric is undoubtedly of late Carboniferous age as shown by our zircon ages. The final deformation is represented by an intense ENE-WSW trending cleavage front surrounding the pluton and steep folds refolding all sequences, including early Carboniferous sediments and volcanic rocks. The age of this fabric is not well constrained but is certainly post-Permian and probably early Triassic as indicated by the ^{40}Ar-^{39}Ar cooling age for a gneiss sample from the northern deformation front of the pluton (Lehmann and others, 2010).

SAMPLE DESCRIPTIONS AND GEOCHRONOLOGY

Single zircons were dated from selected samples using SHRIMP II instruments at the Beijing SHRIMP Center, Chinese Academy of Geological Sciences, and the John de Laeter Center for Mass Spectrometry at Curtin University, Perth, Australia. Precise dating of relatively young zircons (<1000 Ma) by ion-microprobe is best achieved by using concordant ^{206}Pb/^{238}U ages, whereas older zircons usually provide precise ^{207}Pb/^{206}Pb ages (see Black and others, 2003, and Black and Jagodzinski, 2003, for explanation). We therefore mostly report mean ^{206}Pb/^{238}U zircon crystallization ages in this paper, whereas ^{207}Pb/^{206}Pb ages are considered more appropriate for old grains interpreted as xenocrysts. Note that in the case of discordant data the given ^{207}Pb/^{206}Pb age is a minimum value. Single zircons dated by the Pb-Pb evaporation technique were measured using a Finnigan-MAT 261 mass spectrometer in the Max-Planck-Institut für Chemie in Mainz. Mineral separation techniques, cathodoluminescence imaging and analytical procedures for isotopic analyses are detailed in the Appendix.

Lake Zone

Sample M523JC was collected some 45 km east of Chandman village on the saddle between the Zamtyn and Bayantsaagan Ridges, in the Zamtyn Range complex (figs. 3, 4A and 5A). This rock is a medium-grained (up to 1 mm) granite-gneiss composed of plagioclase, quartz, K-feldspar, biotite and minor opaque minerals and shows a solid-state foliation defined by the alignment of biotite and recrystallization of quartz

and feldspars. The zircons are dark brown to yellow-brown, long-prismatic with variably rounded terminations although near-idiomorphic grains also occur. CL-images are rather dark because of uniformly high U-contents, but oscillatory magmatic zoning is well developed, often with lighter cores surrounded by broad, darker rims. Light U-poor rims on some grains were too narrow to be measured on SHRIMP. Inclusions are also common but were avoided during analysis. Eight grains were analyzed (table 1) of which two are concordant and one is very close to concordance, whereas the remaining five grains are variably discordant due to recent Pb-loss (fig. 6A). The most concordant grain has a $^{206}Pb/^{238}U$ age of 955 ± 7 Ma. All grains are well aligned and define a chord (MSWD = 0.03) with an upper Concordia intercept age of 950 ± 16 Ma (fig. 6A) and a lower intercept near zero, suggesting Recent Pb-loss. We interpret the upper intercept age as reflecting the time of protolith emplacement in the early Neoproterozoic.

Sample M150/06-3 was collected near the gravel road 10 km NE of Chandman village, north of the Main Mongolian Lineament, from a granite-gneiss dike cutting banded amphibolites (figs. 3, 4A and 5B) in the high-grade basement of the Zamtyn Range (Rauzer and others, 1987). It is a medium-grained leucocratic granitic gneiss containing quartz, plagioclase, K-feldspar, biotite and muscovite. Biotite is commonly chloritized, and feldspars are altered. Zircons are rare and clear to light redbrown, either idiomorphic and long-prismatic or rounded to oval at their terminations. CL images show oscillatory or striped zoning (fig. 6B, inset), and some grains have narrow, low-U rims which could not be analyzed. Six grains were dated on SHRIMP II of which five are concordant and well grouped (table 1) with a mean $^{206}Pb/^{238}U$ age of 500.8 ± 3.8 Ma. One grain is much older but grossly discordant and has a minimum $^{207}Pb/^{206}Pb$ age of 1490 Ma (fig. 6B). This is undoubtedly a xenocryst, probably reflecting older pre-CAOB basement at depth, perhaps related to the South Mongolian microcontinent (Yarmolyuk and others, 2005) as also suggested for other samples below.

Sample M140 is a felsic volcaniclastic rock from a sequence of volcaniclastic and clastic sediments tectonically above a serpentinite lens. The zircons are transparent, light yellow, subhedral and long-prismatic with oscillatory or striped internal zoning. Of six analyses obtained on SHRIMP II (table 1), four yielded similar and concordant data points with a weighted mean $^{206}Pb/^{238}U$ age of 358.7 ± 5.0 Ma (fig. 6C), whereas two analyses resulted in sub-concordant data points having a minimum $^{207}Pb/^{206}Pb$ age of 350 ± 18 Ma (fig. 6C) which is compatible with the concordant data. We interpret this early Carboniferous age as reflecting the time of volcanic activity.

In a channel within the above volcaniclastic rocks there is a coarse sandstone, in part conglomeratic, with grading and cross-bedding, thin lenses of serpentinite, chert, all variably sheared and isoclinally folded. Sample M141 is a coarse-grained grit from this channel deposit containing angular fragments of serpentinite (figs. 3 and 4A). The detrital zircons are fairly heterogeneous and range from pale yellow, transparent and subhedral to dark colored and well-rounded grains. CL images show oscillatory or striped zoning for the subhedral grains and sector zoning or no structures in the rounded grains. Six zircons of different morphological type analyzed on SHRIMP II produced varying ages from 406 to 553 Ma (table 1, fig. 6D). Consequently, the depositional age of the grit must be younger than 406 Ma, presumably similar to the enclosing early Carboniferous volcaniclastic rock. The detrital input reflects a latest Neoproterozoic to early Paleozoic source.

Higher up in the above sequence is a 1 km wide belt of cleaved, fine-grained turbidite sediments with rare beds of sandstone from which sample M142 was collected (figs. 3 and 4A). This most likely represents a turbiditic sequence, possibly from an accretionary wedge. The detrital zircons are either pale yellow, transparent, long-prismatic and subhedral or dark brown and well-rounded. SHRIMP II analyses of ten zircons (table 1) resulted in three groups of ages spread between 397 and 2594 Ma. At

TABLE 1

SHRIMP II analytical data for spot analyses of zircons from magmatic and sedimentary rocks in southwestern Mongolia

	Sample No.*	U (ppm)	Th (ppm)	$^{206}Pb/^{204}Pb$	$^{208}Pb/^{206}Pb$	$^{207}Pb/^{206}Pb$	$^{206}Pb/^{238}U$	$^{207}Pb/^{235}U$	$^{206}Pb/^{238}U$ age ± 1σ	$^{207}Pb/^{235}U$ age ± 1σ	$^{207}Pb/^{206}Pb$ age ± 1σ
Lake Zone	**M523JC** Zamtyn Range Complex, granitic gneiss, N 45.29058°, E 98.64678°										
	M523-1.1	1946	584	2642	0.0972 ±13	0.0706 ± 6	0.1301 ± 11	1.344 ± 16	834 ± 6	865 ± 7	945 ± 17
	M523-2.1	1650	568	28145	0.1023 ± 6	0.0708 ± 3	0.1583 ± 13	1.544 ± 15	947 ± 7	948 ± 6	950 ± 9
	M523-3.1	740	332	11837	0.1325 ± 13	0.0708 ± 5	0.1596 ± 13	1.558 ± 18	955 ± 7	954 ± 7	952 ± 16
	M523-4.1	828	336	9390	0.1146 ± 13	0.0705 ± 6	0.1529 ± 12	1.486 ± 18	917 ± 7	925 ± 7	943 ± 16
	M523-5.1	1408	675	6768	0.1433 ± 11	0.0708 ± 5	0.1468 ± 12	1.433 ± 16	883 ± 7	903 ± 7	951 ± 14
	M523-6.1	584	229	8604	0.1217 ± 16	0.0707 ± 7	0.1473 ± 12	1.434 ± 19	886 ± 7	903 ± 7	947 ± 20
	M523-7.1	492	180	5048	0.1098 ± 16	0.0708 ± 7	0.1569 ± 13	1.532 ± 21	940 ± 7	943 ± 8	952 ± 21
	M523-8.1	1394	405	10393	0.0881 ± 9	0.0706 ± 4	0.1492 ± 12	1.453 ± 15	896 ± 7	911 ± 6	947 ± 12
	M150/06-3 Zamtyn Range Complex, granitic gneiss dike, N 45.40288°, E 98.08887°										
	M150/06-3.1.1	243	127	4508	0.1637 ± 31	0.0574 ± 11	0.0807 ± 7	0.639 ± 15	501 ± 4	502 ± 9	509 ± 45
	M150/06-3.2.1	534	298	10483	0.1663 ± 18	0.0573 ± 6	0.0808 ± 7	0.638 ± 10	501 ± 4	501 ± 6	503 ± 25
	M150/06-3.3.1	860	210	28911	0.0642 ± 5	0.0931 ± 3	0.2494 ± 23	3.201 ± 33	1435 ± 12	1457 ± 8	1490 ± 6
	M150/06-3.4.1	293	110	6713	0.1261 ± 24	0.0574 ± 10	0.0808 ± 7	0.639 ± 13	501 ± 4	502 ± 8	505 ± 37
	M150/06-3.5.1	369	152	7994	0.1291 ± 22	0.0573 ± 9	0.0809 ± 7	0.639 ± 12	501 ± 4	502 ± 7	503 ± 33
	M150/06-3.6.1	427	511	8987	0.3760 ± 30	0.0574 ± 8	0.0808 ± 7	0.639 ± 11	501 ± 4	502 ± 7	508 ± 29
	M140 Zamtyn Range Complex, felsic volcaniclastic rock, N 45.46675°, E 98.15528°										
	M140-1.1	186	149	264061	0.2522 ± 35	0.05379 ± 9	0.0575 ± 6	0.427 ± 9	361 ± 4	361 ± 6	362 ± 38
	M140-1.2	148	131	7671	0.2686 ± 54	0.05330 ± 19	0.0576 ± 6	0.424 ± 16	361 ± 4	359 ± 11	341 ± 79
	M140-2.1	180	234	18110	0.3911 ± 71	0.0541 ± 25	0.0600 ± 5	0.343 ± 17	290 ± 3	300 ± 12	377 ± 102
	M140-3.1	137	111	82919	0.2485 ± 39	0.0547 ± 11	0.0569 ± 6	0.429 ± 10	357 ± 4	362 ± 7	399 ± 45
	M140-3.2	256	237	23811	0.2757 ± 50	0.0539 ± 19	0.0569 ± 6	0.423 ± 16	357 ± 4	358 ± 11	369 ± 78
	M140-4.1	500	520	34763	0.3158 ± 43	0.0532 ± 16	0.0468 ± 5	0.343 ± 11	295 ± 3	300 ± 9	339 ± 67
	M141 Zamtyn Range Complex, grit, N 45.46467°, E 98.15367°										
	M141-1.1	244	118	86633	0.1488 ± 21	0.0585 ± 8	0.896 ± 6	0.723 ± 11	553 ± 3	552 ± 7	548 ± 29
	M141-2.1	304	47	18858	0.0460 ± 58	0.0565 ± 25	0.0813 ± 6	0.633 ± 29	504 ± 3	498 ± 18	471 ± 99
	M141-3.1	691	227	47065	0.1003 ± 25	0.0545 ± 11	0.0518 ± 3	0.389 ± 8	326 ± 2	334 ± 6	390 ± 45
	M141-4.1	1139	1094	205888	0.2873 ± 20	0.0549 ± 5	0.0439 ± 3	0.333 ± 40	277 ± 2	292 ± 3	410 ± 21
	M141-5.1	263	93	7871	0.0943 ± 38	0.0566 ± 17	0.0759 ± 5	0.592 ± 18	471 ± 3	472 ± 12	475 ± 65
	M141-6.1	419	769	46729	0.6328 ± 48	0.0549 ± 13	0.0473 ± 3	0.358 ± 9	298 ± 2	311 ± 7	408 ± 51
	M142 Zamtyn Range Complex, volcanic sandstone, N 45.45658°, E 98.15367°										
	M142-1.1	132	147	20916	0.3335 ± 42	0.0660 ± 13	0.1342 ± 16	1.221 ± 29	812 ± 9	810 ± 13	807 ± 40
	M142-2.1	335	296	23900	0.2750 ± 39	0.0548 ± 13	0.0637 ± 7	0.481 ± 14	398 ± 4	399 ± 9	404 ± 55
	M142-3.1	313	257	204040	0.2475 ± 20	0.0660 ± 6	0.1337 ± 15	1.217 ± 19	809 ± 9	808 ± 9	806 ± 19
	M142-4.1	808	355	37495	0.1305 ± 17	0.0540 ± 7	0.0645 ± 7	0.480 ± 9	403 ± 4	398 ± 6	370 ± 29
	M142-5.1	609	438	40532	0.2158 ± 32	0.0537 ± 13	0.0643 ± 7	0.476 ± 13	402 ± 4	396 ± 9	360 ± 53
	M142-6.1	548	377	58692	0.2086 ± 14	0.0657 ± 5	0.1355 ± 15	1.226 ± 17	819 ± 9	813 ± 8	796 ± 15

TABLE 1
(continued)

	Sample No.*	U (ppm)	Th (ppm)	$^{206}Pb/^{204}Pb$	$^{208}Pb/^{206}Pb$	$^{207}Pb/^{206}Pb$	$^{206}Pb/^{238}U$	$^{207}Pb/^{235}U$	$^{206}Pb/^{238}U$ age ± 1σ	$^{207}Pb/^{235}U$ age ± 1σ	$^{207}Pb/^{206}Pb$ age ± 1σ
Lake Zone *(continued)*	M142-7.1	317	248	683527	0.2452 ± 35	0.0543 ± 9	0.0633 ± 5	0.474 ± 9	396 ± 3	394 ± 6	383 ± 38
	M142-8.1	405	175	22871	0.1258 ± 22	0.0542 ± 9	0.0633 ± 5	0.473 ± 9	395 ± 3	393 ± 6	380 ± 35
	M142-9.1	465	418	23195	0.2737 ± 59	0.0540 ± 23	0.0631 ± 5	0.469 ± 21	394 ± 3	391 ± 14	370 ± 97
	M142-10.1	520	355	96043	0.1825 ± 9	0.1737 ± 5	0.4973 ± 42	11.914 ± 111	2602 ± 18	2598 ± 9	2594 ± 5
	M275 Zamtyn Range Complex, felsic pyroclastic rock, N 45.37647°, E 98.41317°										
	M275-1.1	119	85	2817	0.2395 ± 91	0.0594 ± 35	0.0808 ± 8	0.662 ± 41	501 ± 5	516 ± 25	582 ± 129
	M275-2.1	150	121	1206	0.2574 ± 129	0.0570 ± 53	0.0806 ± 8	0.634 ± 60	500 ± 5	498 ± 37	492 ± 205
	M275-3.1	148	98	1265	0.2020 ± 117	0.0576 ± 49	0.0812 ± 8	0.644 ± 56	503 ± 5	505 ± 34	513 ± 186
	M275-4.1	461	176	3955	0.1165 ± 35	0.0571 ± 15	0.0812 ± 7	0.640 ± 19	503 ± 4	502 ± 11	496 ± 59
	M275-5.1	362	331	7516	0.2845 ± 50	0.0579 ± 18	0.0804 ± 7	0.642 ± 22	499 ± 4	504 ± 13	526 ± 69
Gobi-Altai Zone (Northern Slope of Gichgene Ridge)	**M103/06-2** Chandman Crystalline Complex, granitoid, N 45.27681°, E 97.95878°										
	M103/06-2.1.1	873	180	5409	0.0714 ± 23	0.0533 ± 10	0.0543 ± 2	0.399 ± 7	341+ 1	341 ± 5	342 ± 40
	M103/06-2.2.1	874	295	6212	0.1078 ± 24	0.0529 ± 10	0.0544 ± 2	0.394 ± 8	341 ± 1	339 ± 5	324 ± 41
	M103/06-2.3.1	583	135	5939	0.0778 ± 33	0.0535 ± 14	0.0543 ± 2	0.401 ± 11	341 ± 1	342 ± 8	351 ± 58
	M103/06-2.4.1	755	192	2679	0.800 ± 30	0.0531 ± 13	0.0544 ± 6	0.398 ± 11	341 ± 3	340 ± 8	332 ± 54
	M103/06-2.5.1	1139	401	210	0.1614 ± 10	0.0537 ± 41	0.0541 ± 6	0.400 ± 32	340 ± 4	342 ± 23	357 ± 175
	M103/06-2.6.1	578	202	6191	0.1465 ± 22	0.0529 ± 10	0.0542 ± 5	0.396 ± 9	340 ± 3	338 ± 6	325 ± 42
	M107 06-2 Chandman Crystalline Complex, granitic gneiss, N 45.26224°, E 98.10258°										
	M107/06-2.1	715	401	4297	0.1421 ± 21	0.0538 ± 8	0.0559 ± 2	0.414 ± 6	351 ± 1	352 ± 5	362 ± 33
	M107/06-2.2.1	823	809	10864	0.2959 ± 22	0.0537 ± 6	0.0559 ± 2	0.413 ± 5	350 ± 1	351 ± 4	356 ± 25
	M107/06-2.3.1	892	538	12510	0.1900 ± 17	0.0538 ± 6	0.0557 ± 2	0.413 ± 5	350 ± 1	351 ± 3	360 ± 24
	M107/06-2.4.1	290	289	2197	0.2612 ± 45	0.0536 ± 16	0.0559 ± 2	0.413 ± 12	350 ± 1	351 ± 9	353 ± 65
	M107/06-2.5.1	313	231	2634	0.2356 ± 41	0.0541 ± 14	0.0560 ± 2	0.417 ± 11	351 ± 1	354 ± 8	373 ± 60
	M107/06-2.6.1	1104	663	7057	0.1884 ± 23	0.0545 ± 9	0.0558 ± 5	0.420 ± 8	350 ± 3	356 ± 6	393 ± 35
	M107/06-2.7.1	463	358	697	0.2109 ± 77	0.0540 ± 31	0.0562 ± 5	0.418 ± 25	353 ± 3	355 ± 17	371 ± 128
Gobi-Altai Zone (Southern Slope of Gichgene Ridge)	**M65/06-1** "Neoproterozoic unit" (Rauzer and others, 1987), cataclastic granite, N 44.82581°, E 97.77161°										
	M65/06-1.1.1	1175	1849	5439	0.4859 ± 31	0.0522 ± 9	0.0455 ± 1	0.327 ± 6	287 ± 1	288 ± 5	294 ± 40
	M65/06-1.2.1	248	118	1674	0.1454 ± 87	0.0537 ± 35	0.0455 ± 2	0.337 ± 22	287 ± 1	295 ± 17	357 ± 148
	M65/06-1.3.1	1091	690	4801	0.1994 ± 25	0.0520 ± 9	0.0456 ± 4	0.327 ± 7	287 ± 3	287 ± 5	287 ± 39
	M65/06-1.4.1	268	313	3045	0.3453 ± 73	0.0528 ± 25	0.0454 ± 4	0.331 ±16	286+ 3	290 ± 12	321 ± 105
	M74/06-6 "Neoproterozoic unit" (Rauzer and others, 1987), tonalitic gneiss, N 44.86185°, E 97.78711°										
	M74/06-6.1.1	677	226	15188	0.1056 ± 14	0.0541 ± 6	0.0584 ± 5	0.436 ± 7	366 ± 3	367 ± 5	375 ± 25
	M74/06-6.2.1	204	140	2551	0.2104 ± 48	0.0542 ± 17	0.0578 ± 5	0.431 ± 15	362 ± 3	364 ± 10	378 ± 72
	M74/06-6.3.1	1060	415	908	0.1209 ± 31	0.0546 ± 13	0.0577 ± 5	0.434 ± 11	362 ± 3	366 ± 8	395 ± 52
	M74/06-6.4.1	143	76	1983	0.1697 ± 63	0.0542 ± 24	0.0578 ± 6	0.432 ± 20	362 ± 3	365 ± 14	379 ± 100
	M74/06-6.5.1	138	102	1506	0.2443 ± 71	0.0551 ± 26	0.0584 ± 6	0.444 ± 22	366 ± 3	373 ± 15	417 ± 104

TABLE 1
(continued)

	Sample No.*	U (ppm)	Th (ppm)	$^{206}Pb/^{204}Pb$	$^{208}Pb/^{206}Pb$	$^{207}Pb/^{206}Pb$	$^{206}Pb/^{238}U$	$^{207}Pb/^{235}U$	$^{206}Pb/^{238}U$ age ± 1σ	$^{207}Pb/^{235}U$ age ± 1σ	$^{207}Pb/^{206}Pb$ age ± 1σ
Gobi-Altai Zone (Southern Slope of Gichgene Ridge) *(continued)*	**M83/06** Granite intruding the Gichgene formation, N 44.99451°, E 97.77270°										
	M83/06-1.1	27222	8791	17412	0.1102 ± 10	0.0518 ± 4	0.0440 ± 4	0.315 ± 4	278 ± 2	278 ± 3	278 ± 18
	M83/06-2.1	6597	22369	3402	0.1368 ± 34	0.0521 ± 13	0.0445 ± 4	0.320 ± 9	281 ± 3	282 ± 7	291 ± 57
	M83/06-3.1	25234	14525	4648	0.1943 ± 18	0.0517 ± 6	0.0444 ± 4	0.317 ± 5	280 ± 2	279 ± 4	273 ± 28
	M83/06-4.1	7237	2461	5342	0.1074 ± 26	0.0518 ± 10	0.0443 ± 4	0.316 ± 7	279 ± 2	279 ± 6	276 ± 46
	M83/06-5.1	9034	3152	5064	0.1082 ± 24	0.0515 ± 10	0.0445 ± 4	0.316 ± 7	280 ± 2	279 ± 5	262 ± 43
	M137 "Neoproterozoic unit" (Rauzer and others, 1987), siltstone, N 45.14506°, E 97.14381°										
	M137-1.1	238	100	43541	0.1281 ± 19	0.0557 ± 8	0.0736 ± 5	0.565 ± 9	458 ± 3	455 ± 6	440 ± 30
	M137-2.1	392	246	456621	0.1976 ± 13	0.0561 ± 4	0.0740 ± 5	0.572 ± 6	460 ± 3	460 ± 4	457 ± 16
	M137-3.1	1205	735	862	0.1931 ± 21	0.0567 ± 9	0.0737 ± 5	0.576 ± 10	458 ± 3	462 ± 6	481 ± 34
	M137-4.1	487	203	2049180	0.1244 ± 9	0.0563 ± 4	0.0734 ± 5	0.570 ± 5	457 ± 3	458 ± 3	463 ± 14
	M137-5.1	185	112	38809	0.1883 ± 27	0.0563 ± 10	0.0734 ± 5	0.570 ± 12	457 ± 3	458 ± 7	466 ± 41
	M137-6.1	693	267	111744	0.1162 ± 8	0.0561 ± 4	0.0740 ± 5	0.572 ± 5	460 ± 3	459 ± 3	454 ± 14
	M135 "Neoproterozoic unit" (Rauzer and others, 1987), foliated granite, N 45.11947°, E 97.11561°										
	M135-1.1	596	979	167168	0.5147 ± 28	0.0518 ± 6	0.0472 ± 5	0.337 ± 6	297 ± 3	295 ± 4	276 ± 26
	M135-2.1	645	1133	288600	0.5581 ± 29	0.0521 ± 5	0.0472 ± 5	0.339 ± 5	297 ± 3	296 ± 4	288 ± 22
	M135-3.1	386	543	124517	0.4455 ± 35	0.0515 ± 8	0.0467 ± 5	0.332 ± 6	294 ± 3	291 ± 5	264 ± 34
	M135-4.1	352	416	396983	0.3701 ± 30	0.0517 ± 6	0.0473 ± 5	0.337 ± 6	298 ± 3	295 ± 4	271 ± 27
	M135-4.2	459	564	183453	0.3869 ± 29	0.0517 ± 6	0.0467 ± 5	0.333 ± 6	294 ± 3	292 ± 4	274 ± 28
	M135-5.1	196	212	13956	0.3142 ± 45	0.0520 ± 14	0.0468 ± 5	0.336 ± 10	295 ± 3	294 ± 8	284 ± 61
	M135-5.2	392	405	275786	0.3201 ± 29	0.0518 ± 7	0.0468 ± 5	0.335 ± 6	295 ± 3	293 ± 5	277 ± 29
	M135-6.1	676	1275	152369	0.5813 ± 30	0.0518 ± 6	0.0468 ± 5	0.334 ± 5	295 ± 3	293 ± 4	276 ± 25
	M132 "Neoproterozoic unit" (Rauzer and others, 1987), foliated diorite, N 45.03658°, E 97.16169°										
	M132-1.1	190	239	17711	0.3785 ± 57	0.0515 ± 17	0.0461 ± 5	0.327 ± 12	291 ± 3	288 ± 9	264 ± 75
	M132-2.1	169	219	26148	0.4147 ± 70	0.0523 ± 22	0.0456 ± 5	0.329 ± 15	288 ± 3	289 ± 11	297 ± 97
	M132-3.1	227	294	16851	0.4013 ± 54	0.0516 ± 16	0.0460 ± 5	0.328 ± 11	290 ± 3	288 ± 8	267 ± 69
	M132-4.1	242	260	562114	0.3314 ± 38	0.0528 ± 9	0.0458 ± 5	0.333 ± 7	288 ± 3	292 ± 5	319 ± 36
	M132-5.1	158	208	13813	0.4150 ± 72	0.0514 ± 23	0.0460 ± 5	0.326 ± 16	290 ± 3	287 ± 12	260 ± 104
	M132-6.1	185	240	23949	0.4081 ± 72	0.0510 ± 25	0.0458 ± 5	0.322 ± 17	289 ± 3	284 ± 13	242 ± 113
Western Mandalovoo Subzone	**M60/06-1** "Early Devonian metamorphic unit" (Rauzer and others, 1987), migmatite leucosome, N 44.60966°, E 99.24146°										
	M60/06-1.1.1	1045	119	7108	0.0394 ± 14	0.0526 ± 7	0.0464 ± 4	0.337 ± 6	292 ± 3	295 ± 4	313 ± 28
	M60/06-1.2.1	368	608	7534	0.5167 ± 48	0.0534 ± 10	0.0465 ± 4	0.342 ± 8	293 ± 3	299 ± 6	344 ±43
	M60/06-1.3.1	391	289	5421	0.2275 ± 35	0.0522 ± 12	0.0469 ± 4	0.338 ± 9	296 ± 3	295 ± 7	293 ± 52
	M60/06-1.4.1	1699	1355	653	0.2613 ± 37	0.0788 ± 14	0.0341 ± 3	0.370 ± 8	216 ± 2	320 ± 6	1166 ± 36
	M60/06-1.5.1	511	859	12074	0.5245 ± 41	0.0529 ± 8	0.0459 ± 4	0.335 ± 6	289 ± 3	293 ± 5	325 ± 34
	M60/06-1.6.1	252	53	4471	0.0702 ± 34	0.0526 ± 15	0.0464 ± 4	0.336 ± 11	292 ± 3	294 ± 8	312 ± 65

TABLE 1
(continued)

	Sample No.*	U (ppm)	Th (ppm)	$^{206}Pb/^{204}Pb$	$^{208}Pb/^{206}Pb$	$^{207}Pb/^{206}Pb$	$^{206}Pb/^{238}U$	$^{207}Pb/^{235}U$	$^{206}Pb/^{238}U$ age ± 1σ	$^{207}Pb/^{235}U$ age ± 1σ	$^{207}Pb/^{206}Pb$ age ± 1σ
Western Mandalovoo Subzone *(continued)*	**M62/06-2** "Early Devonian metamorphic unit" (Rauzer and others, 1987), leucocratic granite, N 44.62950°, E 99.23835°										
	M62/06-2.1.1	2039	161	39171	0.0273 ± 11	0.0522 ± 5	0.0440 ± 1	0.316 ± 3	277 ± 1	279 ± 3	293 ± 22
	M62/06-2.2.1	1690	217	13388	0.0417 ± 12	0.0520 ± 5	0.0441 ± 1	0.317 ± 4	278 ± 1	279 ± 3	287 ± 24
	M62/06-2.3.1	492	167	8944	0.1012 ± 28	0.0586 ± 12	0.0871 ± 3	0.704 ± 15	538 ± 2	541 ± 9	553 ± 43
	M62/06-2.4.1	732	328	8609	0.1414 ± 20	0.0553 ± 8	0.0659 ± 2	0.503 ± 7	411 ± 1	414 ± 5	425 ± 31
	M62/06-2.5.1	789	374	10408	0.1512 ± 19	0.0560 ± 7	0.0656 ± 2	0.507 ± 7	410 ± 1	416 ± 5	453 ± 29
	M62/06-2.6.1	1511	183	17074	0.0426 ± 10	0.0520 ± 5	0.0440 ± 1	0.315 ± 3	277 ± 1	278+ 3	285 + 22
	M62/06-2.7.1	520	239	10183	0.1476 ± 29	0.0549 ± 11	0.0659 ± 2	0.499 ± 11	411 ± 1	411 ± 7	408 ± 46
	M62/06-2.8.1	822	306	4848	0.1211 ± 24	0.0551 ± 10	0.0657 ± 6	0.499 ± 10	410 ± 4	411 ± 7	416 ± 39
	M62/06-2.9.1	636	244	7617	0.1195 ± 22	0.0541 ± 9	0.0658 ± 6	0.490 ± 10	411 ± 4	405 ± 7	374 ± 37
	M200 Indert formation, felsic volcaniclastic rock, N 44.36755°, E 99.51861°										
	M200-1.1	259	113	5731	0.1434 ± 53	0.0547 ± 22	0.0569 ± 4	0.430 ± 18	357 ± 3	363 ± 13	400 ± 91
	M200-1.2	275	120	37912	0.1230 ± 40	0.0534 ± 17	0.0574 ± 4	0.422 ± 14	360 ± 3	358 ± 10	345 ± 70
	M200-2.1	273	212	14091	0.2331 ± 42	0.0527 ± 15	0.0570 ± 4	0.414 ± 13	358 ± 3	352 ± 9	314 ± 65
	M200-3.1	657	625	32630	0.2944 ± 29	0.0532 ± 10	0.0570 ± 4	0.418 ± 9	357 ± 3	355 ± 6	339 ± 41
	M200-4.1	295	144	21539	0.1442 ± 36	0.0567 ± 15	0.0768 ± 6	0.601 ± 17	477 ± 3	478 ± 11	482 ± 58
	M205 Gashuunovoo formation, sandstone, N 44.34167°, E 99.37514°										
	M205-1.1	539	786	54212	0.4605 ± 27	0.0578 ± 6	0.0842 ± 8	0.671 ± 11	521 ± 5	521 ± 6	521 ± 24
	M205-2.1	168	119	240964	0.2104 ± 14	0.1257 ± 7	0.3768 ± 40	6.529 ± 82	2061 ± 19	2060 ± 11	2038 ± 9
	M205-3.1	133	55	55692	0.1189 ± 15	0.1821 ± 9	0.4992 ± 55	12.534 ± 159	2610 ± 24	2645 ± 12	2672 ± 8
	M205-4.1	274	228	35925	0.2671 ± 30	0.0578 ± 10	0.0870 ± 9	0.694 ± 14	538 ± 5	535 ± 8	524 ± 36
	M205-5.1	174	248	70319	0.4592 ± 48	0.0573 ± 11	0.0828 ± 8	0.654 ± 15	513 ± 5	511 ± 9	503 ± 43
	M206 Indert formation, sandstone, N 44.39981°, E 99.32119°										
	M206-1.1	127	81	28868	0.2026 ± 34	0.0677 ± 13	0.1438 ± 15	1.342 ± 31	866 ± 9	864 ± 13	859 ± 39
	M206-2.1	190	80	28107	0.1406 ± 39	0.0543 ± 15	0.0610 ± 6	0.457 ± 14	382 ± 4	382 ± 10	384 ± 64
	M206-3.1	122	82	88992	0.2262 ± 41	0.0556 ± 12	0.0702 ± 7	0.539 ± 14	438 ± 4	437 ± 9	436 ± 49
	M206-4.1	685	419	85353	0.2028 ± 18	0.0551 ± 5	0.0674 ± 7	0.512 ± 8	420 ± 4	420 ± 5	417 ± 22
	M207 Ulanshaand formation, sandstone, N 44.31928°, E 99.59814°										
	M207-1.1	967	405	449236	0.1337 ± 11	0.0575 ± 4	0.0819 ± 8	0.649 ± 8	508 ± 5	508 ± 5	510 ± 15
	M207-2.1	1005	67	139451	0.0182 ± 8	0.0580 ± 5	0.0865 ± 9	0.692 ± 10	535 ± 5	534 ± 6	531 ± 18
	M207-3.1	983	264	76699	0.0857 ± 12	0.0565 ± 5	0.0752 ± 7	0.586 ± 9	467 ± 4	468 ± 5	474 ± 21
	M207-4.1	1087	79	228206	0.0236 ± 6	0.0574 ± 4	0.0822 ± 8	0.650 ± 8	509 ± 5	508 ± 5	505 ± 15
	M207-5.1	715	483	1057	0.2038 ± 36	0.0572 ± 15	0.0841 ± 8	0.664 ± 19	521 ± 5	517 ± 12	499 ± 58
	M208 Ulanshaand formation, sandstone, N 44.31886°, E 99.59325°										
	M208-1.1	381	628	354484	0.4571 ± 15	0.1609 ± 5	0.4518 ± 35	10.020 ± 87	2403 ± 15	2437 ± 8	2465 ± 5
	M208-2.1	683	512	80205	0.2294 ± 21	0.0575 ± 7	0.0827 ± 6	0.656 ± 98	512 ± 4	512 ± 6	511 ± 27
	M208-3.1	425	105	2207505	0.0710 ± 5	0.1198 ± 4	0.3562 ± 27	5.884 ± 52	1964 ± 13	1959 ± 8	1954 ± 6
	M208-4.1	530	223	24353	0.1268 ± 17	0.0574 ± 7	0.0824 ± 6	0.652 ± 98	511 ± 4	510 ± 6	505 ± 27

TABLE 1
(continued)

	Sample No.*	U (ppm)	Th (ppm)	$^{206}Pb/^{204}Pb$	$^{208}Pb/^{206}Pb$	$^{207}Pb/^{206}Pb$	$^{206}Pb/^{238}U$	$^{207}Pb/^{235}U$	$^{206}Pb/^{238}U$ age ± 1σ	$^{207}Pb/^{235}U$ age ± 1σ	$^{207}Pb/^{206}Pb$ age ± 1σ
Mandalovoo Subzone *(continued)*	**M209** Ulanshaand formation, sandstone, N 44.31886°, E 99.59325°										
	M209-1.1	424	205	138581	0.1468 ± 19	0.0577 ± 7	0.0832 ± 6	0.662 ± 10	515 ± 4	516 ± 6	517 ± 27
	M209-2.1	220	224	131441	0.2872 ± 17	0.1170 ± 6	0.3464 ± 28	5.589 ± 57	1918 ± 13	1914 ± 9	1911 ± 10
	M209-3.1	1386	547	740	0.1228 ± 32	0.0584 ± 14	0.0894 ± 7	0.719 ± 18	552 ± 4	550 ± 11	543 ± 51
	M209-4.1	579	208	415973	0.1006 ± 6	0.1168 ± 4	0.3449 ± 26	5.557 ± 48	1910 ± 12	1909 ± 7	1908 ± 6
	M209-5.1	505	289	31903	0.1738 ± 17	0.0675 ± 7	0.1426 ± 10	1.327 ± 17	859 ± 6	858 ± 7	853 ± 20
	M209-6.1	370	200	74482	0.1665 ± 21	0.0572 ± 8	0.0827 ± 6	0.653 ± 10	512 ± 4	510 ± 6	501 ± 29
South Gobi Zone	**R-ortho** Gobi-Tienshan Intrusive Complex, granitic gneiss xenolith, N 43.18239°, E 97.56508°										
	R-ortho-1.1	693	187	909	0.1404 ± 45	0.0520 ± 18	0.0478 ± 2	0.342 ± 12	301 ± 1	299 ± 9	286 ± 78
	R-ortho-2.1	486	179	8279	0.1123 ± 22	0.0536 ± 9	0.0550 ± 2	0.407 ± 7	345 ± 1	347 ± 5	355 ± 37
	R-ortho-3.1	389	166	4278	0.1424 ± 33	0.0533 ± 13	0.0478 ± 2	0.351 ± 9	301 ± 1	305 ± 7	340 ± 55
	R-ortho-4.1	503	189	20011	0.1169 ± 11	0.0686 ± 5	0.1472 ± 5	1.393 ± 11	886 ± 3	886 ± 5	887 ± 14
	R-ortho-5.1	510	292	7654	0.1737 ± 19	0.0568 ± 7	0.0794 ± 3	0.622 ± 8	493 ± 2	491 ± 5	485 ± 26
	R-ortho-6.1	1046	556	17281	0.1708 ± 16	0.0526 ± 5	0.0479 ± 1	0.348 ± 4	302 ± 1	303 ± 3	312 ± 23
	R-ortho-7.1	665	306	5550	0.1420 ± 28	0.0528 ± 11	0.0478 ± 4	0.348 ± 8	301 ± 3	303 ± 6	321 ± 47
	R-ortho-8.1	1063	378	540	0.1181 ± 69	0.0525 ± 28	0.0475 ± 5	0.344 ± 19	299 ± 3	300 ± 14	307 ± 122
	R-ortho-9.1	339	96	1234	0.0895 ± 76	0.0533 ± 31	0.0476 ± 5	0.349 ± 21	300 ± 3	304 ± 16	341 ± 133
	M33/06 Gobi-Tienshan Intrusive Complex, granodiorite, N 43.29281°, E 97.17729°										
	M33/06-1.1	452	362	8035	0.2511 ± 52	0.0532 ± 20	0.0477 ± 2	0.350 ± 13	300 ± 1	304 ± 10	337 ± 85
	M33/06-2.1	410	308	6501	0.2299 ± 47	0.0526 ± 18	0.0476 ± 2	0.345 ± 12	300 ± 1	301 ± 9	313 ± 77
	M33/06-3.1	508	310	3509	0.1913 ± 51	0.0527 ± 20	0.0475 ± 2	0.345 ± 13	299 ± 1	301 ± 10	315 ± 86
	M33/06-4.1	358	146	4716	0.1343 ± 58	0.0522 ± 24	0.0475 ± 2	0.342 ± 16	299 ± 1	299 ± 12	295 ± 103
	M33/06-5.1	350	212	4192	0.1924 ± 45	0.0533 ± 17	0.0478 ± 4	0.351 ± 12	301 ± 3	306 ± 9	343 ± 71
	M33/06-6.1	308	246	1894	0.2344 ± 67	0.0520 ± 25	0.0478 ± 5	0.343 ± 17	301 ± 3	299 ± 13	285 ± 110
	M33/06-7.1	560	376	3198	0.2093 ± 41	0.0533 ± 15	0.0482 ± 4	0.354 ± 11	303 ± 3	308 ± 8	341 ± 64

* 1.1 is spot 1 on grain 1, 1.2 is spot 2 on grain 1, 2.1 is spot 1 on grain 2, etc.

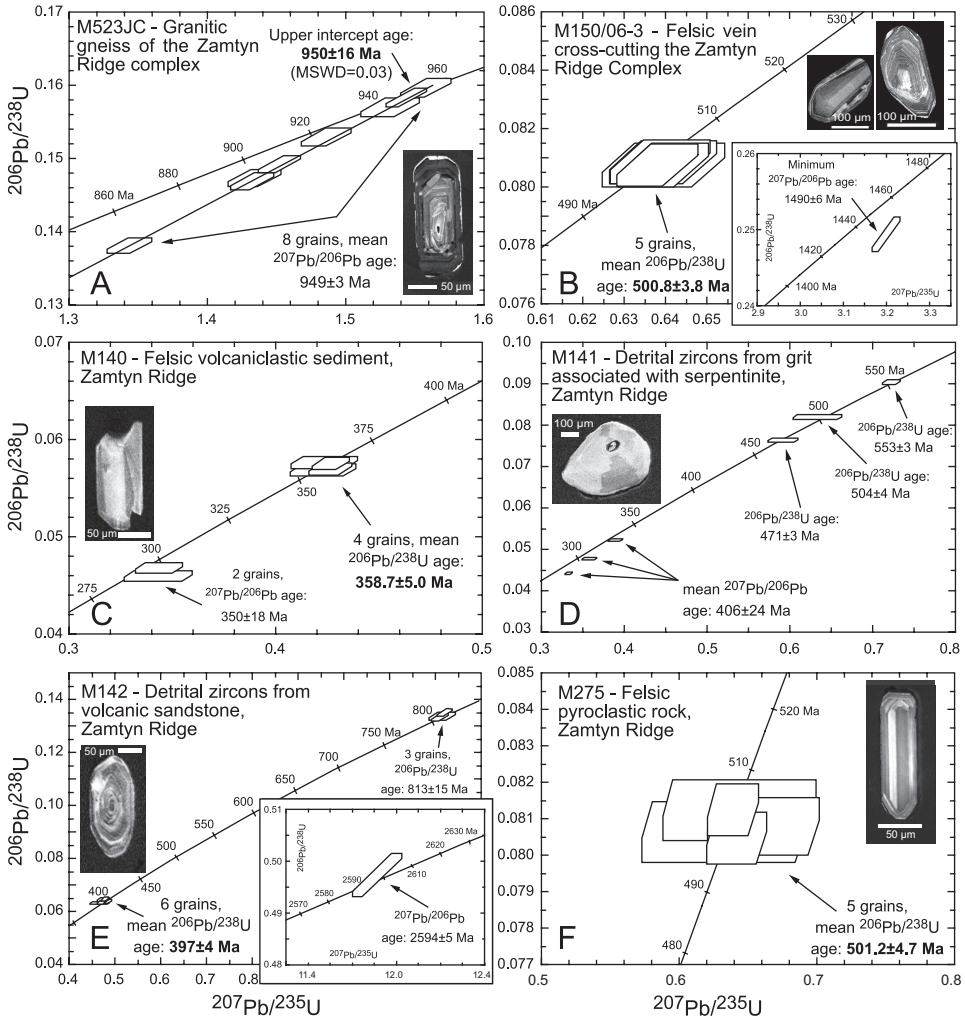

Fig. 6. Concordia diagrams showing SHRIMP II analyses of single zircons for samples from the Lake Zone. Data boxes for each analysis are defined by standard errors in $^{207}Pb/^{235}U$, $^{206}Pb/^{238}U$ and $^{207}Pb/^{206}Pb$. Errors on pooled ages are given at 95% confidence level. Insets show typical CL images of dated zircons.

the lower end of the spread, a cluster of six data points obtained from oscillatory zoned domains of long-prismatic grains has a weighted mean $^{206}Pb/^{238}U$ age of 397 ± 4 Ma (fig. 6E). In the middle of the spread, three analyses from faint sector-zoned domains of rounded grains yielded comparable results with a weighted mean $^{206}Pb/^{238}U$ age of 813 ± 15 Ma. At the upper end of the spread, a single concordant analysis from a metamict domain of a rounded zircon has a $^{207}Pb/^{206}Pb$ age of 2594 ± 5 Ma (fig. 6E). The data at the lower end of the spread suggest a maximum early Devonian depositional age from proximal sources, whereas the remaining ages indicate Neoproterozoic to Archean detrital input, the latter possibly derived from the Baydrag block.

Sample M275 is a well foliated and strongly folded felsic pyroclastic rock from a homogeneous sequence of volcaniclastic rocks in the Zamtyn Range (figs. 3 and 4A). The zircons are translucent to slightly yellow, euhedral and long- to short-prismatic. CL

imaging reveals igneous-related oscillatory zoning and rare rounded, inherited cores. SHRIMP II analyses of oscillatory zoned domains in five zircons yielded a cluster of concordant data (table 1) with a weighted mean $^{206}Pb/^{238}U$ age of 501.2 ± 4.7 Ma (fig. 6F). We interpret this to reflect the time of felsic protolith emplacement.

Gobi-Altai Zone (Northern Slope of Gichgene Ridge)

Sample M103/06-2 was collected some 6 km south of Chandman village on the Gichgene Ridge (figs. 3 and 4B) and in the granitoid core of the granite-migmatite Chandman dome. This rock is a coarse-grained (up to 0.5 cm) granitoid composed of plagioclase, quartz, K-feldspar, biotite, and minor titanite and opaque minerals. The magmatic fabric was weakly reworked by solid state deformation marked by recrystallization of quartz. The zircons are up to 300 μm long, mostly clear, idiomorphic and long-prismatic, rarely rounded at their terminations. Well preserved oscillatory zoning is ubiquitous (fig. 7A, inset), and some cores show evidence of metamictization and were avoided during analysis. Six grains were analyzed on SHRIMP II and produced well grouped and concordant results (table 1) with a mean $^{206}Pb/^{238}U$ age of 340.9 ± 2.5 Ma (fig. 7A). This is considered to approximate the time of granite emplacement in the early Carboniferous.

Granitic gneiss sample M107/06-2 was taken at the eastern termination of the Chandman complex, some 11 km SE of Chandman village on the Gichgene Ridge (figs. 3, 4B and 5C). The rock is composed of quartz, plagioclase, K-feldspar, biotite and epidote and shows a strong planar fabric defined by the alignment of biotite and recrystallization of quartz and feldspars. The zircons are clear to yellow-brown and idiomorphic to slightly rounded at their terminations. Long-prismatic shapes predominate, but stubby grains also occur. CL images display characteristic striped patterns (fig. 7B, inset) or oscillatory zoning, typical of igneous growth and similar to zircons in sample M33/06. SHRIMP II analyses of seven grains yielded well grouped results with little variation in the $^{206}Pb/^{238}U$ isotopic ratios (table 1). The mean age of 350.4 ± 1.7 Ma (fig. 7B) is interpreted to reflect early Carboniferous magmatism in the Chandman complex.

Gobi-Altai Zone (Southern Slope of Gichgene Ridge)

Foliated granite sample M65/06-1 was collected in a "basement terrain" [Neoproterozoic unit on the 1:200,000 Geological Map of Rauzer and others (1987)] located some 30 km south of Erdene village on the Gichgene Ridge (figs. 3 and 4B). The rock is a mylonitic to cataclastic pink granite with K-feldspar and plagioclase porphyroclasts (up to 1.5 mm) set in a fine-grained (0.1 mm) recrystallized matrix of quartz and feldspars, with little muscovite and epidote replacing feldspars. The zircons are clear to light yellow-brown, idiomorphic, and vary in shape from long-prismatic to stubby. CL images show grains with oscillatory zoning (fig. 7C, inset) and grains showing no or only vague zoning. Four zircons were analyzed on SHRIMP II and provided consistent and concordant results (table 1) with a mean $^{206}Pb/^{238}U$ age of 286.8 ± 1.8 Ma (fig. 7C). We interpret this early Permian age to approximate the time of granite emplacement.

Amphibole-rich tonalitic gneiss sample M74/06-6 was collected on the Gichgene Ridge, some 10 km north of sample M65/06-1 and in the same tectonic unit (figs. 3 and 4B). The gneiss is composed of hornblende, plagioclase, quartz, chlorite and minor epidote. It displays a strong foliation defined by alternation of hornblende-rich and plagioclase-quartz rich layers and by preferred orientation of hornblende and plagioclase. Originally large quartz grains (up to 2 mm) are mostly recrystallized in equidistant pockets between the plagioclase grains. Chlorite developed mostly at the expense of amphibole, and epidote replaces plagioclase without preferred orientation. The zircons vary in color and shape from clear to light brown and idiomorphic,

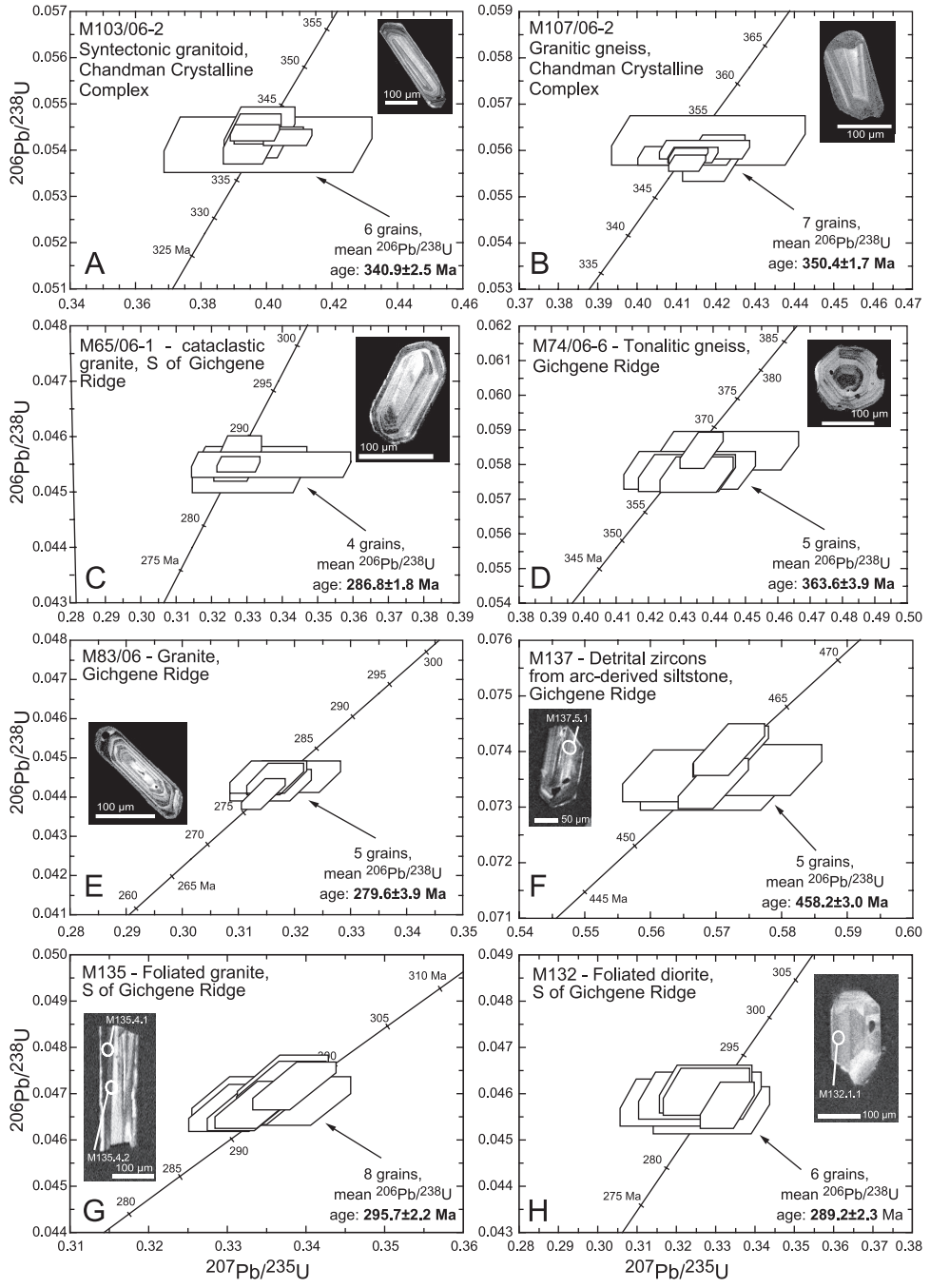

Fig. 7. Concordia diagrams showing SHRIMP II analyses of single zircons for samples from the western Gobi-Altai Zone. Data boxes for each analysis and errors on pooled ages as in fig. 6. Insets show typical CL images of dated zircons.

long-prismatic to stubby and oval. Most grains show oscillatory or sector zoning (fig. 7D, inset). Five grains were analyzed on SHRIMP II, and all yielded concordant and nearly identical results (table 1) which combine to a mean $^{206}Pb/^{238}U$ age of 363.6 ± 3.9 Ma (fig. 7D). We consider this late Devonian age to reflect the time of tonalite emplacement.

Medium-grained (0.5 mm) granite sample M83/06 was collected farther north in the same valley, some 15 km south of Erdene village on the Gichgene Ridge (figs. 3, 4B and 5D). In the field, the granite is associated with leucocratic granitic veins and sills which intruded along the cleavage. The sample is composed of quartz, plagioclase, K-feldspar and biotite. Biotite is commonly chloritized and plagioclase is altered, with local growth of epidote and muscovite inside plagioclase. The texture is magmatic without solid state deformation features. The zircons are mostly clear, colorless, idiomorphic and long-prismatic in shape. Magmatic zoning is well developed under CL, and some grains have homogeneous cores surrounded by oscillatory rims (fig. 7E, inset). Five grains were analyzed on SHRIMP II and produced concordant and well grouped results (table 1) with a mean $^{206}Pb/^{238}U$ age of 279.6 ± 3.9 Ma (fig. 7E) which we interpret as reflecting granite emplacement in the earliest Permian.

Sample M137 is a low-grade, strongly cleaved siltstone from a shale-siltstone sequence of presumed early Devonian depositional age (figs. 3 and 4B). This sequence is exposed N of a large pink, undeformed granite. To the north of this follows a thick, strongly cleaved turbidite sequence. The zircons are mostly clear, light yellow to colorless, idiomorphic and long-prismatic in shape, indicating virtually no sedimentary transport. Minor subrounded and dark-colored grains are also present. CL images reveal typical igneous-related oscillatory zoning and the presence of subrounded inherited cores in some grains. The igneous domains of six idiomorphic grains were analyzed on SHRIMP II and resulted in a cluster of concordant data points (table 1) with a weighted mean $^{206}Pb/^{238}U$ age of 458.2 ± 3.0 Ma (fig. 7F). The uniformity in age and grain morphology suggests derivation of the zircons from a nearby source, probably a late Ordovician volcanic arc.

Sample M135 was collected about 4 km south of sample M137 and represents an isoclinally folded granite sheet, some 20 to 25 m wide, intruding deformed amphibolite. The zircons are homogeneous in shape, clear, yellow to light brown, idiomorphic and long-prismatic with short pyramidal terminations and characterized by striped internal zoning. Eight SHRIMP II analyses produced similar and concordant results (table 1) with a weighted mean $^{206}Pb/^{238}U$ age of 295.7 ± 2.2 Ma (fig. 7G). This early Permian age is considered as the time of granite emplacement.

Foliated diorite sample M132 was collected north of low-grade felsic metavolcanic rocks near the southern margin of the Tseel metamorphic belt. The zircons are clear, pale yellow, mostly long-prismatic with smooth edges, and characterized by sector zoning in CL images. SHRIMP II analyses of six zircons (table 1) define a cluster of concordant results with a weighted mean $^{206}Pb/^{238}U$ age of 289.2 ± 2.3 Ma (fig. 7H) which we interpret as the time of emplacement of the dioritic protolith.

Southern Gobi-Altai Zone (Shine Jinst Area)

Sample M60/06-1 is a migmatitic leucosome collected 8 km north of the Shine Jinst village and was interpreted as early Devonian on the 1:200,000 Geological Map of Rauzer and others (1987) (figs. 3 and 4B). The outcrop consists of banded migmatite showing ptygmatic folds of felsic melt surrounded by biotite stromatites. This rock was originally considered to represent a basement with respect to the surrounding Devonian, Carboniferous and Permian sediments. The sample contains plagioclase, K-feldspar, quartz, muscovite, biotite and epidote. It shows a strong foliation defined by recrystallized augens and bends of K-feldspar, plagioclase and quartz and by fine-grained muscovite strips with epidote formed at the expense of plagioclase. Within the

recrystallized matrix are preserved porphyroclasts of K-feldspar and muscovite of supposed migmatitic origin, whereas the deformation is interpreted as a greenschist-facies overprint. The zircons are mostly clear and colorless and vary in shape between short- and long-prismatic. Some grains have rounded terminations. CL images reveal oscillatory and striped zoning (fig. 8A, inset), and some cores are metamict but were not measured. Six grains were analyzed (table 1) of which five are concordant and form a cluster with a mean $^{206}Pb/^{238}U$ age of 292.4 ± 3.6 Ma (fig. 8A). We interpret this early Permian age to reflect the time of leucosome formation and, by implication, the peak of metamorphism in this rock. One additional grain is grossly discordant and has a minimum $^{207}Pb/^{206}Pb$ age of 1166 ± 36 Ma (table 1, fig. 8A). This is likely to be a xenocryst inherited from a Precambrian source in the deeper crust, and again similar ages have been reported from other parts of the southern Gobi-Altai farther E where such rocks are exposed (for example Baga Bogd Massif, see Demoux and others, 2009c).

Granite sample M62/06-2 was collected some 10 km north of Shine Jinst village to constrain the age of a leucocratic granite intruding the migmatite complex (figs. 3, 4B). The rock is composed of plagioclase, K-feldspar, quartz, muscovite, epidote and calcite. The original structure is marked by equidistant large grains of feldspar and quartz (up to 2 mm). Quartz is recrystallized within the pockets, feldspars are replaced to a large extent by epidote and muscovite. The zircons are predominantly clear, idiomorphic, long-prismatic and show excellent magmatic zonation in CL images. Several grains have wide and zoned magmatic rims around older cores (fig. 8B, inset). Nine grain domains were analyzed on SHRIMP II, and all provided concordant results (table 1). The dominant zircon population is represented by a group of five concordant grains with a mean $^{206}Pb/^{238}U$ age of 410.8 ± 2.0 Ma (fig. 8B). Some rims were wide enough to be analyzed by a 30 μm analytical beam, and three such rims provide identical results with a mean $^{206}Pb/^{238}U$ age of 277.7 ± 2.4 Ma (fig. 8B). One grain is much older at 538 ± 2 Ma and is likely to be a xenocryst inherited from an early Cambrian crustal domain.

We interpret the early Permian rim age of 278 Ma as most likely reflecting the time of emplacement of the leucocratic granite, considering that this rock intrudes the 292 Ma migmatite represented by the sample M60/06-1. The dominant 411 Ma zircon population probably reflects an early Devonian granitoid domain in the lower crust which, on remelting produced the post-metamorphic leucocratic granite now exposed.

Western Mandalovoo Subzone (Shine Jinst Area)

Andesitic volcaniclastic sample M200 was collected within the western termination of the Mandalovoo "terrane" (Badarch and others, 2002) in a formation of presumed middle to late Devonian depositional age (figs. 3 and 4B). The sample comes from the upper part of the Khar member of the Indert formation which contains late Givetian to late Frasnian conodonts and Frasnian radiolarians (Minzhin and others, 2001). The entire sequence is composed of interlayered volcanic-derived sediments, massive felsic volcanic rocks, and silicified shale. The zircons from sample M200 are yellow, translucent, and subhedral and short-prismatic in shape. Of five analyses obtained on SHRIMP II (table 1), four yielded a cluster of concordant data points with a weighted mean $^{206}Pb/^{238}U$ age of 357.8 ± 3.2 Ma (fig. 8C). The fifth analysis produced a much older $^{206}Pb/^{238}U$ age of 477 ± 3 Ma (fig. 8C) which we interpret as a xenocryst inherited from an early Ordovician protolith. The early Carboniferous age is best interpreted as the time of deposition of the felsic volcaniclastic rock.

Sample M205 is a greenish, medium-grained sandstone collected within the Gashuunovoo formation of presumed late Ordovician depositional age (figs. 3 and 4B). This formation consists of mudstone, siltstone, sandstone and carbonates with

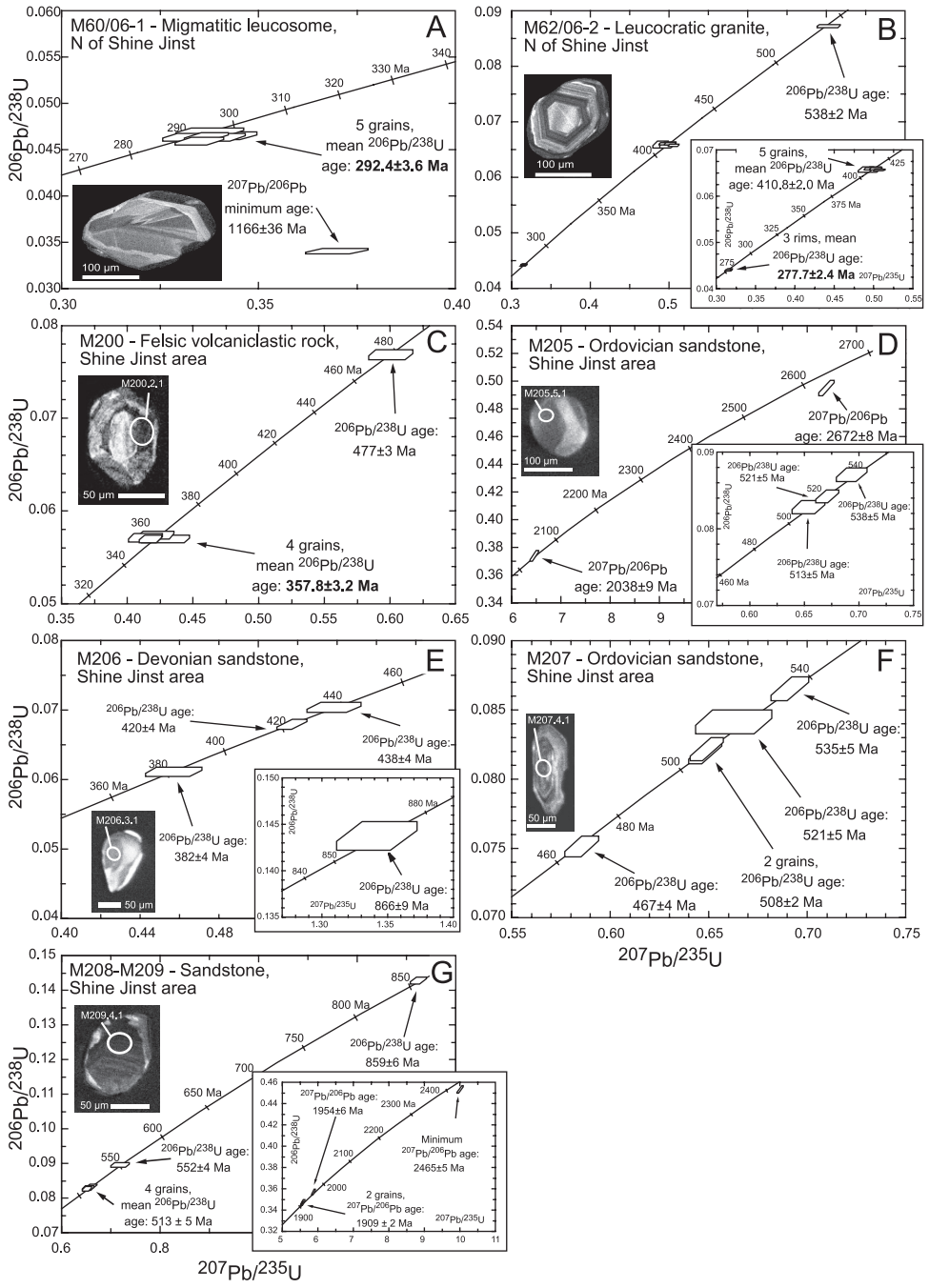

Fig. 8. Concordia diagrams showing SHRIMP II analyses of single zircons for samples from the southern Gobi-Altai Zone (Shine Jinst area). Data boxes for each analysis and errors on pooled ages as in fig. 6. Insets show typical CL images of dated zircons.

Upper Ordovician (Ashgilian) corals (Minzhin and others, 2001). The detrital zircons are translucent, yellow to dark brown in color and subhedral to well-rounded, suggesting long-distance sedimentary transport. The internal structures are homogeneous to faintly zoned or display well developed oscillatory zoning. Five zircons were analyzed on SHRIMP II and produced three concordant results with $^{206}Pb/^{238}U$ ages between 513 and 538 Ma and two much older ages indicating Archean to Paleoproterozoic detrital input (table 1, fig. 8D).

Sample M206 is a greenish, medium-grained sandstone with well-rounded quartz. This sample belongs to the Indert formation of presumed late Devonian depositional age (Minzhin and others, 2001). The detrital zircons are well-rounded with dominant red-brown color and display homogeneous or sector-zoned domains in CL image. SHRIMP II analyses of four zircons produced an age array ranging from 382 to 866 Ma (table 1, fig. 8E). The youngest zircon age suggest a maximum late Devonian depositional age for this sample, and the detrital input is from distant sources as suggested by the strongly abraded zircons.

Samples M207, M208 and M209 were collected within the fossiliferous (Ulaanshand) Upper Ordovician formation (Minzhin and others, 2001) (figs. 3 and 4B). This sequence consists of shale, volcaniclastic siltstone and sandstone and rare interlayered volcanic rocks and limestone beds. The samples are described below, upwards through the sequence.

Sample M207 is a fine-grained sandstone collected from a 3 m thick bed interlayered with siltstone. The zircons are mostly dark yellow, translucent, subhedral and long-prismatic. CL images reveal oscillatory or striped zoning. SHRIMP II analyses of five zircons yielded concordant data points spread along the concordia with $^{206}Pb/^{238}U$ ages of 467 to 535 Ma (table 1, fig. 8F).

Sample M208 is a medium-grained sandstone pebble collected from a 3 to 4 m thick conglomerate that contains well-rounded sandstone pebbles up to 25 cm in diameter. The conglomerate crops out some 400 m above sample M207. The detrital zircons are yellow to red-brown in color and subhedral to well-rounded in shape. CL images reveal oscillatory or sector zoning and rare rounded, inherited cores. Sample M209 is a greenish and fine-grained sandstone collected from a strongly cleaved sequence of several decimeters to meter thick shale beds interlayered with decimeter-thick horizons of sandstone. The detrital zircons are mostly dark colored and well-rounded, indicating long-distance sedimentary transport, and are characterized by homogeneous or oscillatory internal zoning. Zircons of both samples were analyzed on SHRIMP II and yielded ages varying between 513 and 2465 Ma (table 1; fig. 8G). At the lowest end of the spread, four zircons yielded similar results yielding a weighted mean $^{206}Pb/^{238}U$ age of 513 $\pm$ 7 Ma. These samples are compatible with an early Ordovician depositional age but also contain a record of substantial late Archean to Paleoproterozoic input as previously noted for the late Ordovician sandstone M205 from the Gashuunovoo formation.

South Gobi Zone

Sample 2/1054 was taken from a low-strain domain of the Tömörtyn formation on the Tömörtyn Ridge (figs. 2, 3 and 4C) and was dated to constrain the age of the oldest rocks forming the pre-intrusive sequence of the Gobi-Tienshan plutonic complex. The rock is a greenschist-facies mylonitic metarhyolite composed of partly recrystallized K-feldspar as well as micaceous products of decomposition of plagioclase and K-feldspar, surrounding rounded augens of quartz. The zircons are uniformly light yellow to colorless and euhedral, long-prismatic in shape, typical of igneous growth. Four grains were evaporated individually and provided identical $^{207}Pb/^{206}Pb$ ratios (table 2) that combine to a mean early Devonian age of 399.1 $\pm$ 1.1 Ma (fig. 9A). We interpret this to approximate the time of emplacement of the original rhyolite.

TABLE 2

Pb isotopic data from single grain zircon evaporation of samples from the South Gobi Zone, southern Mongolia

Sample Number	Zircon color and morphology	Grain #	Mass scans[1]	Evaporation temperature (°C)	Mean $^{207}Pb/^{206}Pb$ ratio[2] and 2σ (mean) error	$^{207}Pb/^{206}Pb$ age and 2σ (mean) error (Ma)
Tömörtyn Formation, felsic metavolcanic rock, N 42.84596°, E 98.725272°						
		1	99	1598	0.054667±43	398.6±1.8
	Clear to honey-yellow,	2	88	1599	0.054691±45	399.6±1.8
2/1054	idiomorphic	3	110	1597	0.054676±41	399.0±1.7
		4	88	1600	0.054683±41	399.3±1.7
mean of 4 grains		1-4	385		0.054679±21	***399.1±1.1**
Gobi-Tienshan Intrusive Complex, granitic gneiss, N 43.23939°, E 97.56420°						
		1	161	1596	0.052388±38	302.4±1.7
	light gray-brown, stubby	2	163	1998	0.052369±29	301.6±1.3
28/5325	to long-prismatic,	3	108	1598	0.052362±38	301.3±1.7
	idiomorphic	4	106	1600	0.052380±36	302.0±1.6
		5	56	1599	0.052374±54	301.8±2.3
mean of 5 grains		1-5	594		0.052376±20	***301.9±1.2**

[1] Number of $^{207}Pb/^{206}Pb$ ratios evaluated for age assessment.
[2] Observed mean ratio corrected for nonradiogenic Pb where necessary.
Errors based on uncertainties in counting statistics.
* Error based on reproducibility of internal standard.

Leucocratic granite-gneiss sample 28/5325 was collected from the orthogneiss-migmatite base of the Gobi-Tienshan plutonic complex (figs. 2, 3, 4C). This rock type constitutes the structurally deepest part of the pluton and may represent the metamorphosed root of the magmatic arc. It is a medium-grained, partially anatectic granite-gneiss with rare biotite. The homogeneous zircon population consists of clear to yellow-brown, idiomorphic, long- and short-prismatic grains. Five zircons were evaporated individually and yielded identical isotopic ratios, suggesting no disturbance of the Pb isotopic system. The combined mean $^{207}Pb/^{206}Pb$ age is 301.4 ± 1.2 Ma (table 2, fig. 9B), which we interpret as reflecting the time of late Carboniferous emplacement of the orthogneiss protolith.

Sample R-ortho is from a xenolith of leucocratic, medium-grained granitic gneiss with rare biotite, collected in the central part of the Gobi-Tienshan pluton (figs. 2, 3 and 4C) in order to constrain the age of the presumed basement of this magmatic complex. This xenolith occurs in medium- to coarse-grained granodiorite which forms the main part of the pluton. Under the microscope, the rock is composed of quartz, muscovite, sillimanite and rare plagioclase. The structure is formed by equidistant grains of quartz and plagioclase (0.1-0.5 mm) and randomly oriented muscovite aggregates associated with sillimanite. The zircons are clear and colorless and predominantly short-prismatic and idiomorphic. They show well developed oscillatory or striped zoning (fig. 9C, inset), and some grains have metamict cores which were avoided during analysis. Nine grains were analyzed on SHRIMP II, and all are concordant (table 1). Six grains have virtually identical $^{206}Pb/^{238}U$ isotopic ratios and define a late Carboniferous mean age of 301.1 ± 1.6 Ma (fig. 9C), which we consider to reflect the age of emplacement of the granite protolith from which the xenolith was derived. This is identical to the age of granite-gneiss sample 28/5325 discussed above. The other three grains are distinctly older and are interpreted as xenocrysts derived from older rocks during ascent of the granite magma. Two grains with $^{206}Pb/^{238}U$ ages of 345 ± 1 and 493 ± 2 Ma are probably derived from the deeper parts of the pluton which may have earlier Paleozoic ages dating back to the Ordovician, whereas grain 4 with a concordant $^{206}Pb/^{238}U$ age of 886 ± 3 Ma indicates the presence of Precam-

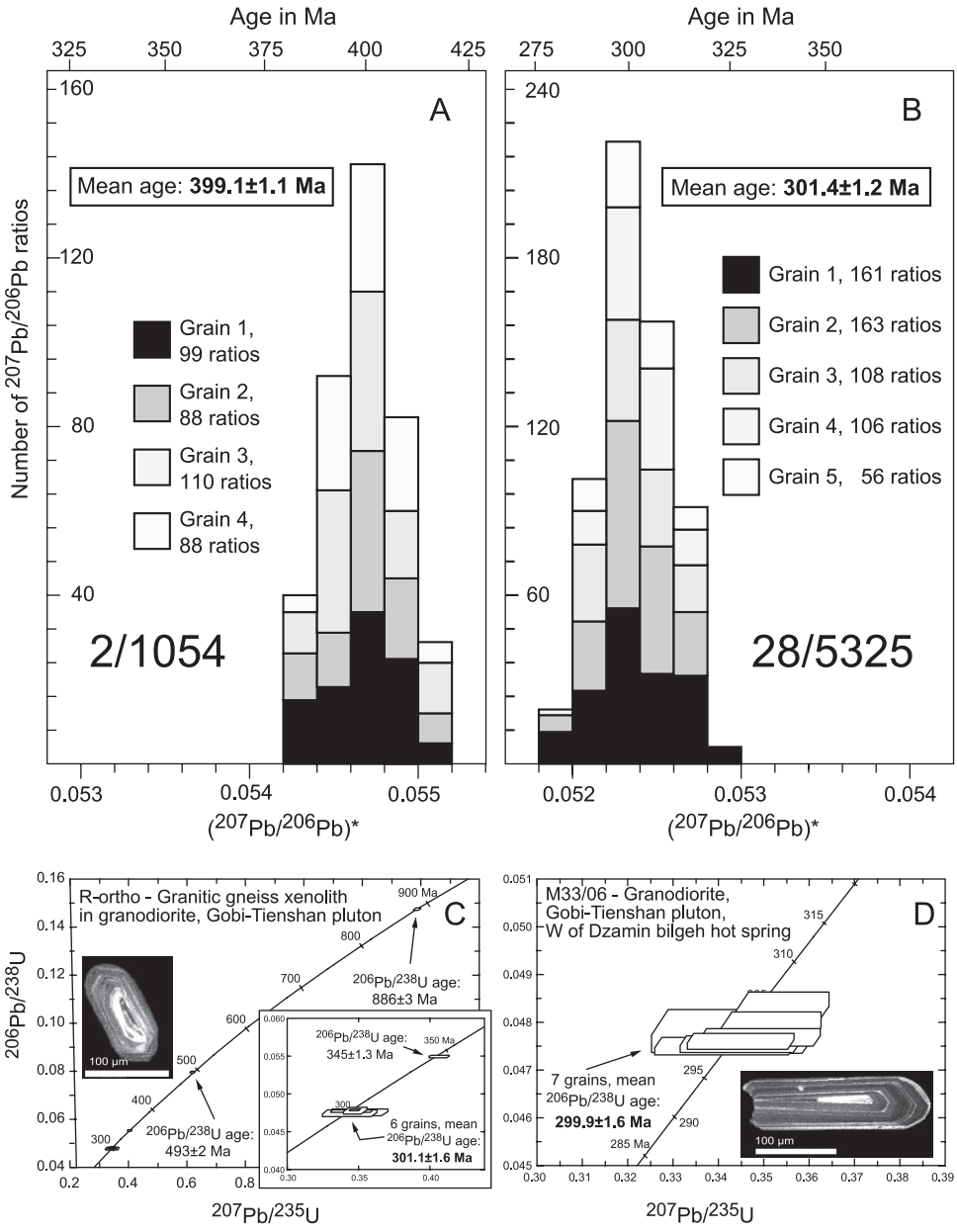

Fig. 9. (A, B). Histograms showing distribution of radiogenic lead isotope ratios from evaporation of single zircons for samples from the South Gobi Zone. (A) Spectrum for four grains from a mylonitic metarhyolite, integrated from 385 ratios. (B) Spectrum for five grains from a leucocratic granite-gneiss, integrated from 594 ratios. (C, D) Concordia diagrams showing SHRIMP II analyses of single zircons for samples from the South Gobi Zone. Data boxes for each analysis and errors on pooled ages as in fig. 6. Insets show typical CL images of dated zircons.

brian crust at depth, probably part of a continental fragment not exposed at the surface. Rocks of this age have also been reported from the South Mongolian microcontinent farther SE in the Gobi Desert (Yarmolyuk and others, 2005).

Sample M33/06 was collected 33 km NW of the Dzamin bilgeh hot spring in a granodiorite terrain representing the NW part of the Gobi-Tienshan magmatic complex. This lithology constitutes the main rock type of the complex (figs. 2, 3, and 4C), and our sample is a coarse-grained granodiorite composed of plagioclase, biotite, amphibole, titanite and rare quartz. Biotite is partially chloritized, and the magmatic fabric is well preserved. Most zircons are clear to slightly yellow-brown and idiomorphic, long-prismatic, but grains with slightly rounded terminations also occur. Grains with small inclusions occur but were avoided during analysis. CL images display spectacular oscillatory zoning or narrow striping, similar to zircons in sample M107/06 (fig. 9D, inset). Seven grains were analyzed on SHRIMP II and provided similar and concordant results (table 1) with a mean $^{206}Pb/^{238}U$ age of 299.9 ± 1.6 Ma (fig. 9D). This is identical to the ages presented above and firmly dates the Gobi-Tienshan complex as latest Carboniferous.

INTERPRETATION OF ZIRCON AGES

The detailed lithological and stratigraphic studies carried out by Russian and Mongolian expeditions during the last century (Markova, 1975; Rauzer and others, 1987; Ruzhentsev and Pospelov, 1992) provide a good basis for identification of accretionary processes and continental growth in the CAOB of southwestern Mongolia. In addition, the currently available isotopic ages (table 3) provide a significant input to better understand thermal processes during crust formation, identification of accretionary episodes and syn- to post-orogenic magmatism during the early and late Paleozoic (fig. 10).

Ages Testifying to Precambrian–Late Cambrian Thermal Events in the Lake Zone

A Proterozoic basement in the Lake Zone had previously not been identified in the study area, and it was the lithological analogy with the Khantaishir Ridge that led us to propose a Precambrian age for gneisses covered by early Paleozoic sediments (fig. 4A). Our oldest zircon crystallization age of 950 ± 16 Ma (sample M523JC) is for a granite-gneiss from the structurally deepest basement unit of the Zamtyn Ridge. Similar ages have previously been reported from western and southern Mongolia, namely in the Dariv and the Khantaishir Complexes (fig. 1B), that are assumed to represent part of the Dzabkhan microcontinent (Kröner and others, 2001; Badarch and others, 2002; Kozakov and others 2002b; Demoux and others, 2009c). In addition, I. K. Kozakov (personal communication, 2007) reports unpublished zircon ages between 840 and 600 Ma from the Dariv Metamorphic Complex. The Havchig basement complex close to Altai City contains ~1127 Ma granite-gneiss (Kröner and others, 2001) and ~840 Ma migmatite (Zhao and others, 2006). Demoux and others (2009c) reported a discrete Grenville-age igneous event from granite-gneisses with zircon protolith emplacement ages between 954 and 983 Ma from the southern slope of the Baga Bogd Massif (Gobi-Altai, southern Mongolia) some 130 km east of our study area along strike. Furthermore, Demoux and others (2009b) reported first evidence for a Grenville-age magmatic event in the Baydrag block south of Bayankhongor Ridge by discovering a 1051 ± 10 Ma granite-gneiss. The broad similarity in late Mesoproterozoic to early Neoproterozoic ages in all these regions may either imply that the Dzabkhan microcontinent is more extensive than previously thought and may underlie large parts of southern Mongolia or, alternatively, this Precambrian continental segment was broken up during late Neoproterozoic to early Paleozoic rifting and now occurs as individual basement blocks or slivers within the Paleozoic arcs.

The second group of zircon ages indicates a late Cambrian thermal event at ~500 Ma (samples M150-06-3, M275) for a leucocratic granite vein crosscutting high-grade basement rocks and for a felsic pyroclastic rock, respectively. These ages indicate an important event associated with intrusion of the adjacent Cambrian Burdnii Gol

granite (~511 Ma, Hanžl and Aichler, 2007) emplaced into Precambrian basement. Importantly, dating of a large granite batholith (Burdnii Gol granite), a dike swarm (sample M150-06-3), and volcanic rocks (sample M275) indicates that the basement rocks were already close to the surface during the late Cambrian. In addition, these ages correspond to late Cambrian magmatism reported by Demoux and others (2009c) for granite, diorite and granodiorite intrusions from the adjacent Baga Bogd Massif. Therefore, the basement of the Lake Zone in the study area shows significant similarities in its thermal evolution to the more easterly exposed Baga Bogd Massif basement marked by late Mesoproterozoic to early Neoproterozoic and Cambrian thermal-magmatic events.

The third group of ages comes from the sedimentary basins covering the basement. Here, the oldest Naran flyschoid formation was traditionally considered to be of Cambrian age (Rauzer and others, 1987; Hrdličková and others, 2008), whereas our study of detrital zircons yielded young ages around 400 Ma (samples M141 and 142), indicating that deposition of these sediments probably occurred in the middle Devonian. The oldest zircons in these sediments yielded early Neoproterozoic to Ordovician ages (813, 553 and 471 Ma; samples M142 and M141, respectively) which suggests input from the underlying basement. Finally, a small sedimentary basin marked by clastic deposits previously considered as Devonian provided early Carboniferous ages of 358 and 350 Ma. It is important to note that no magmatic event of middle Devonian and early Carboniferous age was reported from the Lake Zone and, therefore, clastic flyschoid sedimentation (Naran formation) and the Carboniferous basin presumably reflect erosion of volcanic/magmatic edifices of Devonian-Carboniferous age that were located farther south.

Zircon Ages Reflecting Devonian and Carboniferous Volcanic and Magmatic Event in the Gobi-Altai Zone

The Gobi-Altai high-grade gneisses and granitoids were dated in the area of the Chandman gneiss complex and in the gneiss dome that is interpreted as part of the Tseel "terrane" of Badarch and others (2002). We use here the collective term Gobi-Altai Zone for both the previous Tseel and Gobi-Altai "terranes," as the former was defined as a so-called metamorphic terrane due to lack of modern isotopic ages, whereas the original Gobi-Altai terrane was defined solely on the basis of Paleozoic sedimentary content. In that way our Gobi-Altai Zone corresponds to the Gobi-Altai tectonic zone of some Russian authors (for example, Markova, 1975). Samples taken from a granite body (M103-06-2) and a strongly foliated granite-gneiss (M107-06-2) of the Chandman complex provide two discrete ages of 340 Ma for the former and 350 Ma for the latter rock. This reflects protracted and syntectonic magmatic activity during which early magmatic phases were gneissified before or during intrusion of later magma pulses. A similar age (~345 Ma) was reported for a granitic rock of the Chandman complex (Hrdličková and others, 2008). Dating of a tonalitic gneiss from the southern Gichgene Ridge provided an age of ~364 Ma which corresponds to ages of granitoids (~360 Ma) located farther west in the area of Tsogt (table 3; Kozakov and others, 2002a; Kröner and others, 2007). These ages are also in line with metamorphic zircon ages of ~385 Ma for granulite-facies rocks from the Tseel and Tsogt areas (table 3; Bibikova and others, 1992; Kozakov and others, 2002a). Whole-rock Nd isotopic data published by Kozakov and others (2007a) from the Tseel region suggest that Devonian to Carboniferous granitoids could not have formed from melting of surrounding metasedimentary rocks of the Tugrig formation that show strong Paleoproterozoic inheritance (Kozakov and others, 2009). All geochemical data for these rocks, including the Nd-Sm isotopic systematics, point to a juvenile character for these granitoids and an origin in a mature magmatic arc setting (Kozakov and others, 2007a; Hrdličková and others, 2008). These granitoids exhibit early to late Neoproterozoic Nd model

TABLE 3

Summary table of published geochronological data for the study area

Locality/Unit	Rock type	Age (Ma)	Method[a]	Interpretation	Reference
Lake Zone - Khantaishir ophiolite					
Khantaishir ophiolite	Plagiogranite	568.1±4.0	Zrn U-Pb TIMS	Crystallization	Gibsher and others, 2001
Lake Zone - NE Chandman village					
Zamtyn Range Complex	Orthogneiss	940±44	Zrn U-Pb LA-ICP-MS	Crystallization or inheritance	Hanžl and Aichler, 2007
Zamtyn Range Complex	Orthogneiss	502±31	Zrn U-Pb LA-ICP-MS	Thermal event or crystallization	Hanžl and Aichler, 2007
Zamtyn Range Complex	Orthogneiss	420.3±3 (plateau)	Ms Ar-Ar	Cooling below ~350°C	Hanžl and Aichler, 2007
Zamtyn Range Complex	Diorite	542±4	Zrn U-Pb LA-ICP-MS	Crystallization	Hanžl and Aichler, 2007
Zamtyn Range Complex	Metadiorite	517±5	Zrn U-Pb LA-ICP-MS	Protolith crystallization	Hanžl and Aichler, 2007
Burdnii Gol Granite	Granite	513±4	Mnz Th-Pb LA-ICP-MS	Crystallization	Hanžl and Aichler, 2007
Burdnii Gol Granite	Granite	511±5	Zrn U-Pb LA-ICP-MS	Crystallization	Hanžl and Aichler, 2007
Burdnii Gol Granite	Granite	1511±10	Zrn U-Pb LA-ICP-MS	Inheritance	Hanžl and Aichler, 2007
Burdnii Gol Granite	Granite	467±22	Mnz U-Pb LA-ICP-MS	Crystallization	Hanžl and Aichler, 2007
Burdnii Gol Granite	Pegmatite dike	485.1±3.2	Ms Ar-Ar	Cooling below ~350°C	Hanžl and Aichler, 2007
Tectonic lens along the Main	Leucogranite	518±5	Zrn U-Pb LA-ICP-MS	Crystallization (inheritance)	Hrdličkovà and others, 2008
Mongolian Lineament	Leucogranite	336.6±6	Zrn U-Pb LA-ICP-MS	Uncertain (crystallization)	Hrdličkovà and others, 2008
Metamorphic basement	Felsic pyroclastic rock	501.2±4.87	Zrn U-Pb SHRIMP	Protolith emplacement	This study
Lake Zone - N Chandman village – Zamtyn Range Complex					
Khantaishir formation	Gabbro	973±12	Zrn U-Pb LA-ICP-MS	Unceertain (crystallization)	Hanžl and Aichler, 2007
Khantaishir formation	Gabbro	1.493±33	Zrn U-Pb LA-ICP-MS	Inheritance from protolith	Hanžl and Aichler, 2007
Khantaishir formation	Gabbro	1179±16	Zrn U-Pb LA-ICP-MS	Inheritance from protolith	Hanžl and Aichler, 2007
Undifferenciated Devonian	Felsic volcaniclastic rock	358.7±5.0	Zrn U-Pb SHRIMP	Time of volcanic activity	This study
Undifferenciated Devonian	Grit	406 to 553	Zrn U-Pb SHRIMP	Sediment younger than 406 Ma with Neoproterozoic to Paleozoic source	This study
Naraan formation	Sandstone	397±4	Zrn U-Pb SHRIMP	Maximum age of sediment	This study
Naraan formation Naraan formation	Sandstone	813±15 2594±5	Zrn U-Pb SHRIMP	Neoproterozoic to Archean source	This study
Metamorphic basement	Granitic gneiss dike	1480 (minimum age)	Zrn U-Pb SHRIMP	Inheritance from protolith	This study
Metamorphic basement	Granitic gneiss dike	500.8±3.8	Zrn U-Pb SHRIMP	Crystallization	This study
Metamorphic basement	Granitic gneiss	950±16	Zrn U-Pb SHRIMP	Protolith emplacement	This study
Lake Zone - Baga bogd Massif (East of figs. 2 and 3)					
Neoproterozoic gneiss	Biotite-rich gneiss	498±3	Zrn U-Pb SHRIMP	Crystallization of the protolith	Demoux and others, 2009c
Neoproterozoic gneiss	Granodioritic gneiss	499±3	Zrn U-Pb SHRIMP	Crystallization of the protolith	Demoux and others, 2009c
Neoproterozoic gneiss	Leucogranitic gneiss	501±4	Zrn U-Pb SHRIMP	Crystallization of the protolith	Demoux and others, 2009c
Neoproterozoic gneiss	Augen gneiss	954±8	Zrn U-Pb SHRIMP	Crystallization of the protolith	Demoux and others, 2009c
Neoproterozoic gneiss	Augen gneiss	983±6	Zrn U-Pb SHRIMP	Crystallization of the protolith	Demoux and others, 2009c

TABLE 3
(continued)

Locality/Unit	Rock type	Age (Ma)	Method[a]	Interpretation	Reference
Lake Zone - Baga bogd Massif (East of figs. 2 and 3) continued					
Neoproterozoic gneiss	Fine-grained leucogneiss	502±6	Zrn U-Pb SHRIMP	Crystallization of the protolith	Demoux and others, 2009c
Neoproterozoic gneiss	Granitic gneiss	1519±11	Zrn U-Pb SHRIMP	Crystallization of the protolith	Demoux and others, 2009c
Neoproterozoic gneiss	Granitic gneiss	956±3	Zrn U-Pb SHRIMP	Crystallization of the protolith	Demoux and others, 2009c
North of the Gobi-Altai Zone					
South Bayan Ondor village	Granite	271±7	Zrn U-Pb TIMS	Crystallization	Kozakov and others, 2007a
Chandman Crystallime Complex	Granite	332±29	Mnz CHIME	One grain measured, crystallization	Hrdličkovà and others, 2008
Chandman Crystallime Complex	Granite	345±2	Zrn U-Pb LA-ICP-MS	Crystallization	Hrdličkovà and others, 2008
Northern slope of Gichgene Ridge	Leucocratic orthogneiss	363±3	Zrn U-Pb LA-ICP-MS	Protolith emplacement	Hrdličkovà and others, 2008
Northern slope of Gichgene Ridge	Leucocratic orthogneiss	529±9	Zrn U-Pb LA-ICP-MS	Inheritance from protolith	Hrdličkovà and others, 2008
Northern slope of Gichgene Ridge	Leucocratic orthogneiss	591±10	Zrn U-Pb LA-ICP-MS	Inheritance from protolith	Hrdličkovà and others, 2008
Chandman Crystallime Complex	Granitoid	340.9±2.5	Zrn U-Pb SHRIMP	Crystallization	This study
Chandman Crystallime Complex	Granitic gneiss	350.4±1.7	Zrn U-Pb SHRIMP	Crystallization	This study
South of the Gobi-Altai Zone (« Tseel terrane ») - South of the Erdene village					
Neoproterozoic rhyolite	Feldspar porphyry	278.9±1.8	Zrn U-Pb SHRIMP	Emplacement	Demoux and others, 2009a
Neoproterozoic metavolcaniclastic rock	Rhyolite	397.0±3.2	Zrn U-Pb SHRIMP	Emplacement	Demoux and others, 2009a
Neoproterozoic metavolcaniclastic rock	Rhyolite	396.3±3.3	Zrn U-Pb SHRIMP	Emplacement	Demoux and others, 2009a
Neoproterozoic metavolcaniclastic rock	Cataclastic granite	286.8±1.8	Zrn U-Pb SHRIMP	Crystallization	This study
Neoproterozoic metavolcaniclastic rock	Tonalitic gneiss	363.6±3.9	Zrn U-Pb SHRIMP	Protolith emplacement	This study
Middle Carboniferous granite	Granite	279.6±3.9	Zrn U-Pb SHRIMP	Crystallization	This study
« Tseel terrane » - SW Erdene village					
Neoproterozoic gneiss	Granitic gneiss	360.5±1.1	Zrn Evaporation Pb-Pb	Anatectic melting	Kröner and others, 2007
Neoproterozoic metavolcaniclastic rock	Siltstone	458.2±3.0	Zrn U-Pb SHRIMP	Maximum age of sediment	This study
Neoproterozoic gneiss	Foliated diorite	289.2±2.3	Zrn U-Pb SHRIMP	Crystallization	This study
Middle Carboniferous granite	Foliated granite	295.7±2.2	Zrn U-Pb SHRIMP	Crystallization	This study
« Tseel terrane » - SE Tsogt village					
Polymetamorphic complex	Amphibolite gneiss	384±2	Zrn U-Pb TIMS	High amphibolite facies	Kozakov and others, 2002a
Polymetamorphic complex	Amphibolite gneiss	357.6±5.7	Zrn U-Pb TIMS	Low amphibolite facies	Kozakov and others, 2002a
Polymetamorphic complex	Granitoid gneiss	385±5	Zrn U-Pb TIMS	High amphibolite facies	Bibikova and others, 1992
Polymetamorphic complex	Granitoid gneiss	365±4	Zrn U-Pb TIMS	Low amphibolite facies	Bibikova and others, 1992
Polymetamorphic complex	Granitoid gneiss	371±2	Zrn U-Pb TIMS		Bibikova and others, 1992
« Tseel terrane » - Vicinity Tseel village					
Gashunuur dike complex	Metadiabase porphyrite dike	321±79	Sm-Nd WR	Low amphibolite facies	Baykova and Amelin, 1995
Gashunuur dike complex	Metadiabase porphyrite dike	320±39	Sm-Nd WR		Baykova and Amelin, 1995

Table 3
(continued)

Locality/Unit	Rock type	Age (Ma)	Method[a]	Interpretation	Reference
South of the Gobi-Altai Zone - North of the Shine Jinst village					
Early Devonian migmatite unit	Migmatitic leucosome	292.4±3.6	Zrn U-Pb SHRIMP	Peak of metamorphism	This study
Early Devonian migmatite unit	Migmatitic leucosome	1166±36	Zrn U-Pb SHRIMP	Inheritance from protolith	This study
Early Devonian migmatite unit	Leucocratic granite	410.8±2.0	Zrn U-Pb SHRIMP	Inheritance from protolith	This study
Early Devonian migmatite unit	Leucocratic granite	277.7±2.4 (rims)	Zrn U-Pb SHRIMP	Emplacement	This study
Early Devonian migmatite unit	Leucocratic granite	538±2	Zrn U-Pb SHRIMP	Inheritance from protolith	This study
South of the Gobi-Altai Zone - South of Shine Jinst village					
Lower Permian mafic granitoid	Alcaline granite	231 (mean)	Kfs Ar-Ar	Cooling below ~ 150°C	Lamb and others, 2008
Lower Devonian migmatite	Amphibolite gneiss	295±13 (mean)	Amphibole Ar-Ar	Cooling below ~ 500°C	Lamb and others, 2008
West of the Mandalovoo Subzone – South of Shine Jinst village					
Middle Devonian volcaniclastic rock	Volcanic tuff	170±20 (mean)	Sa Ar-Ar	Thermal event	Lamb and others, 2008
Middle Devonian volcaniclastic rock	Felsic volcaniclastic rock	357.8±3.2	Zrn U-Pb SHRIMP	Emplacement	This study
Middle Devonian volcaniclastic rock	Felsic volcaniclastic rock	477±7	Zrn U-Pb SHRIMP	Detrital age	This study
Late Ordovician to middle Silurian sediment	Sandstone	513 to 2672	Zrn U-Pb SHRIMP	Detrital ages	This study
Late Devonian to Early Carboniferous sediment	Sandstone	382 to 866	Zrn U-Pb SHRIMP	Maximum late Devonian depositional age of the sediment	This study
Early Carboniferous sediment	Sandstone	467 to 535	Zrn U-Pb SHRIMP	Maximum early Ordovician depositional age with Archean to Paleoproterozoic input	This study
Early Carboniferous sediment	Sandstone	513 to 2465	Zrn U-Pb SHRIMP		
Trans-Altai Zone					
S Tsogt village (Khatan Khairkhan uul)	Granitoid	274±6	Zrn U-Pb TIMS	Crystallization	Kozakov and others, 2007a
S of Shine Jinst (Khurvinkharin ridge)	Granitoid	274±5	Zrn U-Pb TIMS	Crystallization	Kozakov and others, 2007a
Edrengin Nuruu	Hornblende diorite	329±1	Zrn U-Pb TIMS	Crystallization	Yarmolyuk and others, 2008b
S Tseel village (Adzh-Bogd massif)	Plagioclase microcline granodiorite	348±1	Zrn U-Pb TIMS	Crystallization	Yarmolyuk and others, 2008b
S Tseel village (Bum massif)	Alkali feldspar granite	294±5	Zrn U-Pb TIMS	Crystallization	Yarmolyuk and others, 2008b

TABLE 3
(continued)

Locality/Unit	Rock type	Age (Ma)	Method[a]	Interpretation	Reference
South Gobi Zone					
NE of Gobi-Tienshan batholith	Granitic gneiss	301.4.1±1.2	Zrn Evaporation Pb-Pb	Protolith crystallization	This study
Central part of Gobi-Tienshan batholith	Granitic gneiss xenolith	301.1±1.6	Zrn U-Pb SHRIMP	Protolith crystallization	This study
Central part of Gobi-Tienshan batholith	Granitic gneiss xenolith	345±1 493±2	Zrn U-Pb SHRIMP	Inheritance from deeper part of the batholith	This study
Central part of Gobi-Tienshan Intrusive Complex	Granitic gneiss xenolith	886±3	Zrn U-Pb SHRIMP	Inheritance from continental fragment	This study
NW of Gobi-Tienshan batholith	Granodiorite	299.9±1.6	Zrn U-Pb SHRIMP	Crystallization	This study
SW Echin-Gol, Tömörtyn Formation, metavolcaniclastic rock (Upper Ordovician? - Lower Devonian?)	Metarhyolite	399.1±1.1	Zrn Evaporation Pb-Pb	Protolith crystallization	This study
Gobi-Tienshan batholith	Granodiorite	302±3	Zrn U-Pb TIMS	Crystallization	Yarmolyuk and others, 2008b

LA-ICP-MS: Laser ablation inductively coupled plasma mass spectrometry. SHRIMP: Sensitive high resolution ion microprobe. TIMS: thermal ionization mass spectrometry; this includes ages derived from single-grain as well as multigrain analyses. CHIME: Chemical Th-U-total Pb isochron method by microprobe. Mineral abbreviations after Kretz (1983); WR refers to whole-rock.

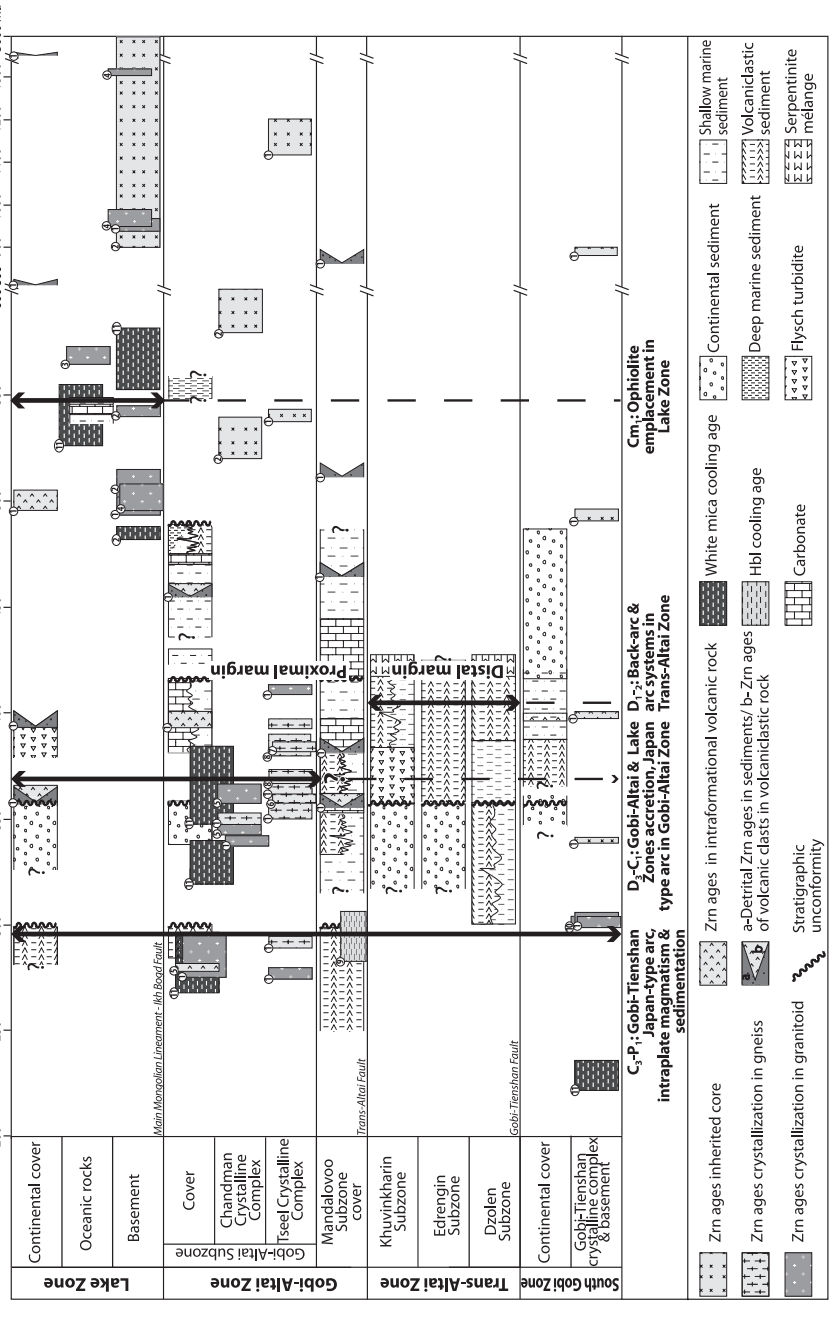

Fig. 10. Summary of published and new zircon ages and published ^{40}Ar-^{39}Ar cooling ages from the Lake, Gobi-Altai, Trans-Altai and South Gobi Tectonic Zones of SW Mongolia. Stratigraphic columns according to the present review and references therein. Circled number in top-left corner of each frame refers to geochronological constraints as follow: 1)—data of this study, 2)—Hanžl and Aichler (2007), 3)—Gibsher and others (2001), 4)—Demoux and others (2009c), 5)—Hrdličková and others (2008), 6)—Kröner and others (2007), 7)—Kozakov and others (2002a), 8)—Bibikova and others (1992), 9)—Lamb and others (2008), 10)—Yarmolyuk and others (2008b), 11)—Lehmann and others (2010). Mineral abbreviations are after Kretz (1983).

ages between 0.95 and 0.60 Ga which broadly correspond to U-Pb zircon ages of Neoproterozoic granitoids from the Lake Zone reported in this study and by Demoux and others (2009c).

The early Devonian cleaved sedimentary rocks (sample M137) provide detrital zircons with a mean age clustering around 458 Ma. The only felsic volcanic rocks in the region that provided an Ordovician age belong to the paleontologically dated Bayantsagaan formation located farther north. More importantly, metarhyolites of the Devonian sequence (previously shown as Neoproterozoic on the 1:200,000 Geological Map of Rauzer and others, 1987) on the southern slope of the Gichgene Ridge provided zircon ages of 396 to 397 Ma, which confirm an early to middle Devonian age for this large basin (Demoux and others, 2009a). The geochemical and Nd isotopic data are consistent with melting of depleted mantle in a transitional back-arc–arc setting, whereas other volcanic rocks indicate an origin from mixed sources involving both juvenile and Precambrian crustal components. Demoux and others (2009a) suggested that the Gobi-Altai magmatic and volcanic association represents the equivalent of a Japan-type arc associated with a juvenile back-arc basin. Finally, dating of a mylonitic quartz porphyry, a pink granite as well as a foliated diorite and granite west of Erdene (samples M65-06-1, M83-06, M132, M135) provide early Permian ages between 280 and 295 Ma which is in line with dating of Demoux and others (2009a) from the same region. This clearly indicates that the Gobi-Altai rock assemblage was affected by widespread early Permian magmatism and volcanism which is a common feature of the boundary between the Lake and Gobi-Altai Zones in SW Mongolia (Coleman, 1989; Kovalenko and others, 1995; Yarmolyuk and others, 2007, 2008c).

Zircon Ages from the Contact of the Gobi-Altai and Mandalovoo Zones

Two samples from the southernmost termination of the Gobi-Altai Zone yielded early Permian zircon ages for a granite leucosome in a migmatite (292 Ma, sample M60/06-1) and a pink granite intrusive into the same migmatite (278 Ma, sample M62/06-2). More importantly, zircon cores from the latter sample show an early Devonian (410 Ma) age which is consistent with ages of volcanism (Demoux and others, 2009a) and is slightly older than high-grade metamorphism from dated samples 70 and 120 km farther west along strike in the same Zone (Bibikova and others, 1992; Kozakov and others, 2002a). These data confirm that this part of the Gobi-Altai Zone was strongly affected by widespread crustal melting during the early Devonian which was probably related to the development of a migmatitic domain and associated intrusive bodies. This melting event most likely affected Devonian protoliths which are the most common volcanic and deep crustal magmatic rocks of the Gobi-Altai Zone.

In contrast, a sample taken from the adjacent Mandalovoo sequence reflects early Carboniferous volcanic activity (~357 Ma, sample M200) affecting late Devonian rocks of the Indert formation (fig. 4B) with Ordovician inheritance and a range of detrital zircons in a Devonian sandstone ranging from 380 to 440 Ma. All these data suggest that the sediments record detrital zircon input from adjacent volcanic provinces which were active between the Silurian and middle Devonian. Late Ordovician sandstones (samples M205 and M207) from the same section provide middle to late Cambrian and middle to late Ordovician ages which indicate a provenance from early Paleozoic material that has so far not been recognized in the Gobi-Altai Zone. Samples M208 and M209 from the same late Ordovician sandstone unit provide a spectrum of ages ranging from early Neoproterozoic to late Cambrian. All these ages are commonly found in different parts of the Lake Zone basement as well as in Khantaishir ophiolitic fragments farther north. In fact, the main difference between the Mandalovoo and Gobi-Altai Zones is seen in the absence of the Tugrig formation of unknown age (probably Neoproterozoic) and of voluminous Devonian to Carboniferous magma-

tism. In contrast, early Ordovician and Neoproterozoic zircons in late Ordovician clastic sediments suggest erosional input from the Lake Zone and an affinity with the Gobi-Altai Zone during the Ordovician.

Protolith-Related Zircon Ages and the Formation of the Late Carboniferous Gobi-Tienshan Magmatic Arc

The oldest age from the South Gobi Zone or Atasbogd "terrane" (Badarch and others, 2002) comes from the presumed late Ordovician Tömörtyn zone where a strongly mylonitic felsic volcanic rock was dated at ~400 Ma (sample 2/1054). This age confirms the importance of early Devonian felsic volcanism in southern Mongolia. In contrast, migmatites, migmatitic orthogneiss and a granodiorite-granite suite of the Gobi-Tienshan pluton provided late Carboniferous ages clustering around 300 Ma. The calc-alkaline character of this intrusion and its large volume of gabbroic rocks suggest that this plutonic complex is part of a late Carboniferous magmatic arc. Our speculative interpretation that this arc evolved on older crust is so far only based on one early Ordovician (493 Ma) and one early Neoproterozoic xenocrystic zircon (886 Ma, sample R-ortho). Nevertheless, these ages correspond to those from other basement regions ("terranes") of south Mongolia such as the nearby Tsagan Uul "terrane" of Badarch and others (2002) where Kozakov (1986) reported a Pb-Pb zircon age of 770 Ma for an aplitic granite and Wang and others (2001) determined a U-Pb zircon age of ~916 Ma for a granite gneiss. Rocks of late Grenvillian age were also reported from the eastern continuation of the South Mongolian basement where Yarmolyuk and others (2005) dated an early Neoproterozoic gneiss (~952 Ma) intruded by an early Paleozoic granodiorite (~433 Ma).

IMPROVED MODEL FOR THE ACCRETIONARY HISTORY OF SW MONGOLIA

Our zircon ages in combination with the established lithostratigraphy (figs. 4A-C) enable us to propose an improved model for the sequence of accretionary events in SW Mongolia (fig. 11). Instead of strike-slip imbrications of the large Tuva-Mongol arc (Şengör and others, 1993) or accretion of exotic terranes (Badarch and others, 2002) we explain the geology of SW Mongolia as resulting from polyphase magmatic reworking of a Silurian-Devonian passive margin of a large microcontinent in the Paleoasian ocean.

Early Cambrian Accretionary Complex Emplacement, Followed by Late Cambrian Magmatism and Volcanism in a Continental Domain (Fig. 11A)

We have shown that the late Mesoproterozoic to early Neoproterozoic basement of the Lake Zone (>1127-755 Ma) was overprinted by a late Cambrian thermal and magmatic event. The zircon ages, corroborated by whole-rock Nd model ages from the Gobi-Altai Zone (Kozakov and others, 2007a), suggest melting of early Neoproterozoic juvenile protoliths. Furthermore, the Tugrig formation, which is the structurally deepest lithostratigraphic unit of the Gobi-Altai Zone, probably received clastic material from a basement of this age (Kozakov and others, 2007a; 2009). Early Neoproterozoic detrital zircons were repeatedly found in Ordovician and Devonian sediments of the Mandalovoo Subzone, and similar age zircon xenocrysts occur in granitoids of the Gobi-Tienshan pluton. These ages suggest that a large area of SW Mongolia contains remnants of a Precambrian basement. The accretionary complex made up of the Khantaishir and Tsakhir Uul formations and obducted on the Lake Zone basement may represent the suture zone of a small oceanic domain closed in early Cambrian times. Because basement rocks of the Lake Zone extend up to the Bayankhonghor ophiolite Zone, some 150 km to the NNE, the only open area where the accreted material could have originated from was located to the south of the E-W trending Lake Zone. Thus we interpret the eclogitic complex as a klippe emplaced

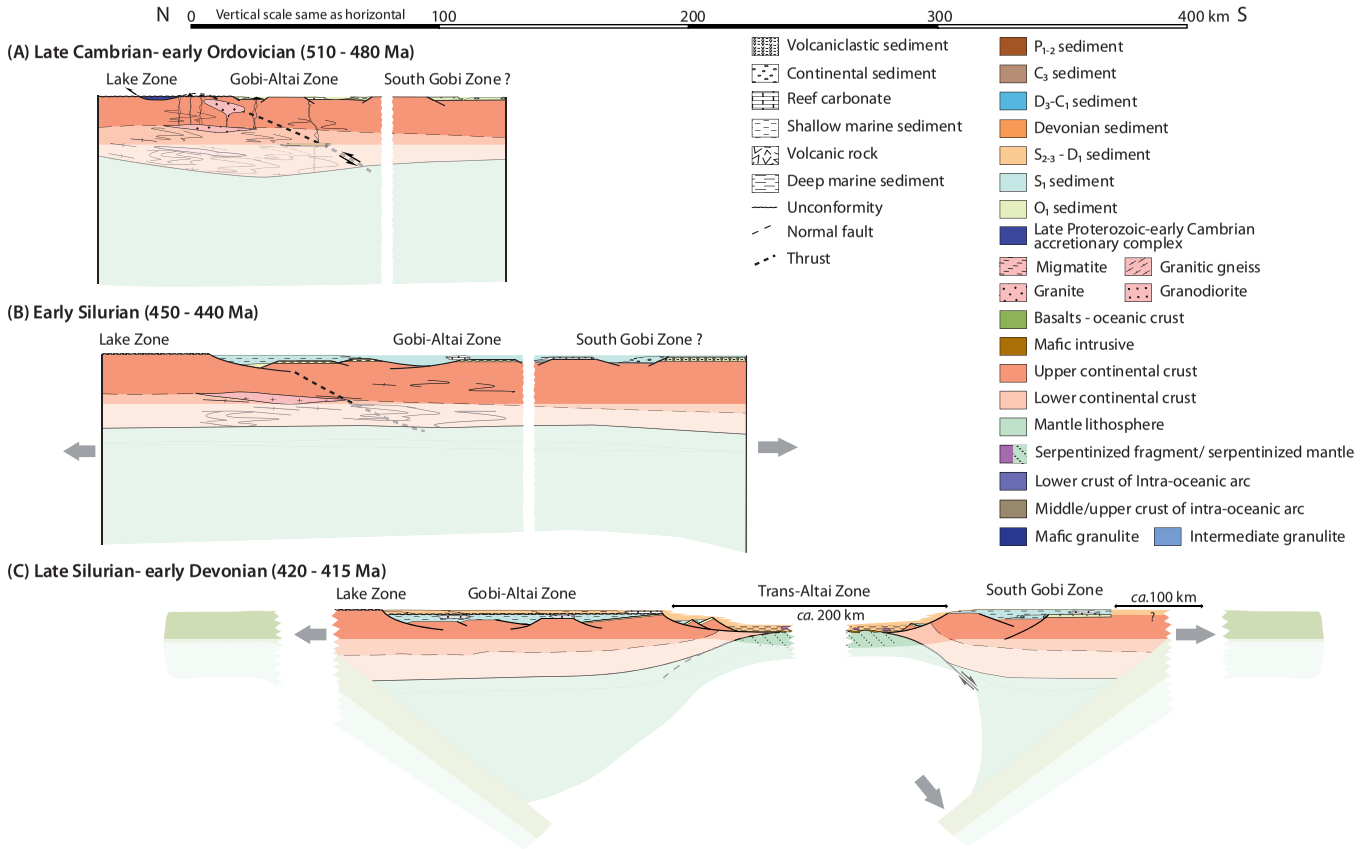

Fig. 11. Tectonic evolution shown as idealized cross sections through time. (A) Late Cambrian to early Ordovician thermomechanic relaxation of the thickened Lake Zone inducing magmatism in Lake and possibly Gobi-Altai Zones. (B) Early Silurian shallow-water sedimentation in Gobi-Altai and South Gobi Zones. (C) Late Silurian to early Devonian opening of the Trans-Altai oceanic domain and exhumation of mantle rocks.

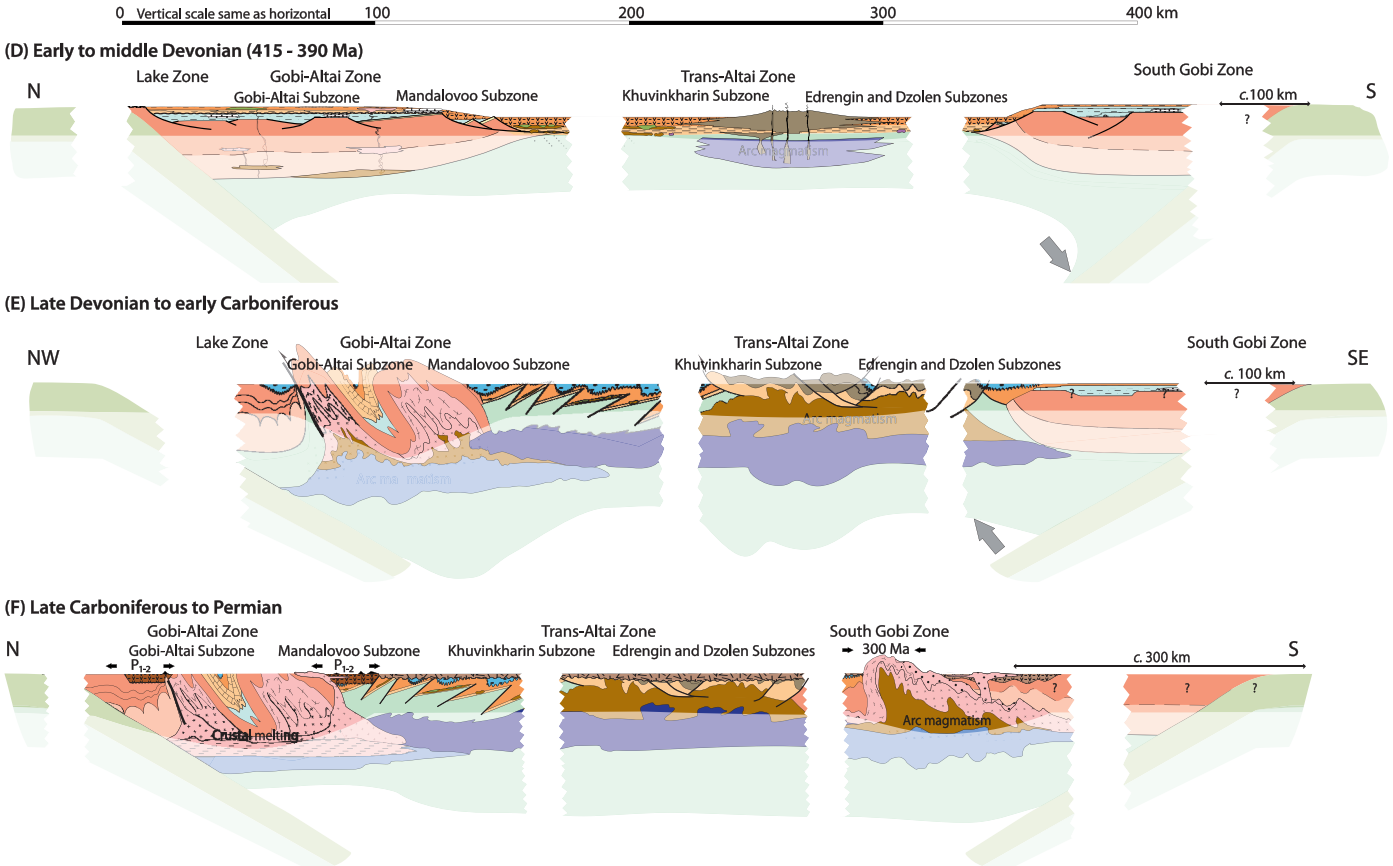

Fig. 11. (Continued) (D) Early to middle Devonian arc/back-arc systems in the Trans-Altai Zone. (E) Late Devonian to early Carboniferous Japan-type arc in the Gobi-Altai Zone with subsequent accretion with Lake Zone. (F) Late Carboniferous Japan-type arc in the South Gobi Zone associated with homogeneous volcaniclastic sedimentation in the Trans-Altai and South Gobi Zones.

during a northward thrusting event. This is in good agreement with obduction kinematics of discrete ophiolitic blocks resting on top of the Lake Zone basement farther west in the Khantaishir and Dariv Ranges (Ruzhentsev and Burashnikov, 1996; Dijkstra and others, 2006). The continental mass which resulted from closure of this small oceanic domain, perhaps part of the Dzabkhan microcontinent (Kozakov and others, 2007b) or the Central Mongolia Terrane assemblage of Badarch and others (2002), experienced a thermal event in late Cambrian times. Isostatic and thermal relaxation after the collision event is shown by ~500 Ma ages in the Lake Zone basement, the age of an angular unconformity marked by the transgression of the Bayantsagaan formation over the deformed basement in the Gobi-Altai Zone (fig. 4B), and the occurrence of 500 Ma zircons in late Ordovician strata of the Mandalovoo Subzone (fig. 4B). The onset of Ordovician clastic sedimentation (Tömörtyn formation) on continental crust of the future Atasbogd "terrane" may have similar significance. The late Cambrian magmatism suggests thermal rejuvenation of the Precambrian crust and the development of Ordovician proximal sedimentary sequences rimming the southern edge of the Dzabkhan microcontinent that culminated in the formation of a late Silurian–early Devonian ocean basin in the future Trans-Altai Zone (Kovalenko and others, 1995) (figs. 11B and C).

Development of a Late Silurian-Devonian Passive Margin and Late Silurian-Devonian Marine Domain (Figs. 11B and 11C)

Heterogeneous stretching of the Dzabkhan lithosphere led to thinning of the continental crust and locally to exhumation of serpentinized mantle as shown on recent and ancient examples of passive margins (Manatschal and others, 2006). At the same time, a carbonate-rich sedimentation occurred on the future Mandalovoo Subzone while Silurian clastic shallow-marine sediments continued to be deposited in the region of the future Gobi-Altai Zone (fig. 4B). This architecture may be interpreted in terms of proximal passive margins, with the Gobi-Altai sedimentary record reflecting areas closer to the continent and Mandalovoo closer to the ocean (for example, Wilson and others, 2001).

Ruzhentsev and others (1991) and Ruzhentsev and Pospelov (1992) proposed that the structurally deepest unit of the entire Trans-Altai domain is represented by Silurian ophiolites and early Devonian radiolarian-bearing jasper sequences. According to these authors, the ophiolite of the Dzolen Ridge and other minor ophiolite fragments dispersed throughout the Trans-Altai Zone represent ocean floor of the Paleoasian Ocean which opened during the early Devonian. Some authors even suggested that continental breakup already occurred during the late Ordovician (Zonenshain and others, 1975; Kovalenko and others, 1995), but no convincing isotopic data exist to support this interpretation. Zonenshain and others (1975) observed an ultramafic mélange in the Dzolen Range that consists of peridotites preserved in blocks of varying sizes and floating in a sheared serpentinite groundmass. Furthermore, Ruzhentsev and others (1991) reported that jaspilite together with serpentinized mantle rocks occurs in mélanges, and the development of tectono-sedimentary breccias occurred before the onset of Devonian volcanism. The development of these tectono-sedimentary breccias above strongly serpentinized peridotite is a typical feature of exhumed mantle and is interpreted as a result of strong normal shearing along lithosphere-scale detachments associated with exhumation of serpentinized mantle domes (Manatschal and others, 2006). In this way the entire geometry of the Lake, Gobi-Altai and Trans-Altai Zones can be regarded as reflecting a passive margin where the former two zones represent proximal and the latter a distal margin related to exhumation of the mantle. The South Gobi Zone reveals a clastic Ordovician sedimentary record, similar to the northern zones, and may be regarded as a conjugate margin related to rifting of the Dzabkhan microcontinent or as a separate block which

was detached from the passive margin and travelled to the south during Silurian and Devonian spreading. This model also satisfies interpretations of previous authors who considered the southern Mongolia basement regions (Tsagan Uul and Hutag Uul "terranes") to be rifted off the main Tuva-Mongolian (or Central Mongolian Massif) continent (for example, Mitrofanov and others, 1981). However, as pointed out by Badarch and others (2002), the Silurian-Devonian strata in these areas do not contain brachiopods of Siberian affinity (Rong and others, 1995) which led them to propose that the South Gobi area has an affinity closer to the Tarim and North China cratons.

Devonian Back-arc Basin and Magmatic Arc Systems (Fig. 11D)

The second important extensional event occurred during the early Devonian and is marked by an unconformity reported from the Gobi-Altai and Mandalovoo Zones (Markova, 1975). Stretching of the crust resulted in the formation of a Devonian basin in the region of the Gobi-Altai Zone with both back-arc and arc affinities as shown by the chemistry of volcanic rocks and new Devonian zircon ages for the basin volcanic rocks (Demoux and others, 2009a). The Devonian clastic sediments of the Mandalovoo Subzone also contain a range of early to middle Devonian zircons that point to important volcanic activity in the region which was well documented by Lamb and Badarch (2001). These authors suggested a back-arc basin, based on both sedimentological and geochemical arguments. Hence, back-arc stretching probably affected the entire Gobi-Altai Zone and probably also adjacent parts of the Trans-Altai Zone. Devonian crustal stretching is not known from the South Gobi Zone, but our zircon age for a volcanic rock of the Tömörtyn formation suggests that some thermal event must have occurred there.

The early Devonian basalt and basalt-andesite volcanism was associated with major volcanic activity in the Trans-Altai Zone and is paleontologically dated by several synchronous bioherms (Markova, 1975; Ruzhentsev and Pospelov, 1992) and subsequently by the isotopic study of Helo and others (2006). The volcanic rocks unconformably overlie late Silurian–early Devonian deep marine sediments and mantle rocks. This major volcanism may suggest increased spreading in the oceanic domain south of the Gobi-Altai Zone (in recent coordinates), associated with the formation of several intra-oceanic arcs in this area as shown, for example, by basalt-andesite volcanism (Ruzhentsev and others, 1991) on the Gurvansaykhan and Dzolen Ridges which clearly shows an intraoceanic arc signature (Lamb and Badarch, 2001; Helo and others, 2006). Thus, the model of earlier Russian authors (Markova, 1975; Ruzhentsev and others, 1991; Ruzhentsev and Pospelov, 1992) that a large oceanic domain existed between the Gobi-Altai Zone in the north and the South Gobi Zone in the south during the Silurian and Devonian receives support from modern studies (fig. 10). The Trans-Altai rocks represent a Silurian ocean floor on which early Devonian back-arc and arc sequences developed that were subsequently juxtaposed during transcurrent faulting and associated folding in a complex puzzle which is not yet satisfactorily resolved.

It is possible, however, that the back-arc and arc structures were established on a previously developed continental margin as shown by early Devonian sediments unconformably overlying Ordovician and Silurian strata in the continent-derived South Gobi Zone and by destruction of the Silurian carbonate platform in the Mandalovoo Subzone as shown by the presence of Ordovician and Silurian corals in basal Devonian conglomerates (Alekseyeva, 1981; 1993). In addition, the volcanic sequence unconformably overlies strongly deformed and weakly metamorphosed tectono-sedimentary breccias and serpentinites of the Trans-Altai oceanic domain (Markova, 1975; Ruzhentsev and others, 1991; Kovalenko and others, 1995). All this may indicate that the early Devonian back-arc and arc sequences did not develop in

continuity with the Ordovician-Silurian margin architecture but during an independent and distinct event superimposed on a previous episode of continental stretching.

Late Devonian–Early Carboniferous Arc Formation and First "Terrane" Accretion (Fig. 11E)

Several zircon ages (Hrdličková and others, 2008; this work), geochemical data (Kozakov and others, 2007a; Economos and others, 2008) and metamorphic petrology (Kozakov and others, 2002a) suggest that the Gobi-Altai Zone constitutes a Japan-type magmatic arc, partly developed on older continental crust and on products of an early back-arc Devonian basin. Most significant are the Devonian Naran flysch basins (previously interpreted as Cambrian) that contain 400 Ma old detrital zircons that are most likely derived from erosion of the volcano-sedimentary upper part of the Gobi-Altai edifice. The younger early Carboniferous basins with clastic rocks (previously late Devonian) in the Lake Zone contain early Carboniferous zircons whose age coincides with that of arc magmatism in the Chandman Mountains but also in other parts of the Gobi-Altai Zone (Bibikova and others, 1992; Kozakov and others, 2002a). We suggest that deposition of clastic material indicates progressive exhumation and erosion of the Gobi-Altai arc province which first yielded early Devonian detrital zircons, followed by early Carboniferous growth of a deep crustal gneiss and granite dome associated with melting of deep magmatic rocks. This corroborates the existence of early Carboniferous intramontane basins, reported by Markova (1975) from both the Lake and Gobi-Altai Zones, which unconformably overlie the early Paleozoic sediments and indicate important tectonic activity in both domains.

In summary, our zircon ages as well as the stratigraphy of the Lake and Gobi-Altai Zones are compatible with welding of both domains during the late Devonian to early Carboniferous (fig. 11C). Docking of the Gobi-Altai arc with the Lake Zone basement must have been soft to avoid severe deformation of the Lake Zone continental margin. The Trans-Altai Zone is characterized by imbrication of strongly schistose Silurian and Devonian deposits (Eengin, 1978) and thrusting of Silurian ophiolites over early to middle Devonian sequences in the Dzolen Ridge (Zonenshain and others, 1975). The age of thrusting is unknown, and Russian authors, although meticulous in stratigraphy, were careful in proposing time constraints for this event. However, it is possible that nappe stacking occurred before onset of clastic late Devonian and early Carboniferous sedimentation and certainly before onset of late Carboniferous volcanism which was not affected by this deformation. This may indicate that contraction occurred there as well, but to a lesser extent than in the northern zones. It is therefore possible that the Trans-Altai Zone records a period of shortening between the late Devonian and Carboniferous that may have been related to thrusting of the Dzolen ophiolites over the early Devonian rocks. The early Carboniferous sediments are also transgressive in the South Gobi Zone, and we speculate that greenschist-facies metamorphism of the Tömörtyn formation as well as lower greenschist-facies deformation of the Devonian sequences may record the same Carboniferous shortening event as in the Trans-Altai Zone. The early Carboniferous unconformity is probably the most important event in all of SW Mongolia, whereas accretion seems only firmly established between the Gobi-Altai and Lake Zones.

Late Carboniferous Arcs and Permian Thermal Event (Fig. 11F)

Late Carboniferous sedimentary, magmatic and volcanic activity is characteristic of the Trans-Altai and South Gobi Zones. The former is characterized by major felsic and andesitic volcanism in the late Carboniferous, pointing to an arc type environment. This volcanic arc was partly superimposed on a previously developed early Devonian back-arc–volcanic arc association and late Devonian clastic sediments. Similarly, the composite Gobi-Tienshan pluton in the South Gobi Zone was generated from both juvenile calc-alkaline magmatism and crustal melting. Migmatites, anatectic

orthogneiss, and a granodiorite-tonalite suite, all dated at ~300 Ma, suggest that a major magmatic arc developed on the older crust of this zone. The fact that subaeral andesitic volcanism occurred in the Trans-Altai region whereas deep arc magmatism affected the Gobi-Tienshan crust may indicate that both volcano-magmatic provinces were not too distant from each other.

In summary, magmatic activity migrated to the south in the late Carboniferous where a large magmatic arc developed in a compressive setting, similar to that of the Gobi-Altai arc. Therefore, the Gobi-Tienshan arc shows many features similar to the Devonian arc such as the presence of migmatites, high temperature/low pressure metamorphism, and a dominance of gabbro-granodiorite magmas together with crustal-melt granites. These features may be interpreted as another Japanese-type arc established on continental crust. Our study shows how arc magmatism migrated over a vast domain from the Devonian continental magmatic arc in the Gobi-Altai in the north, via Devonian and late Carboniferous arcs in the Trans-Altai Zone, to a continental late Carboniferous magmatic arc in the south.

Late Paleozoic magmatism as documented in the Gobi-Altai Zone belongs to a wide zone of early Permian bimodal volcanism (basalt and trachyrhyolite). This belt is genetically related to important Permian grabens that follow the trend of the Main Mongolian lineament and affected the entire Gobi-Altai Zone. The formation of Permian intracontinental basins is related to the intrusions of large volumes of peralkaline magmas (Kovalenko and others, 1995), diorites and gabbros. In the study area, 290 and 270 Ma Permian magmatic and volcanic events were responsible for major thermal perturbations on a crustal scale, leading to local melting of the crust and formation of migmatites. A major deformation event of late Permian to early Jurassic age (Lamb and others, 2008) also affected the entire domain and implies continuous stress transfer across the assembled crust. Kovalenko and others (1995) pointed out that the late Paleozoic in southern Mongolia is characterized by extensive igneous and tectonic activity that was concentrated in two major E-W trending belts (Gobi-Altai and Gobi-Tienshan bimodal complexes) that are reported in this study. Both volcanic and graben provinces evolved on continental crust and cross-cut various "terrane" boundaries (fig. 31 in Kovalenko and others, 1995). We therefore conclude that the proximal and distal passive margins, including the oceanic domain and the southerly continental domain (South Gobi Zone), were assembled into a single continental block prior to the late Paleozoic.

CONCLUSIONS

A review of the published lithological and paleontological database, combined with new zircon dating and a structural analysis (Lehmann and others, 2010) leads us to propose a revised geodynamic model for the evolution of SW Mongolia in the Paleozoic. We argue that neither accretion of suspect terranes nor strike-slip imbrication of a large magmatic arc were responsible for the present geometry of the CAOB in SW Mongolia. Instead, we propose a model of repeated magmatic reworking of proximal and distal passive margin sequences during the Paleozoic.

All litho-tectonic units are interpreted here in terms of heterogeneous stretching of a Precambrian continental basement (Dzabkhan microcontinent?) during the late Ordovician to early Silurian. The northern continental margin (Lake Zone) reveals features of thermal reworking around 500 Ma, whereas the presence of early Neoproterozoic and early Ordovician zircons in Ordovician sediments and the development of a Silurian carbonate platform on adjacent continental domains (Gobi-Altai Zone) reveal characteristics of proximal parts of a passive margin. The Trans-Altai Zone, characterized by tectono-sedimentary breccias and a serpentinite-peridotite mélange, indicates exhumation of mantle rocks during the Silurian on the distal passive margin.

The South Gobi Zone may be regarded either as the conjugated margin of a paleorift or as an independent ribbon continental block.

The early Devonian is characterized by formation of back-arc basins on continental crust (proximal margin), destruction of the Silurian platform, and formation of back-arcs and intra-oceanic volcanic arcs on serpentinized mantle rocks and chert-serpentinite breccias of the distal margin sequences. This event is probably related to opening of an oceanic domain.

The late Devonian to early Carboniferous was a period of emplacement of a large magmatic arc in a compressive regime on the Gobi-Altai continental crust. Exhumation and erosion of Devonian back-arc basins and the high-grade core of the arc are responsible for deposition of Devonian and Carboniferous zircons in intramontane basins on the continental Lake Zone. At this time the oceanic domain was imbricated and subsequently covered unconformably by Carboniferous clastic sediments. The major deformational event affecting the CAOB in SW Mongolia therefore occurred in the early Carboniferous.

The late Carboniferous was characterized by the development of a volcanic arc on the Trans-Altai oceanic crust and a deep-seated Japan-type magmatic arc on the Gobi Tienshan continental crust. Finally, early Permian thermal reworking related to widespread perakaline magmatism, crustal melting and bimodal volcanism affected the boundary between the Gobi-Altai and Lake Zone continental domains.

ACKNOWLEDGMENTS

This is a collaborative study of Strasbourg and Mainz Universities with the Department of Geology and Mineral Resources, Mongolian Academy of Sciences, and was partly funded by the Volkswagen Foundation of Germany, Grant I/76399 to AK, grants of Strasbourg University and the French CNRS to KS, and support of the Beijing SHRIMP Center. The grant MSM0021620855 of the Ministry of Education of the Czech Republic is acknowledged for salary and financial support of Ondrej Lexa. Research of AD was supported by the German Research Foundation (DFG) through grant GK392 "Composition and Evolution of Crust and Mantle." We thank Rita Economos for providing sample R-ortho, Annie Bouzeghaia for helping draw figures 10 and 11, Claude Roquin for helping process the DEM map of figure 2, to Qing Ye for preparing the SHRIMP mounts, and to Hui Zhou for producing most of the CL images. We acknowledge constructive reviews by J. F. Dewey and B. F. Windley. Some of the zircon analyses were carried out on the sensitive high-resolution ion micro-probe mass spectrometer in Perth (SHRIMP II), operated by a consortium consisting of Curtin University of Technology, the Geological Survey of Western Australia, and the University of Western Australia, with the support of the Australian Research Council. This is publication number 630 of the Mainz Research Center "Earth System Science," and also a contribution to the ERAS-Project of the International Lithosphere Program (ILP) and to IGCP 480.

Appendix: Analytical Methods

Cathodoluminescence imaging and SHRIMP zircon dating.—Zircons were handpicked and mounted in epoxy resin together with chips of the Perth zircon standard CZ3. The mount was then ground and polished to expose the interiors of the zircons, and the polished mounts were then imaged under cathodoluminenscence (CL) to reveal the internal structure of the grains and to select suitable domains for analysis. CL imaging in the Beijing SHRIMP Center was performed on a Hitachi SEM S-3000N equipped with a Gatan ChromaCL detector and a DigiSan II data recorder, operating at 9 kV accelerarting voltage and 99 μA beam current. CL imaging in Perth was undertaken in the Centre for Microscopy and Microanalyis at the University of Western Australia on a JEOL 6400 SEM, operating at 15 kV accelerating voltage and 5 nA beam current. The instrumental details of the SHRIMP II instruments in Perth and Beijing are summarized in De Laeter and Kennedy (1998). For data collection, six scans through the critical mass range were made, and the Prawn, WALLEAD and Plonk data reduction programs (Williams and others, 1996; Nelson, 1997) were used for data processing. Details on the analytical procedure and data reduction are summarized in Compston and others (1992), Stern (1997), Nelson (1997), and Williams (1998). Primary beam intensity was

between 2 and 4 nA, and a Köhler aperture of 100 μm diameter was used, giving a slightly elliptical spot size of about 30 μm. Sensitivity was between 20 and 26 cps/ppm/nA ^{206}Pb on the standard CZ3. Analyses of samples and standards were alternated to allow assessment of Pb^+/U^+ discrimination. The 1-σ error in the ratio $^{206}Pb/^{238}U$ during analysis of all standard zircons for each analytical session in Perth and Beijing was between 0.88 and 1.33 percent. Common-Pb corrections have been applied using the ^{204}Pb-correction method. In case of low counts on ^{204}Pb (less than 3 times background) it was assumed that common lead is surface-related (Kinny, 1986), and the isotopic composition of Broken Hill lead was used for correction. For ^{204}Pb counts more than 3 times background the values of Cumming and Richards (1975) were applied. Absolute U and Th concentrations and isotopic ratios were determined relative to the CZ3 standard zircon ($^{238}U/^{206}Pb$ age = 561.5 Ma; ^{238}U = 551 ppm, Nasdala and others, 2008), and ages were calculated using the decay constants recommended by Steiger and Jäger (1977). The analytical data are presented in table 1. Errors on individual analyses are given at the 1-sigma level and are based on counting statistics (for details see Stern and Amelin, 2003) and include the calibration uncertainty in the standard U/Pb age added in quadrature (Nelson, 1997) and the common-Pb correction. Errors for pooled analyses are at the 2-sigma or 95 percent confidence interval. The data are graphically presented on conventional concordia plots.

Single zircon evaporation.—Our laboratory procedures as well as comparisons with conventional and ion-microprobe zircon dating are detailed in Kröner and others (1991) and Kröner and Hegner (1998). Isotopic measurements were carried out on a Finnigan-MAT 261 mass spectrometer at the Max-Planck-Institut für Chemie in Mainz.

The calculated ages and uncertainties are based on the means of all ratios evaluated and their 2σ mean errors. Mean ages and errors for several zircons from the same sample are presented as weighted means of the entire population. During the course of this study we repeatedly analyzed fragments of large, homogeneous zircon grains from the Palaborwa Carbonatite, South Africa. Conventional U-Pb analyses of six separate grain fragments from this sample yielded a $^{207}Pb/^{206}Pb$ age of 2052.2 ± 0.8 Ma (2σ, W. Todt, unpublished data), whereas the mean $^{207}Pb/^{206}Pb$ ratio for 19 grains, evaporated individually over a period of 12 months, was 0.126634 ± 0.000027 (2σ error of the population), corresponding to an age of 2051.8 ± 0.4 Ma, identical to the U-Pb age. The above error is considered the best estimate for the reproducibility of our evaporation data and corresponds approximately to the 2σ (mean) error reported for individual analyses in this study (table 2). In the case of combined data sets the 2s (mean) error may become very low, and whenever this error was less than the reproducibility of the internal standard, we have used the latter value (that is, an assumed 2σ error of 0.000027).

The $^{207}Pb/^{206}Pb$ spectra are shown in histograms that permit visual assessment of the data distribution from which the ages are derived. The evaporation technique provides only Pb isotopic ratios, and there is no *a priori* way to determine whether a measured ratio reflects a concordant age. Thus, all $^{207}Pb/^{206}Pb$ ages determined by this method are necessarily *minimum* ages. However, many studies have demonstrated that there is a very strong likelihood that these data represent true zircon crystallization ages when (1) the $^{207}Pb/^{206}Pb$ ratio does not change with increasing temperature of evaporation and/or (2) repeated analyses of grains from the same sample at high evaporation temperatures yield the same isotopic ratios within error. Comparative studies by evaporation, conventional U-Pb dating, and ion-microprobe analysis have shown this to be correct (see Kröner and others, 1999 for summary and additional references).

References

Afanas'yeva, G. A., 1992, New species of Devonian and Carboniferous Chonetida (Brachiopoda) of Mongolia, *in* Tatarinov, L. P., Lubsandanzan, B., Afanas'yeva, G. A., Barsbold, R., Morozova, I. P., Novitskaya, L. I., Rasnitsyn, A. P., Reshetov, V. Y., Rozanov, A. Y., Sysoyev, V. A., and Trofimov, B. A., editors, New species of fossil invertebrates of Mongolia: Moscow, Nauka Press, Transaction of Joint Soviet-Mongolian Scientific Research Geological Expedition, v. 41, p. 56–60 (in Russian).

Alekseyeva, R. E., 1981, Brachiopods and biostratigraphy of Lower Devonian of Mongolia: Moscow, Nauka Press, Transactions of Joint Soviet-Mongolian Paleontological Expedition, 176 p. (in Russian).

——— 1993, Biostratigraphy of Devonian of Mongolia: Moscow, Nauka Press, Transactions of Joint Soviet-Mongolian Paleontological Expedition, 135 p. (in Russian).

Amantov, V. A., Borzakovskyi, Y. A., Luvsandanzan, B., Chasin, R. A., and Churts, C., 1968, Main features of tectonics of Mongolia, *in* Works of Soviet geologists in XXIII symposium of the International Geological Congress, Problem 3. Orogenic zones: Moscow, Nauka Press (in Russian).

Amantov, V. A., Blagonravov, V. A., Borzakovskiy, Y. A., Durante, M. V., Zonenshain, L. P., Luvsandanzan, B., Matrosov, P. S., Suyetenko, O. D., Filippova, I. B., and Hasin, R. A., 1970, Main features of Paleozoic stratigraphy of Mongolian People's Republic, *in* Zaitsev, N. S., Luvsandanzan, B., and Marinov, N. A., editors, Stratigraphy and tectonics of the Mongolian People's Republic: Moscow, Nauka Press, p. 8–63.

Badarch, G., 1982, Geology of the area of Shine Jinst, Gobi-Altai Province: Ulaanbaatar, Academy Nauka MNR, 95 p. (in Russian).

Badarch, G., Cunningham, W. D., and Windley, B. F., 2002, A new terrane subdivision for Mongolia: implications for the Phanerozoic crustal growth of Central Asia: Journal of Asian Earth Sciences, v. 21, p. 87–110, doi: 10.1016/S1367-9120(02)00017-2.

Baykova, V. S., and Amelin, Y., 1995, The Sm-Nd age of the Gashunnur Dike Complex, Mongolia: Transactions of the Russian Academy of Science: Earth Science Section 336, v. 4, p. 40–44.

Bibikova, E. V., Kirnozova, T. I., Kozakov, I. K., Kotov, A. B., Neymark, L. A., Gorkhovskiy, B. M., and Shuleshko, I. K., 1992, U-Pb ages for polymetamorphic complexes on the southern flank of the Mongolian and Gobi-Altai: Geotectonics, v. 26, p. 166–172.

Black, L. P., and Jagodzinski, E. A., 2003, Importance of establishing sources of uncertainty for the derivation of reliable SHRIMP ages: Australian Journal of Earth Sciences, v. 50, p. 503–512, doi: 10.1046/j.1440-0952.2003.01007.x.

Black, L. P., Kamo, S. L., Allen, C. M., Aleinikoff, J. N., Davis, D. W., Korsch, R. J., and Foudoulis, C., 2003, TEMORA 1: a new zircon standard for Phanerozoic U-Pb geochronology: Chemical Geology, v. 200, p. 155–170, doi: 10.1016/S0009-2541(03)00165-7.

Coleman, R. G., 1989, Continental growth of northwest China: Tectonics, v. 8, p. 621–635, doi: 10.1029/TC008i003p00621.

Compston, W., Williams, I. S., Kirschvink, J. L., Zhang, Z., and Ma, G., 1992, Zircon U-Pb ages for the early Cambrian time scale: Journal of the Geological Society, London, v. 149, p. 171–184, doi: 10.1144/gsjgs.149.2.0171.

Cumming, G. L., and Richards, J. R., 1975, Ore lead isotope ratios in a continuously changing earth: Earth and Planetary Science Letters, v. 28, p. 155–171, doi: 10.1016/0012-821X(75)90223-X.

De Laeter, J. R., and Kennedy, A. K., 1998, A double focusing mass spectrometer for geochronology: International Journal of Mass Spectrometry, v. 178, p. 43–50, doi: 10.1016/S1387-3806(98)14092-7.

Demoux, A., Kröner, A., Hegner, E., and Badarch, G., 2009a, Devonian arc magmatism in the Tseel terrane of SW Mongolia: chronological and geochemical evidence: Journal of the Geological Society, London, v. 166, p. 459–471, doi: 10.1144/0016-76492008-090.

Demoux, A., Kröner, A., Badarch, G., Jian, P., Tomurhuu, D., and Wingate, M. T. D., 2009b, Zircon ages from the Baydrag block and the Bayankhongor ophiolite zone: Time constraints on late Neoproterozoic to Cambrian subduction- and accretion-related magmatism in central Mongolia: Journal of Geology, v. 117, p. 377–397, doi: 10.1086/598947.

Demoux, A., Kröner, A., Liu, D., and Badarch, G., 2009c, Precambrian crystalline basement in southern Mongolia as revealed by SHRIMP zircon dating: International Journal of Earth Sciences, v. 98, p. 1365–1380, doi: 10.1007/s00531-008-0321-4.

Dijkstra, A. H., Brouwer, F. M., Cunningham, W. D., Buchan, C., Badarch, G., and Mason, P. R. D., 2006, Late Neoproterozoic proto-arc ocean crust in the Dariv Range, Western Mongolia: a supra-subduction zone end-member ophiolite: Journal of the Geological Society, London, v. 163, p. 363–373, doi: 10.1144/0016-764904-156.

Economos, R. C., Hanžl, P., Hrdličková, K., Buriánek, D., Said, L. O., Gerdes, A., and Paterson, S. R., 2008, Geochemical and structural constraints on the magmatic history of the Chandman Massif of the eastern Mongolian Altay Range, SW Mongolia: Journal of Geosciences, v. 53, p. 335–352, doi: 10.3190/jgeosci.034.

Eengin, G., 1978, Structure of the sedimentary mantle of the Dzolen Range, Mongolia: Geotectonics, v. 12, p. 54–57.

Gibsher, A. S., Khain, E. V., Kotov, A. B., Sal'nikova, E. V., Kozakov, I. K., Kovach, V. P., Yakovleva, S. Z., and Fedoseenko, A. M., 2001, Late Vendian age of the Han-Taishiri ophiolite complex in western Mongolia: Russian Geology and Geophysics, v. 42, p. 1110–1117.

Hanžl, P., and Aichler, J., 2007, Geological survey of the Mongolian Altai at a scale 1:50,000 (Zamtyn nurru—50): Ulaabaatar, Czech Geological Survey, Brno & MPRAM, 389 p.

Hanžl, P., and Krejči, Z., 2008, Geological map of the Trans-Altay Gobi 1:500,000, *in* Hanžl, P., and Krejči, Z., editors: Prague, Czech Geological Survey, scale 1:500,000.

Hanžl, P., Bat-Ulzii, D., Rejchrt, M., Košler, J., Bolormaa, K., and Hrdličková, K., 2008, Geology and geochemistry of the Palaeozoic plutonic bodies of the Trans-Altay Gobi, SW Mongolia: implications for magmatic processes in an accreted volcanic-arc system: Journal of Geosciences, v. 53, p. 201–234, doi: 10.3190/jgeosci.028.

Helo, C., Hegner, E., Kröner, A., Badarch, G., Tomurtogoo, O., Windley, B. F., and Dulski, P., 2006, Geochemical signature of Paleozoic accretionary complexes of the Central Asian Orogenic Belt in South Mongolia: Constraints on arc environments and crustal growth: Chemical Geology, v. 227, p. 236–257, doi: 10.1016/j.chemgeo.2005.10.003.

Hrdličková, K., Bolormaa, K., Buriánek, D., Hanžl, P., Gerdes, A., and Janoušek, V., 2008, Petrology and age of metamorphosed rocks in tectonic slices inside the Palaeozoic sediments of the eastern Mongolian Altai, SW Mongolia: Journal of Geosciences, v. 53, p. 139–165, doi: 10.3190/jgeosci.027.

Hsü, K. J., 1988, Relic back-arc basins of China and their petroleum potential, *in* Kleinspehn, K., and Paola, C., editors, New Perspectives in Basin Analysis: Berlin, Springer, p. 245–263.

Kepezhinskas, K. B., 1986, Structural-metamorphic evolution of late Proterozoic ophiolites and Precambrian basement in the Central Asian foldbelt of Mongolia: Precambrian Research, v. 33, p. 209–223, doi: 10.1016/0301-9268(86)90022-7.

Khain, E. V., Bibikova, E. V., Sal'nikova, E. E., Kröner, A., Gibsher, A. S., Didenko, A. N., Degtyarev, K. E., and Fedotova, A. A., 2003, The Palaeo-Asian ocean in the Neoproterozoic and early Palaeozoic: new geochronologic data and palaeotectonic reconstructions: Precambrian Research, v. 122, p. 329–358, doi: 10.1016/S0301-9268(02)00218-8.

Kinny, P. D., 1986, 3820 Ma zircons from a tonalitic Amitsoq gneiss in the Godthab district of southern West Greenland: Earth and Planetary Science Letters, v. 79, p. 337–347, doi: 10.1016/0012-821X(86)90190-1.

Koneva, M. P., 1990, Late Devonian radiolarian of the south Mongolian fold system: Doklady Akademii Nauk SSSR, p. 171–173 (in Russian).

Kovalenko, V. I., Yarmolyuk, V. V., and Bogatikov, O. A., 1995. Magmatism, Geodynamics and Metallogeny of Central Asia: Moscow, MIKO, Commercial Herald Publishers, 272 p.

Kozakov, I. K., 1986, Precambrian infrastructures of Paleozoic complexes of Mongolia: Leningrad, Nauka press, 144 p. (in Russian).
Kozakov, I. K., Glebovitsky, V. A., Bibikova, E. V., Azimov, P. Ya., and Kirnozova, T I., 2002a, Hercynian granulites of Mongolian and Gobian Altai: geodynamic setting and formation conditions: Doklady Earth Sciences, v. 38, p. 781–785.
Kozakov, I. K., Sal'nikova, E. B., Khain, E. V., Kovach, V. P., Berezhnaya, N. G., Yakovleva, N. G., and Plotkina, Y. V., 2002b, Early Caledonian crystalline rocks of the Lake zone, Mongolia: Stages and tectonic environments as deduced from U-Pb and Sm-Nd isotopic data: Geotectonics, v. 36, p. 156–166.
Kozakov, I. K., Kovach, V. P., Bibikova, E. V., Kirnozova, T. I., Zagornaya, N. Y., Plotkina, Yu. V., and Podkovyrov, V. N., 2007a, Age and sources of granitoids in the junction zone of the Caledonides and Hercynides in southwestern Mongolia: geodynamic implications: Petrology, v. 15, p. 126–150, doi: 10.1134/S0869591107020026.
Kozakov, I. K., Sal'nikova, E. B., Wang, T., Didenko, A. N., Plotkina, Yu. V., and Podkovyrov, V. N., 2007b, Early Precambrian crystalline complexes of the central Asian microcontinent: Age, sources, tectonic position: Stratigraphy and Geological Correlation, v. 15, p. 121–140, doi: 10.1134/S0869593807020013.
Kozakov, I. K., Kirnozova, T. I., and Plotkina, Yu. V., 2009, Age assessments for siliciclastic metasediments of the Bodonchin tectonic sheet, the south Altai metamorphic belt: Stratigraphy and Geological Correlation, v. 17, p. 36–42, doi: 10.1134/S0869593809010031.
Kretz, R., 1983, Symbols for rock-forming minerals: American Mineralogist, v. 68, p. 277–279.
Kröner, A., and Hegner, E., 1998, Geochemistry, single zircon ages and Sm-Nd systematics of granitoid rocks from the Góry Sowie (Owl Mts.), Polish West Sudetes: evidence for early Palaeozoic arc-related plutonism: Journal of the Geological Society, London, v. 155, p. 711–724, doi: 10.1144/gsjgs.155.4.0711.
Kröner, A., Byerly, G. R., and Lowe, D. R., 1991, Chronology of early Archaean granite-greenstone evolution in the Barberton Mountain land, South Africa, based on precise dating by single zircon evaporation: Earth and Planetary Science Letters, v. 103, p. 41–54, doi: 10.1016/0012-821X(91)90148-B.
Kröner, A., Jaeckel, P., Brandl, G., Nemchin, A. A., and Pidgeon, R. T., 1999, Single zircon ages for granitoid gneisses in the Central Zone of the Limpopo Belt, Southern Africa, and geodynamic significance: Precambrian Research, v. 93, p. 299–337, doi: 10.1016/S0301-9268(98)00102-8.
Kröner, A., Tomurtogoo, O., Badarch, G., Windley, B. F., and Kozakov, I. K., 2001, New zircon ages and significance for crustal evolution in Mongolia, *in* Sklyarov, E. V., editor, Guidebook and abstract volume: Irkutsk, Russia, workshop IGCP-440, p. 142–145.
Kröner, A., Windley, B. F., Badarch, G., Tomurtogoo, O., Hegner, E., Jahn, B. M., Gruschka, S., Khain, E. V., Demoux, A., and Wingate, M. T. D., 2007, Accretionary growth and crust formation in the Central Asian Orogenic Belt and comparison with the Arabian-Nubian-Shield: Geological Society of America, Memoir, v. 200, p. 181–209, doi: 10.1130/2007.1200(11).
Lamb, M. A., and Badarch, G., 1997, Paleozoic sedimentary basins and volcanic-arc systems of southern Mongolia: new stratigraphic and sedimentologic constraints: International Geological Review, v. 39, p. 542–576, doi: 10.1080/00206819709465288.
——— 2001, Paleozoic sedimentary basins and volcanic arc systems of southern Mongolia: new geochemical and petrographic constraints, *in* Hendrix, M. S., and David, G. A., editors, Paleozoic and Mesozoic tectonic evolution of central Asia: From continental assembly to intracontinental deformation, Boulder, Colorado: Geological Society of America, Memoir, v. 194, p. 117–149, doi: 10.1130/0-8137-1194-0.117.
Lamb, M. A., Badarch, G., Navratil, T., and Poier, R., 2008, Structural and geochronologic data from the Shin Jinst area, eastern Gobi Altai, Mongolia: Implications for Phanerozoic intracontinental deformation in Asia: Tectonophysics, v. 451, p. 312–330, doi: 10.1016/j.tecto.2007.11.061.
Lazarev, S. S., and Suur'suren, S., 1992, New Productida (Brachipoda) from the Carboniferous of Mongolia, *in* Tatarinov, L. P., Lubsandanzan, B., Afanas'yeva, G. A., Barsbold, R., Morozova, I. P., Novitskaya, L. I., Rasnitsyn, A. P., Reshetov, V. Y., Rozanov, A. Y., Sysoyev, V. A., and Trofimov, B. A., editors, New species of fossil invertebrates of Mongolia: Moscow, Nauka Press, Transaction of joint Soviet-Mongolian Scientific Research Geological Expedition, v. 41, p. 61–69 (in Russian).
Lehmann, J., Schulmann, K., Lexa, O., Corsini, M., Kröner A., Štípská, P., Tomurhuu D., and Otgonbator, D., 2010, Structural constraints on the evolution of the Central Asian Orogenic Belt in Southern Mongolia: American Journal of Science, p. 575–628, doi: 10.2476/07.2010.02.
Levashova, N. M., Kalugin, V. M., Gibsher, A. S., Yff, J., Ryabinin, A. B., Meert, J. G., and Malone, S. J., 2010, The origin of the Baydaric microcontinent, Mongolia: Constraints from paleomagnetism and geochronology: Tectonophysics, v. 485, p. 306–320, doi: 10.1016/j.tecto.2010.01.012.
Manatschal, G., Engström, A., Desmurs, L., Schaltegger, U., Cosca, M., Müntener, O., and Bernoulli, D., 2006, What is the tectono-metamorphic evolution of continental break-up: The example of the Tasna Ocean-Continent Transition: Journal of Structural Geology, v. 28, p. 1849–1869, doi: 10.1016/j.jsg.2006.07.014.
Marinov, N. A., Zonenshain, L. P., and Blagonravov, V. A., 1973, Geology of the Mongolian People's Republic: Moscow, Nedra Press, 782 p. (in Russian).
Markova, N. G., 1975, Stratigraphy of the Lower and Middle Paleozoic of Western Mongolia: Moscow, Nauka Press, Transactions of Joint Soviet-Mongolian Scientific Research Geological Expedition, 12, p. 119 (in Russian).
Matsumoto, I., and Tomurtogoo, O., 2003, Petrological characteristics of the Hantaishir ophiolite complex, Altai Region, Mongolia: coexistence of podiform chromitite and boninite: Gondwana Research, v. 6, p. 161–169, doi: 10.1016/S1342-937X(05)70967-9.
Menner, V. V., Peyne, A. V., Gerbova, V. G., Krasheninnikov, V. A., and Timofeyev, P. P., 1981, Atlas of the Ordovician fauna of Mongolia: Moscow, Nauka Press, Transactions of the Geological Institute Nauk SSSR, 228 p.

Minzhin, C., Badarch, G., and Tungalag, F., 1993, Stratigraphy of the Shine Jinst Paleozoic deposits: Mongolian Technical University Scientific Transactions, v. 3, p. 3–19 (in Mongolian).
Minzhin, C., Sersmaa, G., Undarya, J., Gereltsetseg, L., Naymsuren, G., Bolortsetseg, M., and Tumenbayar, B., 2001, *in* Webby, B., and Talent, J., editors, The Guide book, Abstract and Ordovician-Silurian correlation chart: The joint field meeting of IGCP 410 and IGCP 421 in Mongolia, 130 p.
Mitrofanov, F. P., Kozakov, I. K., and Palei, I. P., 1981, The Precambrian of western Mongolia and southern Tuva: Leningrad, Nauka, 156 p. (in Russian).
Mossakovsky, A. A., Ruzhentsev, S. V., Samygin, S. G., and Kheraskova, T. N., 1994, Central Asian fold belt: geodynamic evolution and history of formation: Geotectonics, v. 27, p. 445–474.
Nasdala, L., Hofmeister, W., Norberg, N., Mattinson, J. M., Corfu, F., Dörr, W., Kamo, S. L., Kennedy, A. K., Kronz, A., Reiners, P. W., Frei, D., Kosler, J., Wan, Y., Götze, J., Häger, T., Kröner, A., and Valley, J. W., 2008, Zircon M257—a homogeneous natural reference material for the ion microprobe U-Pb analysis of zircon: Geostandards and Geoanalytical Research, v. 32, p. 247–265, doi: 10.1111/j.1751-908X.2008.00914.x.
Nelson, D. R., 1997, Compilation of SHRIMP U-Pb zircon geochronology data: 1996, Geological Survey of Western Australia Record 1997/2, 189 p.
Nyamsuren, G., and Badarch, G., 1994, Devonian conodonts and biostratigraphy of the Shin-Jinst foldbelt, *in* ACOS-1: Nanjing, China, p. 11.
Rauzer, A. A., Zhanchiv, D. I., Golyakov, V. I., Ykhina, I. F., Ivanov, I. G., Tsukernik, A. B., Afonin, V. V., Smirnov, I. G., Bykhover, V. I., Kravtsev, A. V., Baatarkhuyag, A., Skoryukin, M. I., Khodikov, I. V., Mantsev, N. V., Okaemov, S. V., Mischin, V. A., and Enkhsajkhan, T., 1987, Report on results of geological survey at a scale of 1: 200,000, performed in southeast part of the Mongolian Altay, Mongolian National Republic in 1983–1986: Moscow, Tekhnoexport, 769 p. (in Russian).
Rong, J. Y., Boucot, A. J., Zheng, Y., and Strusz, D. L., 1995, Biogeographical analysis of Late Silurian brachiopod faunas, chiefly from Asia and Australia: Lethaia, v. 28, p. 39–60, doi: 10.1111/j.1502-3931.1995.tb01592.x.
Rozman, K. S., and Minzhin, C., 1988, Silurian stratigraphy of the Gobi Altai, southern Mongolia: Doklady Akademii Nauk SSSR, v. 301, p. 932–935 (in Russian).
Ruzhentsev, S. V., 2001, The Variscan belt of south Mongolia and Dzungaria, *in* Dergunov, A. B., editor, Tectonics, Magmatism, and Metallogeny of Mongolia: London, Routledge, p. 61–94.
Ruzhentsev, S. V., and Burashnikov, V. V., 1996, Tectonics of the western Mongolian Salairides: Geotectonics, v. 29, p. 379–394.
Ruzhentsev, S. V., and Pospelov, I. I., 1992, The South Mongolia Variscan fold system: Geotectonics, v. 30, p. 383–395.
Ruzhentsev, S. V., Badarch, G., and Voznesenskaya, T. A., 1985, Tectonics of the Trans-Altai zone of Mongolia (Gurvansaykhan and Dzolen ranges): Geotectonics, v. 19, p. 276–284.
Ruzhenstev, S. V., Rotman, Kh. S., and Minzhin, C., 1991, The formation time of the south Mongolian ocean: Doklady Akademii Nauk SSSR, v. 319, p. 451–455 (in Russian).
Şengör, A. M. C., and Natal'in, B. A., 1996, Paleotectonics of Asia: fragments of a synthesis, *in* Yin, A., and Harrison, M., editors, The Tectonic Evolution of Asia: Cambridge, Cambridge University Press, p. 486–640.
——— 2007, Eduard Suess and the Altaids: What is in a name? *in* Seltmann, R., Borisenko, A., and Fedoseev, G., editors, Magmatism and metallogeny of the Altai and adjacent large igneous provinces: London, United Kingdom, Centre for Russian and Central Eurasian Mineral Studies, Natural History Museum, p. 187–294.
Şengör, A. M. C., Natal'in, B. A., and Burtman, V. S. 1993, Evolution of the Altaid tectonic collage and Paleozoic crustal growth in Eurasia: Nature, v. 364, p. 299–307, doi: 10.1038/364299a0.
Sharkova, T. T., 1986, The governing principles of reef formation in the Silurian and Devonian basins of southern Mongolia, *in* Tatarinov, L. P., editor, Problems of the paleobiogeography of Asia: Moscow, Nauka Press, v. 29, p. 16 (in Russian).
Sinitsyn, V. M., 1956, Principal elements of geological structure of Gobi: Bull., MOIL, geology, v. 61, p. 6 (in Russian).
Šourek, J., Černý, M., and Rejchrt, M., editors, 2003, Geological and geochemical mapping of Trans-Altay Gobi on the scale 1:200,000: Ulaanbaatar, MS, MRPAM, p. 1–64.
Steiger, R. H., and Jäger, E. 1977, Subcommission on Geochronology: Convention on the use of decay constants in geo- and cosmochronology: Earth and Planetary Science Letters, v. 36, p. 359–362, doi: 10.1016/0012-821X(77)90060-7.
Stern, R. A., 1997, The GSC sensitive high resolution ion microprobe (SHRIMP): analytical techniques of zircon U-Th-Pb age determinations and performance evaluation, *in* Radiogenic age and isotope studies: Geological Survey of Canada, Current Research, Report, v. 10, p. 1–31.
Stern, R. A., and Amelin, Y., 2003, Assessment of errors in SIMS zircon U-Pb geochronology using a natural zircon standard and NIST SRM 610 glass: Chemical Geology, v. 197, p. 111–142, doi: 10.1016/S0009-2541(02)00320-0.
Suess, E., 1901, Das Antlitz der Erde: Wien, F. Tempsky, v. 3, part 1, 508 p.
Suyetenko, O. D., 1973, The construction of the Hercynian eugeosynclinal trough of southeastern Mongolia: Geotektonika, v. 7, p. 177–183.
Suyetenko, O. D., Golovchenko, Ye. V., Dobrov, G. M., and Tsukernik, A. B., 1988, Paleozoic structures in the Transaltay Gobi: Izvestiya Akademii Nauk SSSR, seriya Geologicheskaya, v. 4, p. 64–76.
Tomurtogoo, O., 1997, A new tectonic scheme of the Paleozoides in Mongolia: Mongolian Geoscientist, v. 3, p. 12–17.
——— 1998, Geological map of Mongolia: Mineral Resources Authority of Mongolia, Mongolian Academy of Sciences: Ulaanbaatar, 1:1 000 000 (with English summary).

Wang, T., Zheng, Y., Gehrels, G. E., and Mu, Z., 2001, Geochronological evidence for existence of South Mongolian microcontinent; a zircon U-Pb age of granitoid gneisses from the Yagan-Onch Hayrhan metamorphic core complex: Chinese Science Bulletin, v. 46, p. 2005–2008, doi: 10.1007/BF02901917.

Williams, I. S., 1998, U-Th-Pb Geochronology by ion microprobe, *in* McKibben, M. A., Shanks, W. C., III, and Ridley, W. I., editors, Applications in micro-analytical techniques to understanding mineralizing processes: Reviews in Economic Geology, v. 7, p. 1–35.

Williams, I. S., Buick, I. S., and Cartwright, I., 1996, An extended episode of early Mesoproterozoic metamorphic fluid flow in the Reynolds Range, central Australia: Journal of Metamorphic Geology, v. 14, p. 29–47, doi: 10.1111/j.1525-1314.1996.00029.x.

Wilson, R. C. L., Manatschal, G., and Wise, S., 2001, Rifting along non-volcanic passive margins: stratigraphic and seismic evidence from the Mesozoic successions of the Alps and western Iberia, *in* Wilson, R. C. L., Whitmarsh, R. B., Taylor, B., and Froitzheim, N., editors, Non-Volcanic Rifting of Continental Margins: A Comparison of Evidence from Land and Sea: Geological Society, London, Special Publications, v. 187, p. 429–452, doi: 10.1144/GSL.SP.2001.187.01.21.

Windley, B. F., Alexeiev, D., Xiao, W., Kröner, A., and Badarch, G., 2007, Tectonic models for accretion of the Central Asian Orogenic Belt: Journal of the Geological Society, London, v. 164, p. 31–47, doi: 10.1144/0016-76492006-022.

Yarmolyuk, V. V., Kovalenko, V. I., Sal'nikova, E. B., Kozakov, I. K., Kotov, A. B., Kovach, V. P., Vladykin, N. V., and Yakovleva, S. Z., 2005, U-Pb age of syn- and post-metamorphic granitoids of south Mongolia: evidence for the presence of Grenvillides in the Central Asian foldbelt: Doklady Earth Sciences, v. 404, p. 986–990.

Yarmolyuk, V. V., Kovach, V. P., Kovalenko, V. I., Terent'eva, L. B., Kozakov, I. K., Kotov, A. B., and Eenjin, G., 2007, Isotopic composition of the Hercynian crust of southern Mongolia: Substantiation of the Hercynian juvenile crust-forming event: Doklady Earth Sciences, v. 417, p. 1178–1182, doi: 10.1134/S1028334X07080090.

Yarmolyuk, V. V., Kovalenko, V. I., Anisimova, I. V., Sal'nikova, E. B., Kovach, V. P., Kozakov, I. K., Kozlovsky, A. M., Kudryashova, E. A., Kotov, A. B., Plotkina, Yu. V., Terent'eva, L. B., and Yakovleva, S. Z., 2008a, Late Riphean alkali granites of the Zabhan microcontinent: evidence for the timing of Rodinia breakup and formation of microcontinents in the Central Asian Fold Belt: Doklady Earth Sciences, v. 420, p. 583–588, doi: 10.1134/S1028334X08040132.

Yarmolyuk, V. V., Kovalenko, V. I., Sal'nikova, E. B., Kovach, V. P., Kozlovsky, A. M., Kotov, A. B., and Lebedev, V. I., 2008b, Geochronology of igneous rocks and formation of the late Paleozoic south Mongolian active margin of the Siberian continent: Stratigraphy and Geological Correlation, v. 16, 162–181, doi: 10.1134/S0869593808020056.

Yarmolyuk, V. V., Kovalenko, V. I., Kozlovsky, A. M., Kovach, V. P., Sal'nikova, E. B., Kovalenko, D. V., Kotov, A. B., Kudryashova, E. A., Lebedev, V. I., and Eenzhin, G., 2008c, Crust-forming processes in the Hercynides of the Central Asian Foldbelt: Petrology, v. 16, p. 679–709, doi: 10.1134/S0869591108070035.

Zaitsev, N. S., Luwsandansan, B., Marinov, N. A., Menner, V. V., Pavlova, T. G., Peive, A. V., Timofeev, P. P., Tomurtogoo, O., and Yanshin, A. L., 1970, Stratigraphy and tectonics of the Mongolian Peoples Republic, v. 1: Moscow, Nauka Press, Transactions of Joint Soviet-Mongolian Scientific Research Geological Expedition, 148 p. (in Russian).

Zhao, Y., Song, B., and Zhang, S. H., 2006, The Central Mongolian microcontinent: Its Yangtze affinity and tectonic implications, *in* Jahn, B. M., and Chung, L., editors, Abstract volume: Continental growth and orogeny in Asia: Taipei, Taiwan, March 19–26, Symposium in Taipei, p. 135–136.

Zonenshain, L. P., 1967, Tectonics of the folded regions of central Asia (the structural patterns of geosynclinals regions): Geotectonics, v. 1, p. 356–365.

——— 1972, The geosynclinal theory and its application to the Central Asia's Orogenic Belt: Moscow, Nedra, 240 p. (in Russian).

——— 1973, The evolution of Central Asiatic geosynclines through sea-floor spreading: Tectonophysics, v. 19, p. 213–232, doi: 10.1016/0040-1951(73)90020-6.

Zonenshain, L. P., and Kuzmin, M. I., 1978, Khan-Taishir ophiolite complex of western Mongolia, its petrology, origin and comparison with other ophiolitic complexes: Contributions to Mineralogy and Petrology, v. 67, p. 95–109, doi: 10.1007/BF00371637.

Zonenshain, L. P., Suyetenko, O. D., Jamyandamba, L., and Eengin, G., 1975, Structure and the axial part of South Mongolian eugeosyncline in the Dzolen Range: Geotectonics, v. 9, p. 214–220.